CONTROL OF TRIBOFILMS FORMATION IN MACHINING HARD MATERIALS

CONTROL OF TRIBOFILMS FORMATION IN MACHINING HARD MATERIALS

BY
JUNFENG YUAN, M. Sc., B. Eng.

A Thesis

Submitted to the School of Graduate Studies

in Partial Fulfillment of the Requirements

for the Degree

Doctor of Philosophy

McMaster University

Hamilton, Ontario, Canada

Doctor of Philosophy (2017) McMaster University

(Mechanical Engineering) Hamilton, Ontario, Canada

TITLE: CONTROL OF TRIBOFILMS FORMATION IN MACHINING HARD MATERIALS

AUTHOR: Junfeng Yuan M. Sc., B. Eng., Mechanical Engineering

SUPERVISOR: Dr. Stephen C. Veldhuis

Department of Mechanical Engineering

McMaster University

NUMBER OF PAGES: xx, 191

ABSTRACT

The study of factors governing cutting tool performance and life is driven by manufacturers' need to increase economic efficiency in their production facilities. Tooling and process optimization represent an ongoing opportunity for realizing substantial improvements, thus manufacturers continue to focus on promoting design and development of cutting tools and surface treatment technology relevant to machining. The central goal of cutting tool technology is to increase productivity while simultaneously reducing cost and meeting the quality targets of the machined parts.

This thesis considers a nano-tribological approach to explain some of the past performance improvements in cutting tools used in dry machining applications and to look for opportunities to make further improvements in this field. The approach considers tribofilms, which are often described as tribo-oxides composed of either the base cutting tool material or freshly cut workpiece material transferred to the tool that have formed on the friction surface through interaction with the environment (air or cutting fluids) and a tribo-oxidation process. In general, the formation of tribofilms plays an important role in friction and wear behaviour by offering thermal protection and/or in-situ lubrication, which is especially important during dry machining of hard workpiece materials. The formation of various tribofilms on cutting tools have been reported through: 1) cutting tools with surface modification and further tribo-oxidation during the

cutting process; 2) mass transfer from freshly cut workpiece material due to tool/chip contact in machining; and 3) interaction between the cutting tool surface and the cutting environment.

This dissertation presents a novel method to control the formation of tribofilms on the cutting tool surface during machining of hard materials such as Inconel DA 718 and hardened steels (AISI T1 and AISI D2), with coated and uncoated tools. In particular, the frictional conditions experienced by the cutting tool during the initial period of cutting (the running-in stage) are shown to strongly influence whether or not beneficial processes related to adaptability will trigger. Employing a more aggressive cutting speed during the running-in stage noticeably enhances the generation of protective/lubricious tribo-ceramic films on the friction surface. When the cutting speed is subsequently reduced, the accelerated formation of beneficial tribofilms previously initiated is not fully removed and therefore the rate of tool wear is considerably less than if the tool is run at the lower cutting speed for its entire life.

In addition, preliminary results are presented regarding tribofilms formation under the influence of the cutting environment, specifically the nature of the cooling medium used, which demonstrates an entirely different avenue to explore in terms of fine-tuning of tribofilms generation.

The overall objective of this dissertation is to highlight different approaches to control the tribofilms formed on the cutting tool surface in order to benefit the machining process and to improve cutting tool life, material remove rate and the machined surface quality. Additionally, little work has been found demonstrating the formation of tribofilms on the tool surface through mass transfer from the workpiece material or through interaction with the cooling medium. Thus a secondary objective of this work is to demonstrate the formation of tribofilms through these different means and to investigate the effect of cutting parameters on their formation.

ACKNOWLEDGEMENT

I am grateful and thankful for all the people who advised me, supported me and helped me. Without your help, the completion of this thesis would have been impossible.

First and foremost, I would like to express my great appreciation to my supervisor, Dr. Stephen Veldhuis, for his continuous guidance, critical review and support throughout my research. Dr. Veldhuis, for the past four years I have been deeply impressed by your great enthusiasm, insight and rigor for research, as well as your humour and wisdom about personal life. The opportunities you have provided me and the doors which you have opened have immensely broadened my horizons. The advice you have given me will benefit me for the rest of my life. Thank you!

Great appreciations are also expressed to Dr. German Fox-Rabinovich and Dr. Julia Dosbaeva for their invaluable guidance, academic enthusiasm, and dedication in helping me succeed in my research.

I would like to thank Dr. Igor Zhitomirsky and Dr. Joseph McDermid for their time and valuable suggestions offered while serving as members of my supervisory committee.

I would like to thank Terry Wagg for his fine work and help in experiments and training me on the operation of so many machines. I would like to thank Jeremy Boyd for his dedicated assistance in my experiments and publication, and for working with me for many days and nights to make sure projects were delivered on time.

I also want to express my thanks to all my colleagues and friends from McMaster Manufacturing Research Institute (MMRI) for being such a great team and for making our laboratory such a pleasant place in which to work.

Finally, I would like to thank my family and my dearest parents and grandparents in particular. 感谢我的父母苑振宝与魏华珍，外公外婆魏仓典和单美兰，在读博期间安息的爷爷苑修启以及从未见面的奶奶。I thank them for their constant love and care for all my life. Without their support, I would have never reached this far.

CONTENTS

ABSTRACT iv

ACKNOWLEDGEMENT vii

CONTENTS ix

LIST OF FIGURES xv

LIST OF TABLES xix

Chapter 1 Introduction 1

1.1 Background 1

1.1.1 High Speed Dry Machining 2

1.1.2 Wear Patterns and Mechanisms 4

1.1.3 Heat Generation in Machining 7

1.1.4 Environment (Natural Air) and Tribofilms Generation 8

1.1.5 Sources of Tribofilms 11

1.2 Motivation and Research Objective 11

1.3 Thesis Outline 13

Chapter 2:.....14

Chapter 3:.....15

Chapter 4:.....16

Chapter 5:.....17

Appendix: 18

1.4 A Note to the Reader 19

1.5 References 20

Chapter 2.....25

Influence of Workpiece Material on Tool Wear Performance and Tribofilms Formation in Machining Hardened Steel 25

Abstract:.....28

Keywords:.....29

2.1 Introduction 30

2.2 Experimental Work 32

2.3 Results and Discussion 38

2.4 Conclusion 48

Acknowledgement 49

References 50

Chapter 3 56

Study of Tribofilms Generation at Different Cutting Speeds in Dry Machining Hardened AISI T1 and AISI D2 Steel 56

Abstract 59

Key words: 60

3.1 Introduction 60

3.2 Experimental work 64

3.3 Results and Discussion 67

3.4 Conclusions 82

Acknowledgement: 84

References 85

Chapter 4.....91

Tribofilms Control in Adaptive TiAlCrSiYN/TiAlCrN Multilayer PVD Coating by Accelerating the Initial Machining Conditions 91

Keywords:.....94

Abstract.....95

4.1 Introduction 96

4.2 Material and Methods 98

4.3 Results and Discussion 103

4.4 Conclusions 123

Acknowledgement 124

References 125

Chapter 5.....131

Control of Tribofilms Formation in Dry Machining of Hardened AISI D2 Steel by Tuning the Cutting Speed 131

Abstract.....133

Keywords:.....134

5.1 Introduction 134

5.2 Experimental.....138

5.3 Result and Discussion 142

5.4 Conclusion.....154

Acknowledgement 156

References 157

Chapter 6 Conclusions and Future Work.....162

6.1 General Conclusions 162

6.2 Research Contributions.....165

6.3 Recommendations for Future Research 167

Appendix 168

Preliminary Results of Tribofilms Control with Influence of Cutting Environment and Various Surface Techniques to Characterize Tribofilms 168

A.1 Tribofilms Formation under Influence of Cutting Environment.....168

A.2 Various Methods to Characterize Tribofilms.....178

LIST OF FIGURES

Figure 1.1 The common wear forms in metal machining [9, 10] 5

Figure 1.2 Common wear mechanisms in machining [11] 6

Figure 1.3 General development of flank wear in machining [14].....7

Figure 2.1 Metallography of hardened workpiece materials: (a) AISI T1, (b) AISI D2....34

Figure 2.2 Flank wear land width versus cutting length during turning tests.....38

Figure 2.3 Worn rake and flank faces of ceramic insert after cutting (a) T1 steel to 3304 m, and (b) D2 steel to 3468 m. 41

Figure 2.4 High-resolution XPS spectra from the worn rake surface of ceramic inserts after cutting (a) T1 steel, and (b) D2 steel.....43

Figure 2.5 Cutting force measurements during the first machining pass with unworn inserts 47

Figure 2.6 Measured friction coefficient of individual tribometer tests between TiAlN-coated carbide pins against discs of T1 and D2 steel, under 1000 N load and various elevated temperatures 47

Figure 3.1 Metallography of hardened workpiece materials: (a) AISI T1, (b) AISI D2....65

Figure 3.2 Wear curves in machining T1 (left) and D2 steel (right).....69

Figure 3.3 SEM of ceramic inserts in turning T1 steel at S50, S80 and S100.....72

Figure 3.4 SEM of ceramic inserts in turning D2 steel at S50, S80 and S100 74

Figure 3.5 High resolution spectra on tool rake face after 900 meters cutting length..77

Figure 3.6 Chip undersurface morphology at 80 and 100 m/min 80

Figure 4.1 Wear curves at different cutting speed with CNGG inserts 103

Figure 4.2 Cutting edge at 200 meters length of cut with SPG inserts. 106

Figure 4.3 Elemental mapping of Tungsten (A-S40, B-S60, C-S60/40) and Nickel (D-S40, E-S60, F-S60/40) on rake face.....109

Figure 4.4 Areas of crater wear and build-up edge with SPG inserts.....110

Figure 4.5 Area of crater wear. (A-S40, B-S60, C-S60/40) 111

Figure 4.6 Photoelectron spectra of Al2p Cr2p and Ti2p on rake face after turning of 200 meters.....117

Figure 4.7 Auger depth profile for Thickness of the tribo-films.....122

Figure 5.1 Wear curves at different cutting speeds 143

Figure 5.2 Cutting edge after 200 meter length of cut.....144

Figure 5.3 Wear curve and photoelectron spectra of tuned cutting speeds (120-100 m/min).....148

Figure 5.4 Wear curve of tuned cutting speeds 120-100-80 m/min.....150

Figure 5.5 Cutting edge under different tuned cutting speeds around 4300 meters cutting length.....151

Figure 5.6 Rake face after 200 cutting length at 100 m/min 152

Figure A.1 Flank wear at wet and dry-wet conditions.....170

Figure A.2 Curling types of chips at S40 and S60.....172

Figure A.3 SEM image of chip under surface.....173

Figure A.4 Optical microphotograph of chip cross-section (etched by Aqua regia) 174

Figure A.5 BSE of chip cross-section (etched by 15ml HF+ 15ml 2% Acetic acid).....175

Figure A.6 Cutting edge at 200m and elemental mapping of W and Ni 176

Figure A.7 Cutting edge at 200m after etching and elemental mapping of W and Ni.177

Figure A.8 Tool life of TiAlCrSiYN-based mono- and multilayer coatings vs. length of cut 184

Figure A.9 SEM images of surface morphology vs. length of cut of the worn coated ball-nose end mills with a) TiAlCrSiYN mono-layered and b) TiAlCrSiYN/TiAlCrN multi-layered coatings during running-in stage.....185

Figure A.10 Short time impact fatigue fracture resistance data at 25 mN for the TiAlCrSiYN and TiAlCrSiYN/TiAlCrN coatings that corresponds to the running in stage.....186

Figure A.11 TEM analysis of worn surface for monolayer coating a) at the length of cut of: a) 15m (running-in stage); b) 30 m (post running-in stage).....188

Figure A.12 HRTEM analysis of worn surface with SAED diffraction pattern for monolayer coating at the length of cut of 15m (running-in stage).....189

Figure A.13 TEM analysis of worn surface for multilayer coating. TEM cross-section with SAED diffraction patterns of the marked areas for multilayer coating at the length of cut of a) 15m (running-in stage,) in comparison to b) the post running-in stage (30 m length of cut).....190

Figure A.14 EDS line scan profile of the multilayer coating at the length of cut of 15m (running-in stage) 191

LIST OF TABLES

Table 2.1 Chemical composition of workpiece materials.....33

Table 2.2 Heat treatment processes applied to workpiece materials. 33

Table 2.3 Material properties and geometry of the cutting inserts and tool holder.....35

Table 2.4 Roughness measurements of workpiece surfaces machined with unworn inserts 46

Table 3.1 Chemical composition of workpiece material 65

Table 3.2 XPS on insert for T1 after 900m turning 78

Table 3.3 XPS on insert for D2 after 900m turning.....78

Table 4.1 Structure and micro-mechanical characteristics of TiAlCrSiYN/TiAlCrN coatings at room and elevated temperatures.....99

Table 4.2 Cutting experiments.....101

Table 4.3 AES parameters.....102

Table 4.4 Phase and chemical composition of worn surface 119

Table 5.1 Chemical composition of workpiece material 138

Table 5.2 Tool inserts detail properties.....140

Table 5.3 XPS on tool tip for D2 within running-in stage 146

Table 5.4 Normalized AES results of O, Fe & Cr at 100 m/min 153

Table A.1 Phase and chemical composition of the worn surface (XPS data) at the different stages of wear (15 m-running-in stage; 30 m-beginning of the stable stage).....182

Table A.2 Cutting parameters used for the tool life evaluation.....183

Chapter 1 Introduction

1.1 Background

Machining plays an important role in realizing the critical parts which support a wide range of industries including: automotive, aerospace/space, medical devices, energy, mining and mold/die. Machining is capable of producing complex, high value parts to tight dimensional tolerances and surface quality requirements, cost effectively and often in large volumes. In the last 50 years, innovations in cutting tool materials, geometries and, specifically, coatings, have led to significant advancements in machining performance [1]. However, there is still substantial room for further improvement in this field [2]. Areas with great potential include:

1. Increased material remove rates for a wide range of workpiece materials, including difficult-to-machine materials
2. Higher final part quality
3. Enhanced process robustness
4. Reduced tooling cost
5. Dry or near dry cutting

6. Realization of novel products and services through the efficient processing of new high performance materials and generation of new innovative processes.

Although tooling accounts for only 3-5% of direct machining costs, it indirectly impacts productivity per machine, quality and often triggers the need for extra labour to monitor production as well as considerable labor costs associated with changing and maintaining tooling.

1.1.1 High Speed Dry Machining

The economic efficiency and productivity of a manufacturing facility is a central issue when implementing cutting technology. Thus, high productivity machining, often involving high cutting speeds, is preferred by industry [3, 4]. Currently, high speed machining processes are predominantly focused on aluminium and magnesium machining [1], because of the relatively low mechanical and thermal load they apply to the cutting tool and the high temperature properties of these materials. However, there is great potential in extending the benefits of high cutting speeds to hard materials, as has been shown for the high speed machining of hardened mold/die steels where the thermal softening that takes place in this process enables the cost effective machining of hardened tool steels in the 50-60 HRC range. The research presented in this dissertation seeks to better understand how the surface of the tool withstands these extreme

conditions to increase the efficiency of high speed machining and extend its application to other materials.

In machining, coolant is often used to remove heat from the cutting zone and provide lubrication at the friction surface. However, under the cutting conditions typically used in high speed machining, the use of coolant introduces excessive thermal shock to the tool, greatly reducing its life. To address this limitation and reduce the cost associated with using coolants and lubricants, solid lubrication can be designed into the surface layers of the cutting tool itself through a proper understanding of tribofilms and their formation. In general, tribofilms are generated on the surface of the tool during the frictional interactions between the tool and workpiece materials and reaction with the environment (air or cutting fluids). Many of the thin tribofilms formed can serve as a thermal barrier and enhance the oxidation resistance of a surface, thereby protecting the surface of a tool [5]. When machining without coolant, especially during dry high speed machining of hard materials, the tools are exposed to harsh tribological conditions and chips are not easily flushed out of the cutting zone, especially when machining sticky materials like aluminum or stainless steel, or when performing deep hole drilling. Chip motion along the secondary shear deformation zone can generate extremely high temperatures at the cutting tool / chip interface that may reach or exceed the diffusion and bonding limits of the cutting tool materials. This situation leads to rapid tool wear and poor surface finish of the machined parts [2, 6, 7]. Reducing t

thermal shock makes dry machining more attractive but presents the challenge of harsh tribological conditions for the tool to endure. Tight control of the tribofilms formed on the tool surface represents a way to reduce friction and wear, especially when cutting hard materials [8], thus increasing the viability of dry machining.

1.1.2 Wear Patterns and Mechanisms

Tool wear is a significant issue that limits productivity and quality while contributing substantially to the cost of machining. The tool and workpiece material, the nature of the process, and the local cutting conditions determine the specific wear phenomena and overall wear rate. The common wear patterns in metal cutting include: a) Flank wear, b) Crater wear, c) Notch wear, d) Nose radius wear, e) Comb (thermal) cracks, f) Parallel (mechanical) cracks, g) build up edge, h) Gross plastic deformation, i) Edge chipping or frittering, j) Chip hammering and k) Gross fracture [9, 10], as shown in Figure 1.1.

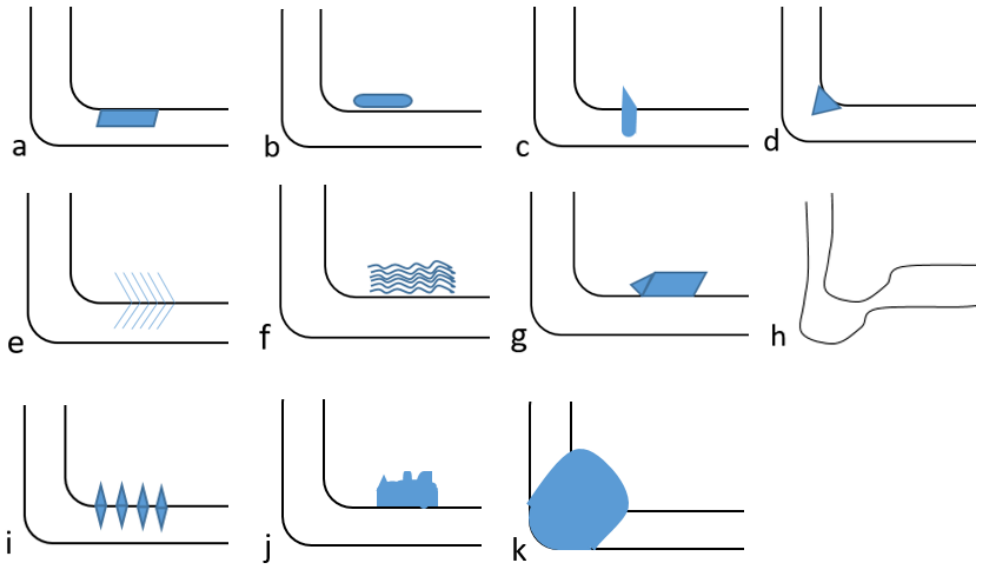

a) Flank b) Crater c) Notch d) Nose radius e) Comb (thermal) cracks f) Parallel (mechanical) cracks g) BUE h) Gross plastic deformation i) Edge chipping or frittering j) Chip hammering k) Gross fracture

Figure 1.1 The common wear forms in metal machining [9, 10]

In metal cutting, common tool wear mechanisms include adhesion, abrasion, diffusion and oxidation, which dominate wear at different temperatures [11], as shown in Figure 1.2. Abrasion occurs due to sliding between the tool and hard constituents from the workpiece material. It can be significant when the workpiece contains hard particles, is by its nature hard, or, in some cases, experiences work hardening during machining. Adhesion occurs when particles of the cutting material adhere to the surface of the tool and then over time are pulled off, removing parts of the cutting tool material with the adhered particle. Diffusion wear commonly occurs at higher temperatures and also depends on the friction pair materials' affinity for one another. Oxidation wear

occurs at higher temperatures and is usually due to chemical attack by the corrosive workpiece surface or liquids that are present at the friction interface [12].

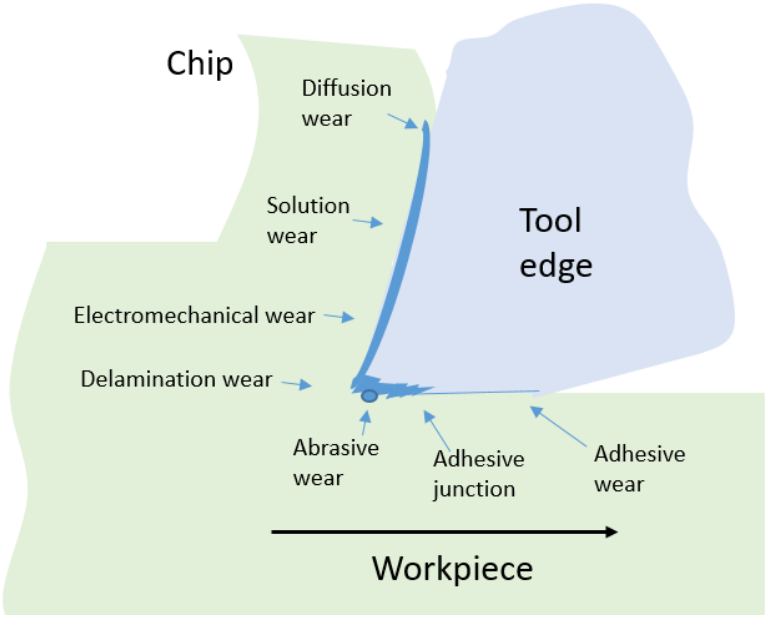

Figure 1.2 Common wear mechanisms in machining [11]

In general, there is no single, universally accepted definition of tool life; tool life needs to be specified taking the process objectives into consideration [13]. A common way to quantify the end of tool life, whether in industry or laboratory research, is to set a limit on the average or maximum flank wear, or sometimes combined with crater wear. Figure 1.3 illustrates the general behavior of flank wear in machining, in which tool life can be generally divided into three phases [14]. Phase I is the running-in stage, during which the sharp edge is worn rapidly with an initial high rate of wear and a finite wear land is established. Phase II is the steady wear stage, where a steady increase in flank wear occurs in proportion to the cutting length. Phase III is severe wear, which

generally begins near the end of the tool's functional life. It is characterized with a marked increase in wear rate after the wear reaches a critical limit where sufficient internal damage to the tool has occurred.

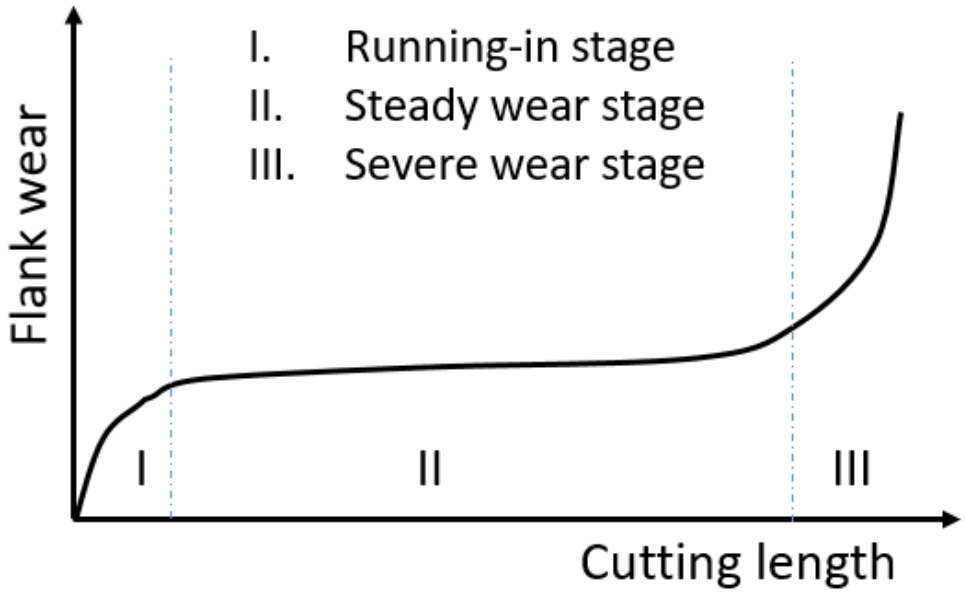

Figure 1.3 General development of flank wear in machining [14]

1.1.3 Heat Generation in Machining

During the metal cutting process, a substantial portion of the energy generated from the metal plastic deformation supplied by the moving tool is converted to heat. The cutting temperature is mostly determined by cutting velocity, which is directly related to the productivity and, ultimately, the cost efficiency of the machining process. Cutting temperature has a significant influence on tool wear. Therefore, the development of new tool materials and coatings is mostly focused on their ability to

sustain high cutting temperatures. Around three quarters of the cutting energy is expended at the Primary deformation zone while one quarter is spent at the Secondary shear zone [15]. The tool-chip interface temperature is determined by the energy from the Secondary shear zone and it directly influences the intensity and the crater tool wear rate [12]. When the cutting speed is increased, less time is available for the heat to transfer into the workpiece and the tool; thus, less heat flows into the workpiece and the cutting tool [13]. It has been reported that during high speed machining, around 80-90% of the heat generated during cutting is transferred to the chip while 10-20% of the heat goes to the cutting tool and workpiece material [16-18]. When coatings with low thermal conductivity are used to protect the cutting tools, an even higher portion of the heat is forced to the chip reducing the thermal load on the tool.

1.1.4 Environment (Natural Air) and Tribofilms Generation

The environment, in particular air with approximately 80% nitrogen and 20% oxygen plays a significant role in metal cutting, especially in dry cutting or high speed cutting due to the reactivity of oxygen with most materials. Oxygen plays two counterbalancing roles in machining [19]. The air itself acts to some extent as a coolant, removing heat from the cutting zone and clearing debris. Oxygen from the air can penetrate along the chip-tool contact edge and react with active elements near the surface. The freshly generated workpiece surface produced by cutting and the

corresponding fresh tool surface exposed from gradual wear are clean and thus chemically very active, enough to react rapidly with the oxygen from the air, or with elements present in other liquids such as water or oil based lubricants used during wet cutting [19].

In general, the formation of tribofilms plays an important role in the friction and wear behaviour of cutting tools, especially during dry machining of hardened material. Tribofilms are generated from the base cutting tool material or transferred workpiece material often through interaction with the environment and further tribo-oxidation. The formation of these films are part of an adaptive response of the tribo-system to the external environment. In an equilibrium system, the energy is uniform, while in a non-equilibrium system with rapidly changing temperatures, such as the extreme tribological conditions which are typical of the cutting process [20], metastable structures can be formed. Their initial formation and replenishment over time in a process is referred to as self-organization [20]. These metastable structures (tribofilms) can remain on the friction surface long enough to provide value in terms of lubrication and protection [20]. The driving force for their formation is self-organization, which is the inherent tendency of a system to organize itself to protect and stabilize itself [21]. Under harsh machining conditions tribofilms must be formed initially during the running-in stage or the tool will be rapidly destroyed. Since the tribofilms are only metastable they are constantly being destroyed and regenerated as part of the friction

process [22]. Thus, to be beneficial, the films need to be continuously regenerated over the life of the tool. In this way, energy is directed to the formation of metastable structures, i.e. tribofilms instead of being spent on system damage, i.e. severe wear [23]. Reliable evaluation of the portion of energy consumed in forming tribofilms is not possible at the moment; however, the reduction in intensity of wear can be observed in the experimental data collected during machining [20, 22].

In a high temperature and heavily loaded tribo-system, the formation of tribofilms has a large impact on tool life and process performance [24, 25]. Complex tribofilms are formed on the friction surface under severe cutting conditions. These thin films work as a dynamic, nanostructured often oxide based layer that serves to protect and lubricate the underlying tool substrate at the tool/chip or tool/workpiece interface. Tribofilms are generated as a result of a self-adaptive process that occurs between the tool and the workpiece at the friction interface [20]. Tribofilms can act as a thermal barrier and help reduce thermal shock as well as protect the surface from oxidation wear. They can also act as high temperature lubricants. Thus both the physical and chemical properties on the friction surface are significantly improved due to the formation of beneficial tribofilms [26-28].

1.1.5 Sources of Tribofilms

The formation of various tribofilms have been reported as a result of tribo-oxidation of cutting tools [22], as well as the result of workpiece material transfer during tool/chip interaction [26, 27]. In general, there are three major sources of tribofilms:

a) cutting tool surface modification with further tribo-oxidation during the cutting process [22];
b) mass transfer from workpiece material during tool/chip contact in machining [26], and lastly;
c) tribofilms formation through the interaction between the tool surface and the cutting environment, for instance partially or totally from material supplied through the cutting coolant, lubricants, etc. [20, 29].

1.2 Motivation and Research Objective

Beneficial tribofilms have demonstrated their ability to provide thermal protection and surface lubrication in order to improve tool life and enhance machined surface quality.

The study of tribofilms has evolved from the research of adaptive coatings; subsequently generated tribofilms from cutting tools and coatings have been studied

and published in the past. However, limited studies have been published on tribofilms formation due to mass transfer from the workpiece material or under the influence of different cutting (cooling) environments. As well, controlling tribofilms formation by shifting a tribo-system to short-term severe frictional conditions during running-in stage, thereby accelerating beneficial processes related to adaptability [30] has not been explicitly demonstrated. Also there is a lack of knowledge in the literature on how to practically accomplish this, regardless of the specific source from which tribofilms arise. Thus, the overall objective of this dissertation is to understand tribofilms formation and, more importantly, to determine conditions under which tribofilms formation can be controlled and most importantly accelerated and stabilized. The specific objectives can be articulated as:

i. To demonstrate the existence of tribofilms generation due to mass transfer from workpiece material in dry machining of hardened materials.
ii. To study the influence of cutting conditions, specifically cutting speeds, on tribofilms formation in cutting of different hardened workpiece materials.
iii. To develop a novel method to control tribofilms generation preferentially by changing cutting conditions in order to improve tool life, material removal rate and surface quality using the following three groups of experiments:

iii-a. To investigate the control of tribofilms formation using a surface engineered layer (coated tools), aimed at determining the effect of an initial acceleration of tribofilms formation with self-adaptive coatings.

iii-b. To study control of tribofilms generation due to mass transfer of workpiece material, in order to enhance tribofilms formation by tuning cutting parameters.

iii-c. To investigate control of tribofilms formation under the influence of changing cutting environments, for the purpose of increasing tribofilms generation due to external change of environment resulting in internal variation in cutting circumstance or gain/loss of compounds caused by altering external environments.

1.3 Thesis Outline

In compliance with the regulations of McMaster University, the main body of this dissertation is assembled in a sandwich thesis format composed of four journal articles (3 published and 1 under review) addressing the objectives above, except for iii (3). Each chapter contains an outline of the contribution made by each of the authors to the paper. An introductory chapter as well as a final chapter, containing overall conclusions and recommendations for future study, have been added. The preliminary results regarding iii (3) will be described in the Appendix and will assist to explain the

recommendations for future study portion of the final chapter. The chapters consisting of the four complete journal articles and Appendix are arranged as follows:

Chapter 2:

This chapter consist of a journal article that was published in Lubricants:

Yuan, Junfeng, et al. "Influence of Workpiece Material on Tool Wear Performance and Tribofilms Formation in Machining Hardened Steel." Lubricants 4.2 (2016): 10.

Preface: This article showed evidence of tribofilms formed as a result of workpiece material mass transfer to the friction surface, which play a significant role in friction control in addition to the bulk properties of a workpiece material. This is especially true in the cutting of hardened materials, where it is very difficult to use liquid based lubricants. To better understand wear performance and the formation of beneficial tribofilms, this study presents an assessment of uncoated mixed alumina ceramic tools (Al2O3+TiC) in the turning of two grades of steel, AISI T1 and AISI D2. Both workpiece materials were hardened to 59 HRC then machined under identical cutting conditions. Comprehensive characterization of the resulting wear patterns and the tribofilms formed at the tool/workpiece interface were made using X-ray Photoelectron Spectroscopy (XPS) and Scanning Electron Microscopy (SEM). Metallographic studies on

the workpiece material were performed before the machining process, and the surface integrity of the machined parts was investigated. This study further validated tribofilms formation resulting from elements supplied by the workpiece.

Chapter 3:

This chapter contains an accepted journal article in Proceedings of the Institution of Mechanical Engineers, Part J: Journal of Engineering Tribology, titled:

Yuan, Junfeng, et al. “Study of tribofilms generation at different cutting speeds in dry machining hardened AISI T1 and AISI D2 steel”

Preface: After the demonstration of tribofilms formation when machining hardened T1 and D2 steels in chapter 2, this paper studied the effect of cutting conditions on the generation of tribofilms at different cutting speeds which effectively means different temperatures. Cutting speeds of 50 m/min, 80 m/min and 100 m/min in hard dry machining of AISI T1 and AISI D2 steels at comparable hardness (around 59 HRC) were used. Comprehensive assessment of uncoated ceramic inserts in machining of T1 and D2 at different cutting speeds was made by optical microscope, SEM and XPS. It was shown that higher cutting speeds increased the formation of thermal protective and/or lubricating tribofilms. In machining D2 steel, more intensive formation of Cr-O tribo-oxides resulted in a lower wear rate; while when cutting T1 steel, a higher amount

of W-O tribofilms generation provided better lubrication. This work showed that hardened D2 was more suitable to study tribofilms formation than T1 steels, and that tribofilms formation is enhanced at higher cutting speed within an appropriate speed range.

Chapter 4:

The published journal article in Surface and Coating Technology:

Yuan, Junfeng, et al. "Tribofilms control in adaptive TiAlCrSiYN/TiAlCrN multilayer PVD coating by accelerating the initial machining conditions." Surface and Coatings Technology 294 (2016): 54-61.

Preface: This article presented a novel approach to control tribofilms formation during the running-in stage of a cutting process using coated carbide in machining DA 718 Inconel. A nano-multilayer TiAlCrSiYN/TiAlCrN coating was deposited by Physical Vapor Deposition (PVD) on cemented carbide turning inserts. Assessment of the performance of the coated inserts in machining of DA718 Inconel was made at various cutting speeds during the initial, running-in stage of wear. Three different machining conditions were used: i. Regular cutting speed (40 m/min) commonly used in industrial practice; ii. Higher cutting speed of 60 m/min, and iii. Accelerated (higher speed followed by regular cutting speed). Comprehensive characterization of the tribofilms

formed on the surface of the worn cutting tools was made using Auger Electron Spectroscopy (AES) and XPS analyses. SEM/Energy Dispersive X-ray Spectrometry (EDS) elemental mapping was used for evaluation of the wear patterns. It was shown that an initial short-term increase in the cutting speed during the running-in stage (condition iii) noticeably improved tool life. This was attributed to the enhanced formation of protective/lubricious tribo-ceramic films on the friction surface which takes place due to the higher initial cutting speed (temperature), with the subsequent slowdown in speed preventing total wearing away of the beneficial tribofilms. In this way, the process of tribofilms formation can be enhanced at the start of the wear process and the benefits of these films can be realized over the life of the tool.

Chapter 5:

This chapter consists of a journal article submitted to Wear and presently under review, titled:

Yuan, Junfeng, et al. “Control of tribofilms formation in dry machining of hardened AISI D2 steel by tuning the cutting speed”. Submitted to Wear, under review

Preface: Chapter 4 focused on control of tribofilms formation with coated tools in which the components of the tribofilms were sourced from adaptive coatings; Chapter 5 presents the study performed on controlling tribofilms generation with

uncoated tools where the tribofilms arise from transferred workpiece materials. This article focuses on the tuning of the tribofilms formation formed as a result of mass transfer of workpiece material to the tool surface with further tribo-oxidation occurring through their interaction with the environment. Based on the current understanding, the formation of tribofilms is enhanced by high temperatures which are brought on by higher cutting speeds, with their beneficial properties further impacting the friction and wear process. Wear performance of uncoated ceramic (mixed alumina and TiCN) tools were studied at different constant cutting speeds (50; 80; 100 and 120 m/min) and tuned cutting speeds (120-100 and 120-100-80 m/min) during hard dry turning of AISI D2 tool steel. The tuning of the cutting speed was performed in order to enhance the generation of favourable tribofilms and obtain an extended tool life. During the tuning of the cutting speed, tribofilms generated at higher speeds were not completely worn out and were found to improve the friction/wear process when the cutting process was subsequently shifting to a lower cutting speed.

Appendix:

The appendix consists of an unpublished section on the tribofilms formation under changing environments like dry-wet conditions. The appendix also includes a section from a journal article with Dr. Fox-Rabinovich as the first author. My contributions as a co-author of this journal article are included in this thesis to highlight

the results of my research involving selected machining tests, surface sample preparation methods, surface characterization and methods used to analyze the results.

1.4 A Note to the Reader

As this thesis consists of a series of journal articles, some overlap or repetition of material might be found during reading. In particular, there is some overlap in the introduction section of some chapters. In addition, the sections describing tests and experimental facilities and measurement methodology in some of the chapters contain significant repetition since the same facilities were used in all experiments. However, each background section contains more specific references related to the study presented in each paper.

Also note that all cutting tests (wear curves) in this article were repeated more than six times. The wear curves were repeatable with the most representative wear curve selected for the figure shown in the article.

1.5 References

[1] Byrne G, Dornfeld D, Denkena B. Advancing cutting technology. CIRP Annals-Manufacturing Technology 2003;52:483-507.

[2] Davim JP. Machining of hard materials: Springer; 2011.

[3] Song J, Huang C, Lv M, Zou B, Liu H, Wang J. Cutting performance and failure mechanisms of TiB2-based ceramic cutting tools in machining hardened Cr12MoV mold steel. The International Journal of Advanced Manufacturing Technology 2013:1-6.

[4] Fox-Rabinovich GS, Kovalev AI, Aguirre MH, Beake BD, Yamamoto K, Veldhuis SC, et al. Design and performance of AlTiN and TiAlCrN PVD coatings for machining of hard to cut materials. Surface and Coatings Technology 2009;204:489-96.

[5] Dudzinski D, Devillez A, Moufki A, Larrouquère D, Zerrouki V, Vigneau J. A review of developments towards dry and high speed machining of Inconel 718 alloy. International Journal of Machine Tools and Manufacture 2004;44:439-56.

[6] Chou YK, Evans CJ. White layers and thermal modeling of hard turned surfaces. International Journal of Machine Tools and Manufacture 1999;39:1863-81.

[7] Matsumoto Y, Hashimoto F, Lahoti G. Surface integrity generated by precision hard turning. CIRP Annals-Manufacturing Technology 1999;48:59-62.

[8] Sreejith P, Ngoi B. Dry machining: machining of the future. J Mater Process Technol 2000;101:287-91.

[9] Stephenson DA, Agapiou JS. Metal cutting theory and practice: CRC press; 2005.

[10] Penalva M, Arizmendi M, Diaz F, Fernandez J, Katz Z. Effect of tool wear on roughness in hard turning. CIRP Annals-Manufacturing Technology 2002;51:57-60.

[11] Kopac J, Sokovic M, Dolinsek S. Tribology of coated tools in conventional and HSC machining. J Mater Process Technol 2001;118:377-84.

[12] Toenshoff HK, Denkena B. Basics of cutting and abrasive processes: Springer; 2013.

[13] Ning L. Nano-multilayered self-adaptive hard PVD coatings for dry high performance machining, McMaster PhD Disertation, 2008.

[14] Wen S, Huang P. Principles of tribology: John Wiley & Sons; 2012.

[15] Shaw MC, Cookson J. Metal cutting principles: Oxford university press New York; 2005.

[16] El-Wardany T, Kishawy H, Elbestawi M. Surface integrity of die material in high speed hard machining, Part 1: Micrographical analysis. Journal of manufacturing science and engineering 2000;122:620-31.

[17] Snr D, Dimla E. Sensor signals for tool-wear monitoring in metal cutting operations—a review of methods. International Journal of Machine Tools and Manufacture 2000;40:1073-98.

[18] Dewes R, Ng E, Chua K, Newton P, Aspinwall D. Temperature measurement when high speed machining hardened mould/die steel. Journal of Materials Processing Technology 1999;92:293-301.

[19] Trent EM, Wright PK. Metal cutting: Butterworth-Heinemann; 2000.

[20] Fox-Rabinovich G, Totten GE. Self-organization During Friction: Advanced Surface-engineered Materials and Systems Design: CRC Press; 2010.

[21] Gershman IS, Bushe NA. Elements of Thermodynamics of Self-Organization during Friction. Self-Organization during Friction Advanced Surface-Engineered Materials and Systems Design 2006:13-58.

[22] Fox-Rabinovich GS, Yamamoto K, D Beake B, S Gershman I, I Kovalev A, C Veldhuis S, et al. Hierarchical adaptive nanostructured PVD coatings for extreme tribological

applications: the quest for nonequilibrium states and emergent behavior. Science and Technology of Advanced Materials 2012;13:043001.

[23] Fox-Rabinovich GS, Gershman IS, Yamamoto K, Biksa A, Veldhuis SC, Beake BD, et al. Self-Organization during Friction in Complex Surface Engineered Tribosystems. Entropy 2010;12:275-88.

[24] Jacobson S, Hogmark S. Tribofilms—on the crucial importance of tribologically induced surface modifications. Recent developments in wear prevention, friction and lubrication 2010;661:197-225.

[25] Bouzakis K-D, Michailidis N, Skordaris G, Bouzakis E, Biermann D, M'Saoubi R. Cutting with coated tools: Coating technologies, characterization methods and performance optimization. CIRP Annals-Manufacturing Technology 2012;61:703-23.

[26] Fox-Rabinovich GS, Gershman I, Hakim MAE, Shalaby MA, Krzanowski JE, Veldhuis SC. Tribofilm Formation As a Result of Complex Interaction at the Tool/Chip Interface during Cutting. Lubricants 2014;2:113-23.

[27] Yuan J, Boyd JM, Covelli D, Arif T, Fox-Rabinovich GS, Veldhuis SC. Influence of Workpiece Material on Tool Wear Performance and Tribofilm Formation in Machining Hardened Steel. Lubricants 2016;4:10.

[28] Shalaby M, El Hakim M, Abdelhameed MM, Krzanowski J, Veldhuis S, Dosbaeva G. Wear mechanisms of several cutting tool materials in hard turning of high carbon–chromium tool steel. Tribology International 2014;70:148-54.

[29] Voevodin A, Zabinski J. Nanocomposite and nanostructured tribological materials for space applications. Composites Science and Technology 2005;65:741-8.

[30] Gershman I, Bushe N, Mironov A, Nikiforov V. Self-organization of secondary structures in friction. Trenie i Iznos 2003;24:329-34.

Chapter 2

Influence of Workpiece Material on Tool Wear Performance and Tribofilms Formation in Machining Hardened Steel

Complete citation:

Yuan, Junfeng, Jeremy M. Boyd, Danielle Covelli, Taib Arif, German S. Fox-Rabinovich, and Stephen C. Veldhuis. "Influence of Workpiece Material on Tool Wear Performance and Tribofilm Formation in Machining Hardened Steel." Lubricants 4, no. 2 (2016): 10.

Relative Contributions:

Junfeng Yuan:	Designed and performed all experiments, interpretation and analysis of the data and wrote the manuscript including all figures and text.
Jeremy M. Boyd:	Performed the tribometer experiments and helped in data analysis of tribometer results, assisted in promotion of writing.
Danielle Covelli:	Performed XPS analyses and assigned peaks.
Taib Arif:	Assisted with cutting experiments and SEM characterization.
G. S. Fox-Rabinovich:	Offered assistance with experiments, analysis of results and suggestions for writing.
Stephen C. Veldhuis:	Provided thesis supervisor for the experiments and was responsible for the final draft submitted to the journal.

Preface:

A deep cut before each test was used to eliminate the effect of surface hardening from the previous pass.

The XPS showed the highest concentration of elements involving tribofilms formation as Tungsten in T1 and Chromium in D2 separately, which was found to be higher than the other elements and played the most important role during machining.

According to the working mechanism of the heated pin-on-disk device used in this chapter, the coating had to be conductive. TiAlN was the best choice to simulate the actual friction situation during turning D2 steel process with mixed Alumina inserts (TiN as the binder).

Influence of workpiece material on tool wear performance and tribofilms formation in machining hardened steel

Junfeng Yuan[1], Jeremy M. Boyd[1], Danielle Covelli[2], Taib Arif[1], German S. Fox-Rabinovich[1], Stephen C. Veldhuis[1*]

1. Department of Mechanical Engineering, McMaster University, 1280 Main St., W. Hamilton, Ontario, Canada L8S 4L7

2. Biointerfaces Institute, McMaster University, 1280 Main St., W. Hamilton, Ontario, L8S 4L7, Canada

* Correspondance: veldhu@mcmaster.ca; Tel. : (905) 525-9140 e. 27044

Abstract:

In addition to the bulk properties of a workpiece material, characteristics of the tribofilms formed as a result of workpiece material mass transfer to the friction surface play a significant role in friction control. This is especially true in cutting of hardened materials, where it is very difficult to use liquid based lubricants. To better understand wear performance and the formation of beneficial tribofilms this study presents an

assessment of uncoated mixed alumina ceramic tools (Al2O3+TiC) in the turning of two grades of steel, AISI T1 and AISI D2. Both workpiece materials were hardened to 59 HRC then machined under identical cutting conditions. Comprehensive characterization of the resulting wear patterns and the tribofilms formed at the tool/workpiece interface were made using X-ray Photoelectron Spectroscopy and Scanning Electron Microscope/Energy-Dispersive X-Ray Spectroscopy. Metallographic studies on the workpiece material were performed before the machining process and the surface integrity of the machined part was investigated after machining. Tool life was 23% higher when turning D2 than T1. This improvement in cutting tool life and wear behavior was attributed to a difference in: 1) tribofilms generation on the friction surface and 2) the amount and distribution of carbide phases in the workpiece materials. The results show that wear performance depends both on properties of the workpiece material and characteristics of the tribofilms formed on the friction surface.

Keywords:

Hard turning, X-ray photoelectron spectroscopy, tribofilms, tool wear, AISI T1, AISI D2.

2.1 Introduction

Dry machining has been gaining some traction among manufacturers nowadays, as industry recognizes its benefits over conventional wet machining, such as eliminating costs and health/environmental risks associated with coolant, and reducing thermal shock in interrupted cutting operations [1-3]. As such, the technique has also been increasingly applied to hard materials (typically in the range of 58 to 68 HRC) and is even replacing conventional grinding processes in some instances, due to reduced machining costs as well as improved surface integrity [4, 5]. However, the application of dry high speed machining of hard materials introduces the problems of harsh tribological conditions at the tool-chip interface and excessive tool wear. Indeed, most limitations and drawbacks to hard machining relate to the high rates of tool wear, e.g., tooling cost per unit is significantly higher than in grinding, the surface finish of machined parts can deteriorate even within tool life [4], and “white layer” formation is prominent [6, 7].

Under extreme tribological conditions, cutting tools must simultaneously withstand high temperatures, easily above 700 °C and even 1000 °C in some cases, and heavy mechanical stress, around 1-3 GPa [4, 8, 9]. Cutting tools for hard turning typically

employ negative rake angles to ensure adequate strength at the tool tip; although this adversely intensifies the sticking zone and heat generation. Similarly, relatively light feed rates and depths of cut are employed to prevent immediate fracture of the cutting edge. Of the range of cutting tool materials available, ceramics (based on alumina (Al2O3) or silicon nitride (Si3N4)) and polycrystalline cubic boron nitride (PcBN) are most widely used for hard and high-speed machining in industry [4, 10]. Compared to alumina ceramic inserts, PcBN inserts cost more and are primarily used in finish hard turning [11, 12]. Although pure alumina possesses relatively low thermal shock resistance and toughness [13], improvement in its physical properties can be realized by additives such as ZrO2, SiC, TiC and TiCN [14, 15].

Tribofilms are dynamic structures, forming as a result of self-adaptive behaviour at the frictional interface, which favourably alter or benefit the friction and wear process, particularly under heavy loaded and high temperature conditions [16]. Various tribofilms formed by tool surface modification with further tribo-oxidation in cutting process have been found to date: Franz et al. reviewed vanadium containing self-adaptive hard coatings for high-temperature applications and Fox-Rabinovich et al. investigated hierarchical adaptive nanostructured PVD coatings for extreme tribological applications [17]. Recently, the generation of tribofilms due to workpiece material transfer during tool/chip interaction was reported [18].

Most previous studies on the formation of tribofilms were focused on medium hardness workpiece materials, such as hot work tool steel AISI H13 (50-53HRC) [19-21], cold work steel AISI D2 (52HRC) [22] and high speed steel (HSS) AISI T15 (52HRC) [23]. However, very few studies have discussed tribofilms formation during machining of harder materials (57 HRC and above).

When using small depth of cut and feed rate, the material removal rate (MRR) is so small that ploughing may dominate over cutting and result in unpredictable surface quality and tool wear. Additionally, the low MRR is not practical for industry, which is also the potential problem in Shalaby's paper (DOC = 0.06 mm and f = 0.05 mm/rev) [22]. Cutting under more aggressive conditions is possible, as demonstrated by Arsecularatne [24], who investigated variations of cutting speed and feed rate in turning hardened AISI D2 steel of 62 HRC with PCBN tools. Combinations of cutting speed ranging from 70–120 m/min and feed rate in the range of 0.08–0.20 mm/rev were all found to be feasible.

2.2 Experimental Work

2.2.1 Workpiece material

AISI T1 high tungsten HSS and AISI D2 high chromium cold work tool steel were selected as workpiece materials and hardened to 59.0 HRC and 58.7 HRC separately.

The chemical composition of both steels is shown in Table 2.1, while the heat treatments applied to each of the annealed workpieces is presented in Table 2.2. Figure 2.1 shows the microstructure of both workpiece materials after heat treatment. Compared to T1, the D2 workpiece is seen to feature less of the carbide phase, in agreement with [25], which is present in smaller and more evenly distributed particles.

Table 2.1 Chemical composition of workpiece materials.

wt%	C	Si	Mn	S	P	Ni+Cu	Cr	Mo	V	W	N
T1	0.74	0.37	0.25	0.001	0.03	0	4.1	0	1.03	18.1	0
D2	1.52	0.32	0.28	0.001	0.026	0.3	11.54	0.73	0.58	0	0

Table 2.2 Heat treatment processes applied to workpiece materials.

	Austenitization temperature/℃	Tempering temperature/℃	Hardness/HRC
T1 HSS	1250-1260	560-570, twice	59.0(±0.5)
D2 tool steel	1000–1040	430-450, twice	58.7(±0.5)

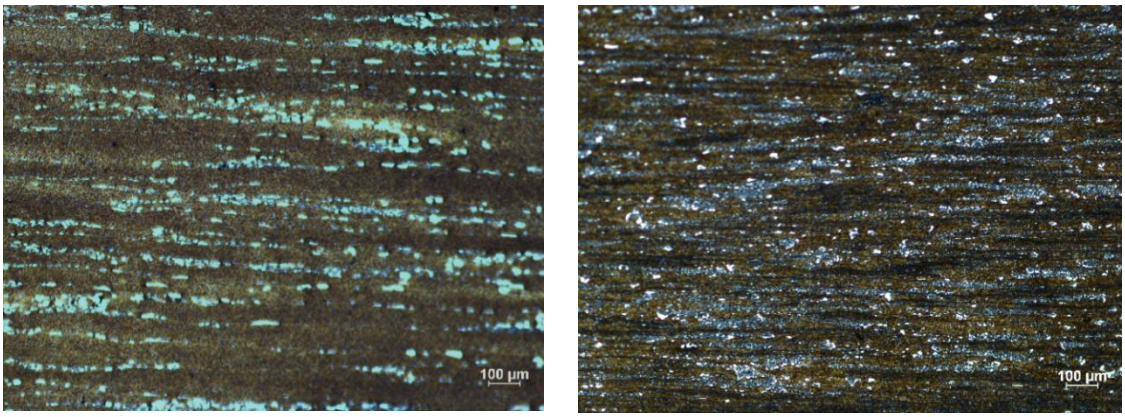

(a) (b)

Figure 2.1 Metallography of hardened workpiece materials: (a) AISI T1, (b) AISI D2.

2.2.2 Cutting tool and turning tests

Turning tests were performed using Sumitomo CNGA432NB90S (Al2O3+TiN) mixed alumina inserts held in a Kennaclamp DCLNL166DKC4 tool holder (Table 2.3 for details). All tests were conducted under a constant cutting speed V = 100 m/min, feed rate f = 0.075 mm/rev and depth of cut DOC = 0.10 mm, without coolant. Prior to each cutting pass, the workpiece was pre-machined using a separate insert at a lower cutting speed (V = 30 m/min) and higher depth of cut (DOC = 1 mm) to remove any work hardened layer from the previous pass.

Tool life tests were carried out on an Okuma Crown L1060 CNC lathe, removing the inserts after each pass for inspection of flank wear land width (Vb) using a Mitutoyo TM microscope. Chips were collected after the first few passes, and tool life was quantified as the accumulated length of cut upon reaching Vb = 300 µm.

Cutting force measurements were acquired for three successive passes, with intermittent cleaning passes as described above, on a Nakamura-Tome SC-450 CNC lathe with a Kistler 9121 tool dynamometer.

Table 2.3 Material properties and geometry of the cutting inserts and tool holder.

Inserts material	Chemical compositions	Hardness	Nose Radius	Tool holder
Mixed Alumina	70%Al2O3+30%TiC	2000 HV	0.313 inch	rake angel -5°; clearance angle 0°; setting angel 95°

2.2.3 Characterization

A JEOL-6610 scanning electron microscope (SEM) was used to study the wear mechanism and morphology of the worn cutting inserts.

The rake surface of the worn cutting inserts were characterized by X-ray photoelectron spectroscopy (XPS) to reveal details about tribofilms formations. The XPS equipment consisted of a Physical Electronics (PHI) Quantera II spectrometer with a hemispherical energy analyzer, an Al anode source for X-ray generation, and a quartz crystal monochromatic for focusing the generated X-rays. The X-ray source was from a monochromatic Al K-α (1486.7eV) at 50W-15kV and the system base pressure was between 1.0x10-9 to 2.0x10-8 Torr. At the beginning, the samples were sputter-cleaned

for 5 minutes with a 4kV Ar+ beam before collecting the data. The beam diameter for data collection was 200 µm, and all spectra were obtained at a 45˚ take off angle. A dual beam charge compensation system was utilized to ensure neutralization of all samples. The pass energy to obtain all survey spectra was 280eV, while to collect all high resolution data it was 69eV. The instrument was calibrated with a freshly cleaned Ag reference foil, where the Ag 3d5/2 peak was set to 368eV. All data analysis was performed in PHI Multipak version 9.4.0.7 software.

Roughness measurements of the machined workpiece surfaces were taken from the beginning of the first cutting pass were obtained using a white light interferometer (Zygo NewView 5000).

2.2.4 Friction tests in tribometer

Friction tests were performed on a custom heavy-load, high-temperature tribometer in order to elucidate lubricating properties of tribofilms arising from the two grades of steel. The tests involve loading a ball-tipped pin, made of the tool material, against a flat disc of work material. The greater hardness of the pin generates considerable plastic strain in the disc, thereby forming a hemispherical imprint. After reaching the desired load, electric current is drawn through the pin-disc interface in order to heat the specimen contact zone. Finally, the disc is rotated about the axis of the pin, resulting in primarily adhesive interactions between the materials in isolation of

macroscopic ploughing. The applied load and the resulting frictional torque and imprint diameter are used to calculate a friction coefficient under the given load and temperature condition. Additional details about the tribometer can be found in Ning and Boyd's publication [26, 27]. Due to the requirement for electrical conductivity of the sample materials, TiAlN-coated tungsten carbide was used in the place of mixed alumina as the pin material, while discs were prepared from the bar stock of T1 and D2 steel used in the cutting tests. Testing occurred under an applied load of 1000 N (generating mean contact pressures on the order of 2.5-4 GPa) elevated temperatures in the range of about 550 – 900 °C.

2.3 Results and Discussion

2.3.1 Tool life and tool wear

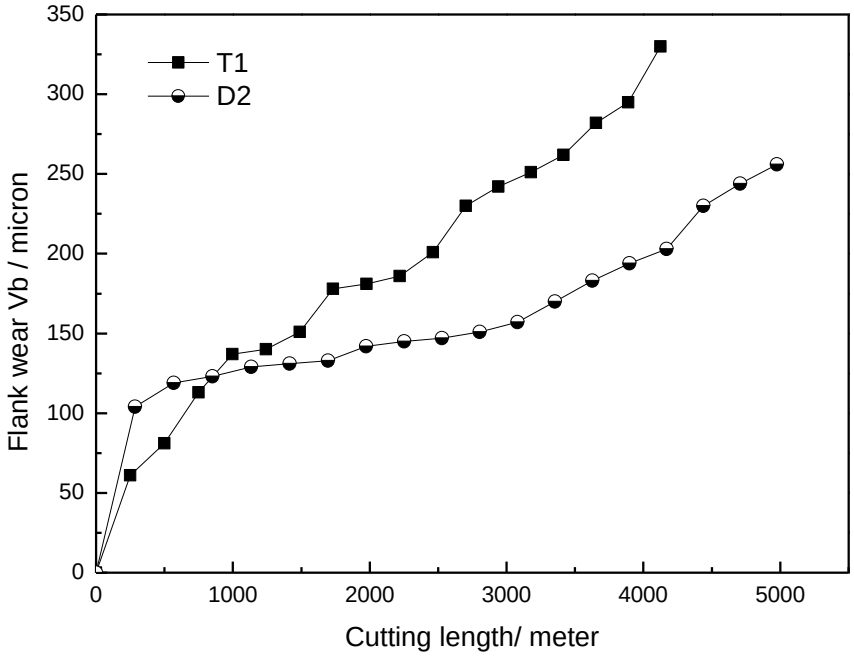

Figure 2.2 Flank wear land width versus cutting length during turning tests

Figure 2.2 presents the progression of flank wear land width, Vb, with cutting length in the hard turning of T1 and D2 steels. It should be noted that testing on D2 steel was stopped prior to Vb = 300 μm on account of catastrophic failure of the cutting edge that occurred during the last pass, attributed to chipping. Nonetheless, despite the equivalent hardness values of the two workpieces, the ceramic inserts exhibited longer tool life (by 23%) when dry turning D2 steel (4976 m) as compared to T1 steel (4124 m). From about 1000 m length of cut (i.e., post-running-in stage) until the end of tool life,

flank wear on the insert was distinguishably lower when cutting D2 steel, which would suggest generally higher quality machined surfaces for this material over T1 steel.

It is postulated that the improved tool life for the ceramic inserts when cutting D2 steel compared with T1 steel is due to 1) differences in the amount and size of carbide phases present in each workpiece material, and 2) differences in tribofilms generated on the tool friction surfaces in contact with each workpiece, due to their different alloying content.

Carbide phases within both workpiece materials will cause abrasive wear of the cutting inserts, manifesting in flank wear. The higher amount of carbide phase present in the T1 workpiece, as well as its generally larger particle size (Figure 2.1) would thus contribute to more intensive abrasive wear of the ceramic inserts during cutting than would the carbide phases in the D2 workpiece.

In conjunction, the differences in alloying content in each workpiece (Table 2.1) allow for different tribofilms with distinct protective properties to form at the friction surfaces between tool and workpiece. The nature of these tribofilms, in turn, can affect tool wear rates as well as cutting forces and machined surface integrity. However, the formation of these tribofilms necessitates mass transfer of workpiece material to the tool surface (i.e., adhesion) as a pre-requisite.

Repeat tests were performed under identical conditions in order to achieve a moderate level of cutting insert flank wear, stopping after a similar length of cut to allow for a more detailed inspection of the worn surfaces.

Figure 2.3 shows the cutting edge of the ceramic inserts after turning T1 for 3304 m (reaching Vb = 240 µm) and D2 for 3468 m (reaching Vb = 193 µm). Both inserts exhibited signs of abrasive wear on their flank face, which was more extensive for T1 turning. Crater wear, a crucial consideration in tool life assessment according to ISO standards [28], was also much more pronounced on the insert used to cut T1 steel. In contrast, more significant built-up edge was observed on the rake surface of the insert used to cut D2 steel, along with evidence of attrition or peeling away of the ceramic insert at the rear of the crater on the rake surface. No such attrition or peeling was observed on the insert used to cut T1 steel.

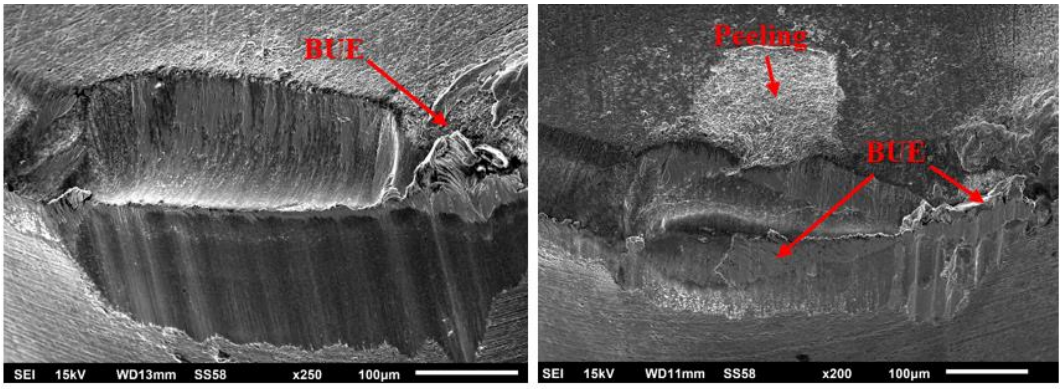

Figure 2.3 Worn rake and flank faces of ceramic insert after cutting (a) T1 steel to 3304 m, and (b) D2 steel to 3468 m.

2.3.2 Adaptive behaviour

Tribofilms formation during friction plays a significant role in the wear behaviour, especially in heavily loaded tribo-systems such as hardened metal machining processes [29, 30], and can offer protection to the underlying coating and substrate in two ways: (1) as a thermal barrier due to ultra-low thermal conductivity; and/or (2) as an in-situ lubricant, reducing the intensity of work material sticking [19].

The tribofilms formed on the worn rake surfaces of the inserts after cutting (to the same cutting length as described earlier in Figure 2.3) were characterized by XPS. In agreement with the predominant alloying elements listed in Table 2.1, survey spectra of insert that cut T1 showed significant tungsten (W) signal and some chromium (Cr), while spectra from the D2 insert showed only Cr signal.

High resolution spectra revealed different types of chemical bonds of W and Cr (Figure 2.4), in simple and complex oxide tribofilms, on the T1 and D2 inserts, respectively. These meta-stable phases have been observed on the worn surface of coated tools [31, 32], and uncoated tools [18] during different cutting processes. Photoelectron lines might be slightly shifted from the binding energy values of pure elements in various offsets (W-O in Figure 2.4 (a) and Cr2O3 in Figure 2.4 (b)), which indicates various degrees of oxidation with the formation of nonequilibrium phases and 'nonphase' clusters[32].

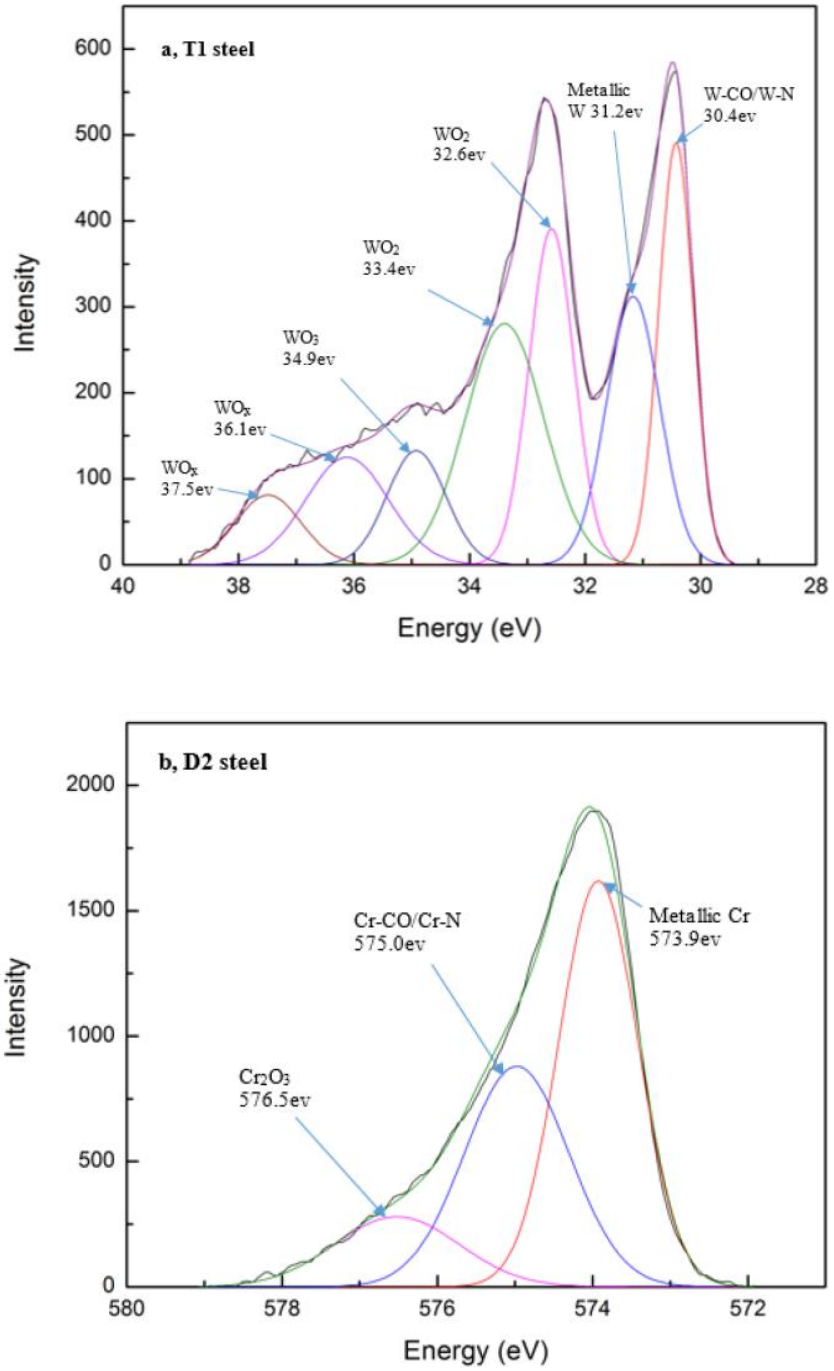

Figure 2.4 High-resolution XPS spectra from the worn rake surface of ceramic inserts after cutting (a) T1 steel, and (b) D2 steel

W-O based tribofilms have been demonstrated to improve the wear behavior during cutting processes; the W-O carries energy dissipating properties [30] and WO3 is a high-temperature lubricant [33], due to its low shear strength [21]. A variety of Cr-O oxides have been previously reported as providing a lubricious function at friction surfaces [34].

According to the high-resolution data of Figure 2.4, acquired from the inserts during the stable-stage of wear, W-O tribofilms constituted 65% of the W signal present on the rake surface of the T1 insert, while Cr-O tribofilms comprised just shy of 15% of the total Cr signal on the D2 insert. In addition, the proportion of tungsten in T1 (18.1%) is higher than the proportion of chromium in D2 (11.54%). This would suggest that more intensive lubricant and energy dissipating W-O tribofilms form on the tool during dry cutting of hardened T1 than do Cr-O tribofilms in dry cutting of hardened D2. As was shown in Figure 2.2, the T1 insert exhibited a lower initial wear rate than did the D2 insert, which is attributed to intensive formation of W-O tribofilms, which is not possible when cutting D2. The energy dissipating qualities of W-O would decrease the micro damage of tool surface while its lubricious aspects would lessen the seizure between tool and workpiece material, as reflected in the noticeably lesser build-up of material on the insert used to cut T1 as compared to D2 (Figure 2.3). Nonetheless, for the majority of the cutting length (beyond roughly 1000 m of cut), the D2 insert exhibited lower flank wear and demonstrated longer tool life than the T1 insert. This is attributed to lower

amount of carbide phase, as well as its smaller size and more even distribution within the steel matrix. In the long run, the damage to the tool surface due to aggressive abrasive action of the more plentiful and larger-sized carbide phase in the T1 workpiece would accumulate and result in shorter tool life.

2.3.3 Cutting performance during early stages of tool wear

Table 2.4 presents the average (R_a) and peak-to-valley (PV) roughness values of obtained from the surface of each work material at the far end of the bar stock, where the tool first engages the workpiece, after machining with an unworn insert. Machining of T1 steel resulted in much lower surface roughness than did machining of D2 steel (50% lower R_a, 35% lower PV). Cutting force measurements obtained during the first pass (approximately 150 m length of cut) with unworn inserts were also consistently lower in feed and tangential directions when cutting T1 steel (Figure 2.5). Chips collected from these trials were of a golden brown and bluish colour, corresponding to tool-chip interfacial temperatures of roughly 850-950 °C [26]. As shown in Figure 2.6, heavy-load, high-temperature tribometer tests demonstrated nearly identical coefficient of friction (COF) for TiAlN-coated carbide against both materials at 550-600 °C (COF = 0.22-0.23); however, between 800-900 °C friction had dropped considerably for T1 steel (COF = 0.16-018) but remained the same for D2 steel. The combination of lower surface roughness and lower cutting forces when machining T1 steel with an unworn insert

suggests the formation of lubricating tribofilms on the cutting insert friction surfaces, arising from the work material, which is corroborated by the drop in friction coefficient and generally lower friction seen in tribometer results for T1 steel in the expected temperature range at the tool-chip interface.

Table 2.4 Roughness measurements of workpiece surfaces machined with unworn inserts

Workpiece Material	Surface Roughness	
	Ra (μm)	PV (μm)
T1	0.40±0.01	3.23±0.18
D2	0.79±0.01	4.92±0.38

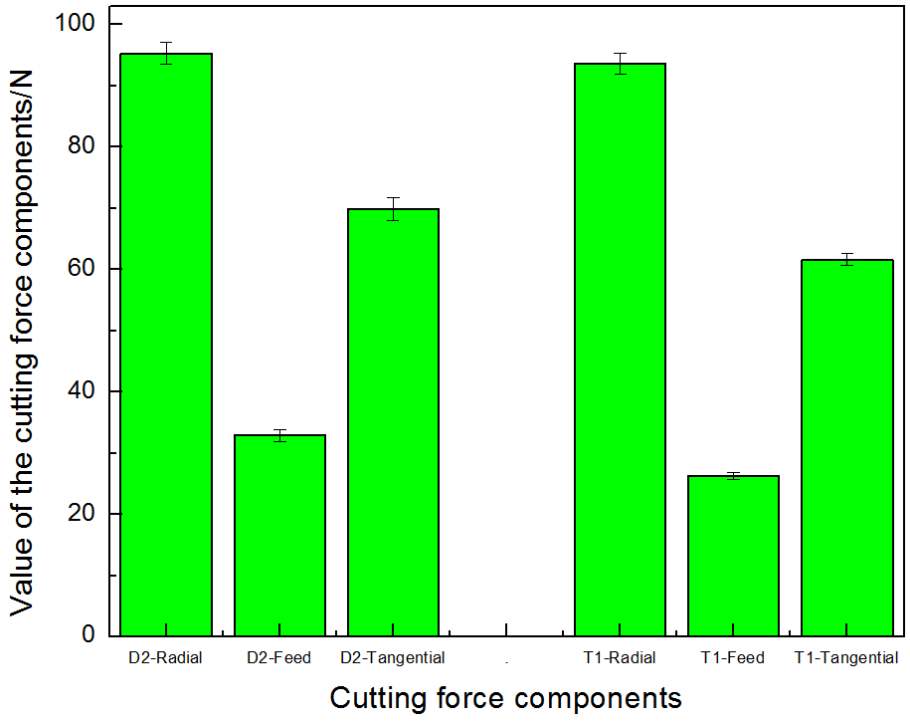

Figure 2.5 Cutting force measurements during the first machining pass with unworn inserts

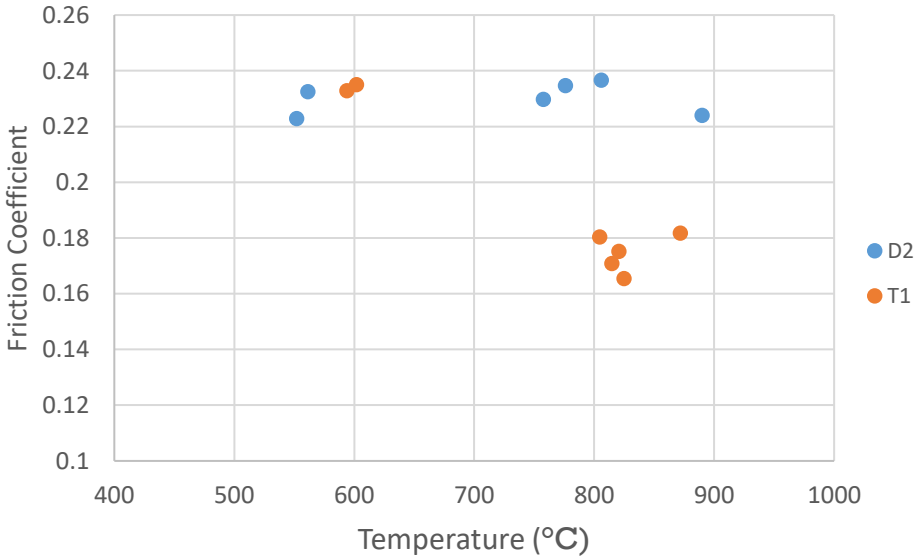

Figure 2.6 Measured friction coefficient of individual tribometer tests between TiAlN-coated carbide pins against discs of T1 and D2 steel, under 1000 N load and various elevated temperatures

2.4 Conclusion

Hard, dry turning of AISI T1 and AISI D2 steels, of comparable hardness, with uncoated mixed alumina ceramic tools was studied under identical cutting conditions. Metallography of workpiece steels, wear mechanisms of the tool inserts and tribofilms formed on the tools were studied with optical microscope, SEM/EDX and X-ray photoelectron spectroscopy. Abrasive wear dominated in both hard turning processes, but tool life was 23% higher in turning of AISI D2 as compared to T1.

Metallographic studies showed AISI D2 steel feature less of the carbide phase, which is smaller and more evenly distributed compared to AISI T1 steel. XPS analysis was used to detect the variety of tribofilms formed during cutting; a variety of lubricious Cr-O tribofilms was shown in turning of D2 while energy dissipating W-O and lubricious WO3 were presented in turning of T1. The tribological properties of these two tribofilms were assessed on a heavy-load, high-temperature tribometer with similar conditions to hard turning. The friction coefficient in the tribometer tests agreed well with the analysis from hard turning, with a noticeably lower friction for the T1 steel than D2 in the range of 800-900 °C.

Conventionally, the carbide phase has been the only determining factor for wear conditions and tool life in turning of similar hardness steels. This study presented a new, nano-scale perspective to help explain the observed results: Besides the amount

and distribution of carbide phase in the workpiece material, tribofilms generation on friction surface of the tool insert is also playing a significant role in determining the tribological conditions and tool life.

Acknowledgement

Authors gratefully acknowledge funding support from the NSERC discovery grant program.

References

[1] G. Byrne, D. Dornfeld, B. Denkena, Advancing cutting technology, CIRP Annals-Manufacturing Technology, 52 (2003) 483-507.

[2] P. Sreejith, B. Ngoi, Dry machining: machining of the future, Journal of Materials Processing Technology, 101 (2000) 287-291.

[3] D. Dudzinski, A. Devillez, A. Moufki, D. Larrouquère, V. Zerrouki, J. Vigneau, A review of developments towards dry and high speed machining of Inconel 718 alloy, International Journal of Machine Tools and Manufacture, 44 (2004) 439-456.

[4] J.P. Davim, Machining of hard materials, Springer2011.

[5] F. Hashimoto, Y. Guo, A. Warren, Surface integrity difference between hard turned and ground surfaces and its impact on fatigue life, CIRP Annals-Manufacturing Technology, 55 (2006) 81-84.

[6] Y.K. Chou, C.J. Evans, White layers and thermal modeling of hard turned surfaces, International Journal of Machine Tools and Manufacture, 39 (1999) 1863-1881.

[7] Y. Matsumoto, F. Hashimoto, G. Lahoti, Surface integrity generated by precision hard turning, CIRP Annals-Manufacturing Technology, 48 (1999) 59-62.

[8] E. Ezugwu, J. Bonney, Y. Yamane, An overview of the machinability of aeroengine alloys, Journal of Materials Processing Technology, 134 (2003) 233-253.

[9] C. Claudin, J. Rech, W. Grzesik, S. Zalisz, Characterization of the frictional properties of various coatings at the tool/chip/workpiece interfaces in dry machining of AISI 4140 steel, International Journal of Material Forming, 1 (2008) 511-514.

[10] E.M. Trent, P.K. Wright, Metal cutting, Butterworth-Heinemann2000.

[11] C. Lahiff, S. Gordon, P. Phelan, PCBN tool wear modes and mechanisms in finish hard turning, Robotics and Computer-Integrated Manufacturing, 23 (2007) 638-644.

[12] J. Barry, G. Byrne, Cutting tool wear in the machining of hardened steels: part II: cubic boron nitride cutting tool wear, Wear, 247 (2001) 152-160.

[13] N. Richards, D. Aspinwall, Use of ceramic tools for machining nickel based alloys, International Journal of Machine Tools and Manufacture, 29 (1989) 575-588.

[14]J. Barry, G. Byrne, Cutting tool wear in the machining of hardened steels: Part I: Alumina/TiC cutting tool wear, Wear, 247 (2001) 139-151.

[15] E. Ayas, A. Kara, Pressureless Sintering of Al2O3-TiCN Composites, Key Engineering Materials, 264 (2004) 849-852.

[16] G. Fox-Rabinovich, G.E. Totten, Self-organization During Friction: Advanced Surface-engineered Materials and Systems Design, CRC Press2010.

[17] G.S. Fox-Rabinovich, K. Yamamoto, B. D Beake, I. S Gershman, A. I Kovalev, S. C Veldhuis, M. H Aguirre, G. Dosbaeva, J. L Endrino, Hierarchical adaptive nanostructured PVD coatings for extreme tribological applications: the quest for nonequilibrium states and emergent behavior, Science and Technology of Advanced Materials, 13 (2012) 043001.

[18] G.S. Fox-Rabinovich, I. Gershman, M.A.E. Hakim, M.A. Shalaby, J.E. Krzanowski, S.C. Veldhuis, Tribofilm Formation As a Result of Complex Interaction at the Tool/Chip Interface during Cutting, Lubricants, 2 (2014) 113-123.

[19] G.S. Fox-Rabinovich, K. Yamamoto, B.D. Beake, I.S. Gershman, A.I. Kovalev, S.C. Veldhuis, M.H. Aguirre, G. Dosbaeva, J.L. Endrino, Hierarchical adaptive nanostructured PVD coatings for extreme tribological applications: the quest for nonequilibrium states and emergent behavior, Science and Technology of Advanced Materials, 13 (2012) 043001.

[20] G.S. Fox-Rabinovich, K. Yamomoto, S.C. Veldhuis, A.I. Kovalev, G.K. Dosbaeva, Tribological adaptability of TiAlCrN PVD coatings under high performance dry machining conditions, Surface and Coatings Technology, 200 (2005) 1804-1813.

[21] G.S. Fox-Rabinovich, K. Yamamoto, S.C. Veldhuis, A.I. Kovalev, L.S. Shuster, L. Ning, Self-adaptive wear behavior of nano-multilayered TiAlCrN/WN coatings under severe machining conditions, Surface and Coatings Technology, 201 (2006) 1852-1860.

[22] M. Shalaby, M. El Hakim, M.M. Abdelhameed, J. Krzanowski, S. Veldhuis, G. Dosbaeva, Wear mechanisms of several cutting tool materials in hard turning of high carbon–chromium tool steel, Tribology International, 70 (2014) 148-154.

[23] M. El Hakim, M. Abad, M. Abdelhameed, M. Shalaby, S. Veldhuis, Wear behavior of some cutting tool materials in hard turning of HSS, Tribology International, 44 (2011) 1174-1181.

[24] J. Arsecularatne, L. Zhang, C. Montross, P. Mathew, On machining of hardened AISI D2 steel with PCBN tools, Journal of Materials Processing Technology, 171 (2006) 244-252.

[25] Y. Geller, Moscow, Mashinostroenie, DOI (1979) 353.

[26] Y. Ning, M. Rahman, Y. Wong, Investigation of chip formation in high speed end milling, Journal of Materials Processing Technology, 113 (2001) 360-367.

[27] K.H. J. M. Boyd, S. C. Veldhuis & E. Ng., Improved prediction of cutting forces via finite element simulations using novel heavy-load, high-temperature tribometer friction data., The International Journal of Advanced Manufacturing Technology, DOI (2016).

[28] A.N.S. Institute, Tool Life Testing with Single-point Turning Tools, American Society of Mechanical Engineers1986.

[29] S. Jacobson, S. Hogmark, Tribofilms—on the crucial importance of tribologically induced surface modifications, Recent developments in wear prevention, friction and lubrication, 661 (2010) 197-225.

[30] K.-D. Bouzakis, N. Michailidis, G. Skordaris, E. Bouzakis, D. Biermann, R. M'Saoubi, Cutting with coated tools: Coating technologies, characterization methods and performance optimization, CIRP Annals-Manufacturing Technology, 61 (2012) 703-723.

[31] J.-M. Lehn, Toward self-organization and complex matter, Science, 295 (2002) 2400-2403.

[32] G. Fox-Rabinovich, A. Kovalev, S. Veldhuis, K. Yamamoto, J. Endrino, I. Gershman, A. Rashkovskiy, M. Aguirre, D. Wainstein, Spatio-temporal behaviour of atomic-scale tribo-ceramic films in adaptive surface engineered nano-materials, Scientific reports, 5 (2015).

[33] A. Kovalev, D. Wainstein, G. Fox‐Rabinovich, S. Veldhuis, K. Yamamoto, Features of self‐organization in nanostructuring PVD coatings on a base of polyvalent metal nitrides under severe tribological conditions, Surface and Interface Analysis, 40 (2008) 881-884.

[34] G. Fox-Rabinovich, A. Kovalev, M. Aguirre, K. Yamamoto, S. Veldhuis, I. Gershman, A. Rashkovskiy, J. Endrino, B. Beake, G. Dosbaeva, Evolution of self-organization in nano-structured PVD coatings under extreme tribological conditions, Applied Surface Science, 297 (2014) 22-32.

Chapter 3

Study of Tribofilms Generation at Different Cutting Speeds in Dry Machining Hardened AISI T1 and AISI D2 Steel

Complete citation:

Junfeng Yuan, Julia Dosbaeva, Danielle Covelli, Jeremy Boyd, German S. Fox-Rabinovich, Stephen C. Veldhuis, "Study of tribofilms generation at different cutting speeds in dry machining hardened AISI T1 and AISI D2 steel", accepted by Proceedings of the Institution of Mechanical Engineers, Part J: Journal of Engineering Tribology, 2017.

Copyright:

Relative Contributions:

Junfeng Yuan:	Designed and performed all experiments, interpretation and analysis of the data and wrote the manuscript including preparation of all figures and text.
Julia Dosbaeva:	Assisted in cutting experiments and SEM analysis.
Danielle Covelli:	Performed XPS analyses and assigned peaks.
Jeremy M. Boyd:	Assisted with cutting experiments and reviewed the writing.
G. S. Fox-Rabinovich:	Offered help with design of experiments and provided suggestions for experiments and writing.
Stephen C. Veldhuis:	Provided thesis supervisor for the experiments and was responsible for the final draft submitted to the journal.

Preface:

This chapter studied two major factors affecting tool life, 1) tribofilms formation; 2) distribution and size of carbide phases. The purpose of this chapter was to assess the influence of these two factors on tool life under a changing speed condition when machining T1 and D2. The carbides phases have less of an impact on tool life

under changing speed conditions. This was done to stress the influence of tribofilms formation on tool life. A further consideration in this chapter was to choose a suitable material to study the control of tribofilms formation during a machining process, in order to obtain longer tool life, elevated machined surface as well as higher material removal rate.

The largest difference between cutting T1 and D2 was the wear rate decrease when machining D2 steel. Carbide phases in D2 were smaller so the tool experienced increased levels of wear compared to when machining T1. This makes D2 a better choice for die/mold tool steel. However, it would also accumulate more damage in the cutting tool which would lead to a higher wear rate in the beginning and an early failure with massive peeling even with protective tribofilms present.

Study of tribofilms generation at different cutting speeds in dry machining hardened AISI T1 and AISI D2 steel

Junfeng Yuan, Julia Dosbaeva, Danielle Covelli, Jeremy Boyd, German S. Fox-Rabinovich, Stephen C. Veldhuis

Department of Mechanical Engineering (JHE 310), McMaster University

1280 Main St., W. Hamilton, ON, Canada L8S 4L7

Abstract

Hard dry machining of AISI T1 and AISI D2 steels at comparable hardness (around 59 HRC) were performed at 50 m/min, 80 m/min and 100 m/min cutting speeds separately with uncoated alumina ceramic tool inserts (Al_2O_3+TiC), in order to study the effect of cutting conditions on the generation of tribofilms. Comprehensive assessment of uncoated ceramic inserts in machining of T1 and D2 at different cutting speeds was made by optical microscope, Scanning Electron Microscope and X-ray Photoelectron Spectroscopy. It was shown that higher cutting speeds increased the formation of thermal protective and/or lubricating tribofilms. In machining D2 steel, more intensive

formation of Cr-O tribo-oxides brought a lower wear rate; while in cutting T1 steel, a higher amount of W-O tribofilms generation provided better lubrication. At higher cutting speeds, wear/friction behaviour changes were attributed to differences in two factors: first, from a traditional micro-scale standpoint, the distribution of carbide within steels and the accumulation of thermal and mechanical damages during different cutting conditions; second, from a new nano-scale viewpoint, the generation of protective/lubricating tribofilms due to change of machining conditions.

Key words:

Tribofilms, Dry machining, Tool wear, X-ray photoelectron spectroscopy, Hardened steel

3.1 Introduction

Since the 1980s, many mechanical components such as bearings, gears, cams, shafts, axles, etc, have been produced by means of a hard turning process. In recent years, dry or near dry machining has become a preferred option by an increasing number of industries [1]. This is generally because the cost of cutting fluids and their management are significant representing in some cases fourfold of the cost of the

consumable tooling used. Wet machining also trigger environment and health concerns related to cutting fluids disposal and handling [2]. In addition, thermal cracking problems of cutting tools caused by intermittent engaged cutting fluids during machining --- the tool passes from heating during cutting then rapid cooling from exposure to the coolant flow --- can be resolved through dry machining [3]. As such, the concept of dry machining has been applied to hard materials and has started to replace grinding in order to reduce machining costs and improve surface integrity [4, 5].

However, dry high speed machining of hard materials introduces extreme tribological conditions involving high temperatures and heavy mechanical loads [4, 6, 7]. Without coolant, chips are not easily flushed out of the cutting zone especially when machining sticky materials or in deep hole drilling. As well, heat build-up in the tool is more severe. With increased heat and little lubrication, considerable physical and thermal stress is placed on the tool's cutting edge, which generates harsh tribological conditions at the tool-chip interface and excessive tool wear [8, 9].

Among available cutting tool materials, mixed ceramic (comprising TiC and either Al_2O_3 or Si_3N_4) and polycrystalline cubic boron nitride (PcBN) have been widely used in machining of hardened steels, especially for dry conditions and relative high cutting speeds [10]. Compared to PcBN inserts, ceramic inserts are less expensive and widely used in hard turning [11, 12].

Thermally protective hard coating are widely applied to cemented carbide and high speed steel (HSS) cutting tools for dry machining applications. In high speed cutting of hardened steels, however, traditional hard, thermal-barrier coatings applied to ceramic tools performed even worse than uncoated tools [13]. Alternatively, there are soft/non-stick coatings which have been designed for dry machining with the aim of increasing in-situ lubrication and reducing built-up edge formation; however, these soft coatings are unable to withstand the severe tribological conditions imposed by dry hard machining.

Tribofilms are well-known to play an important role in the friction and wear process in general, and have been shown to be generated during machining and influence machining. Tribofilms are dynamic structures generated due to self-adaptive behaviour at the frictional interface, particularly under heavy load and high temperature conditions [14]. In extreme tribological conditions, the features of tribofilms ensuring higher tool life can be outlined as follows: lubricant tribofilms reduce sticking intensity of the chip to the tool, especially for dry cutting conditions, and help minimize or eliminate built-up edge; while protective tribofilms function as a thermal barrier and reduce chemical/oxidative wear during machining [14]. Basically, there are two sources for tribofilms formation: cutting tool surface modification and workpiece material transfer. Surface modification to form tribofilms has been studied extensively in the literature. Fox-Rabinovich [15] reviewed various self-adaptive PVD coatings and Franz [16]

investigated adaptive vanadium coatings, both for high temperature/ high load tribological applications. Tribofilms formation from workpiece material at the tool/chip interface during the machining process has also been reported recently [17-19].

The cutting conditions, such as cutting speed and lubricating condition, also affect tribofilms formation greatly during machining. The authors previously studied the impact of cutting speeds on tribofilms formation on adaptive PVD coated inserts in turning DA718 [20]. Little study showed that the influence of cutting speeds to generation of tribofilms in machining hardened steels. W Grzesik [10] studied the influence of surface roughness on tool wear during hard turning, using various geometries of ceramic tools. The workpiece was hardened AISI5140 (60HRC) and the tool material was a mixed alumina containing Al_2O_3 and TiC. The material was machined under dry conditions with the cutting speed ranging from 90 to 120 m/min. Tugrul Ozel [21] investigated the effects of wiper ceramic inserts on surface finish and tool flank wear in turning of hardened AISI D2 steel. The cutting parameters were organized as follows: cutting speed of 80, 115 and 150 m/min, feed rate of 0.05–0.10 and 0.15 mm/rev and depth of cut of 0.2 mm. V.N. Gaitonde [22] investigated machinability of hardened AISI D2 cold work tool steel with conventional and wiper ceramic inserts. The average hardness of D2 was 59/61 HRC and the chemical composition of the ceramic tool was 70% Al_2O_3 and 30% TiC. The cutting speed and feed were selected to be 80m/min and 0.10 mm/rev respectively.

Negative rake angles are applied for cutting inserts in this application to obtain adequate strength at the tool tip, however the sticking zone and heat generation are intensified. Meanwhile, feed rate and depth of cut were selected to be relatively light to eliminate the immediate fracture of tool inserts. Combinations of cutting speed ranging from 70–120 m/min with a small feed rate and depth of cut were all found to be feasible in machining hardened steels [23]. The present study investigates the influence of cutting speed on tribofilms formation in dry machining of different hardened steels.

3.2 Experimental work

3.2.1 Workpiece material

AISI T1 is a high tungsten high speed steel (HSS), whereas AISI D2 is a high chromium cold worked tool steel. Both of them are the most commonly used steels in their own category of steels and were selected as workpiece material in this study. Table 3.1 shows the chemical composition of both steels as supplied. Both materials were sent out for manufacturer recommended heat treatment in order to increase hardness to the range of 58-60 HRC. T1 was subjected to austenization at 1250-1260℃, followed by quenching and two rounds of tempering at 560-570℃, resulting in a final hardness of 59.0 ± 0.5 HRC. D2 was subjected to austenization at 1000-1040℃, quenching and two rounds of tempering at 430-450℃, leading to a hardness of 58.7 ±0.5 HRC.

Table 3.1 Chemical composition of workpiece material

wt%	C	Si	Mn	S	P	Ni+Cu	Cr	Mo	V	W	N
T1	0.74	0.37	0.25	0.001	0.03	0	4.1	0	1.03	18.1	0
D2	1.52	0.32	0.28	0.001	0.026	0.3	11.54	0.73	0.58	0	0

Figure 3.1 presents the metallography of T1 and D2 steels after hardening. T1 steel features relatively larger sized carbide particles while D2 steel had much smaller and more evenly distributed carbide particles. As per Table 3.1, D2 steel contains higher carbon and both D2 and T1 have different amount of tungsten, chromium and other alloying elements, which elevating red hardness or hardenability, leading to the observed differences in metallography even with both samples having the same hardness [24, 25].

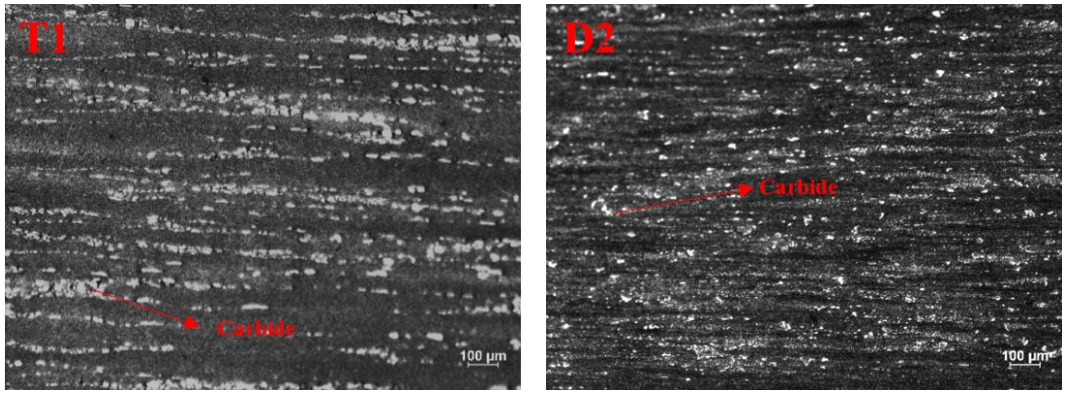

Figure 3.1 Metallography of hardened workpiece materials: (a) AISI T1, (b) AISI D2.

3.2.2 Cutting experiments

For both T1 and D2 steels separately, machining experiments were performed at three different cutting speeds: 50 m/min, 80 m/min and 100 m/min, which are herein

designated as S50, S80 and S100 respectively. These speeds fall within the typical range for machining steels of this hardness, save for 50 m/min which is slightly lower. All turning tests were performed on an Okuma Crown L1060 CNC lathe. Cutting inserts were removed after each pass for inspection of flank wear land width (Vb) using a Mitutoyo TM microscope. The tool life was quantified as the accumulated length of cut upon reaching Vb = 300 μm.

All tests were carried out in a dry cutting condition and under a constant feed rate f = 0.075 mm/rev and depth of cut DOC = 0.10 mm. All experiments were conducted with Sumitomo CNGA432NB90S (70% Al_2O_3+ 30% TiC) mixed alumina inserts held in a KenClamp DCLNL166DKC4 tool holder. The hardness of the inserts are 2000 HV and the nose radius is 0.313 inch. The rake angle, clearance angle and setting angle of the tool holder are -5, 0° and 95° respectively. Prior to each cutting pass, the workpiece was pre-machined using a separate insert at a relative lower cutting speed (V = 30 m/min) and higher depth of cut (DOC = 1 mm) to remove any possible work hardened layer from the previous pass.

3.2.3 Tool surface characterization

Wear mechanisms and morphology of the worn cutting inserts were assessed with the aid of a JEOL-6610 scanning electron microscope (SEM). To understand the nature of tribofilms forming at different cutting speeds, the rake surface of the worn

cutting inserts were characterized by X-ray photoelectron spectroscopy (XPS). The XPS equipment consisted of a Physical Electronics (PHI) Quantera II spectrometer with a hemispherical energy analyzer, an Al anode source for X-ray generation, and a quartz crystal monochromatic for focusing the generated X-rays. The X-ray source was from a monochromatic Al K-α (1486.7eV) at 50W-15kV and the system base pressure was between 1.0x10-9 to 2.0x10-8 Torr. At the beginning, the samples were sputter-cleaned for around 5 minutes with a 4kV Ar+ beam before collecting the data. The beam diameter for data collection was 50 μm, and all spectra were obtained at a 45˚ take off angle. A dual beam charge compensation system was utilized to ensure neutralization of all samples. The pass energy to obtain all survey spectra was 280eV, while to collect all high resolution data it was 69eV. The instrument was calibrated with a freshly cleaned Ag reference foil, where the Ag 3d5/2 peak was set to 368eV. All data analysis was performed in PHI Multipak version 9.4.0.7 software.

3.3 Results and Discussion

3.3.1 Cutting performance: Tool life and wear mechanism

Turning tests were applied to better understand the influence of cutting speed on tribofilms formation arising from work material transfer and how such formed tribofilms affect tool life. Figure 3.2 illustrates the progression of flank wear in dry turning of T1 and D2 steels with the ceramic tool as a function of cutting length at

different cutting speeds (S50, S80 and S100). Interestingly, tool life was shortest at the lowest cutting speed (S50) for both steels. Increasing cutting speed to S80 led to more than doubling of tool life, while further speed increases (S100) saw slight reductions in tool life. In the case of D2, testing was halted during the later stages of wear prior to Vb = 0.300 mm due to massive peeling/attrition of the rake surface.

It should be noticed that for D2 steel, the stable stage of the S100 wear curve begins at a noticeably lower level of flank wear than the S80 curve, suggesting the tool may have experienced better protection during the stable wear period of the S100 test. One possible reason for this may be the accelerated formation of protective tribofilms on the tool surface under the more aggressive cutting speed, which will be explored further in later sections.

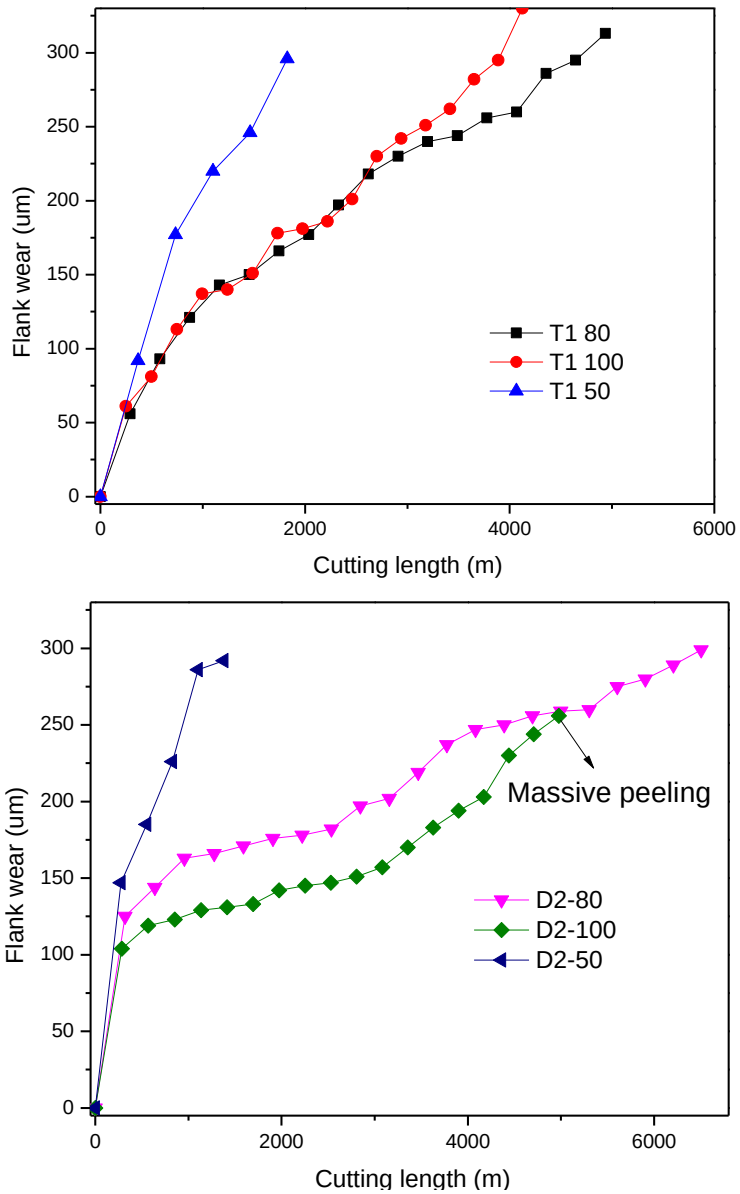

Figure 3.2 Wear curves in machining T1 (top) and D2 steel (bottom).

Figure 3.3 presents the SEM images of tool inserts after turning T1 for approximately 850 m length of cut at S50, S80 and S100. All three inserts exhibit wear on both flank and rake surfaces. Noticeably, the flank wear on the S50 insert is more extensive than on either of the S80 or S100 inserts. As well, the S50 insert features

regions of large fracture/pull out of tool material. In contrast, wear of the S80 and S100 inserts appears more regular with flank wear most likely due to abrasion and the rake wearing in part due to diffusion (manifesting in a crater).

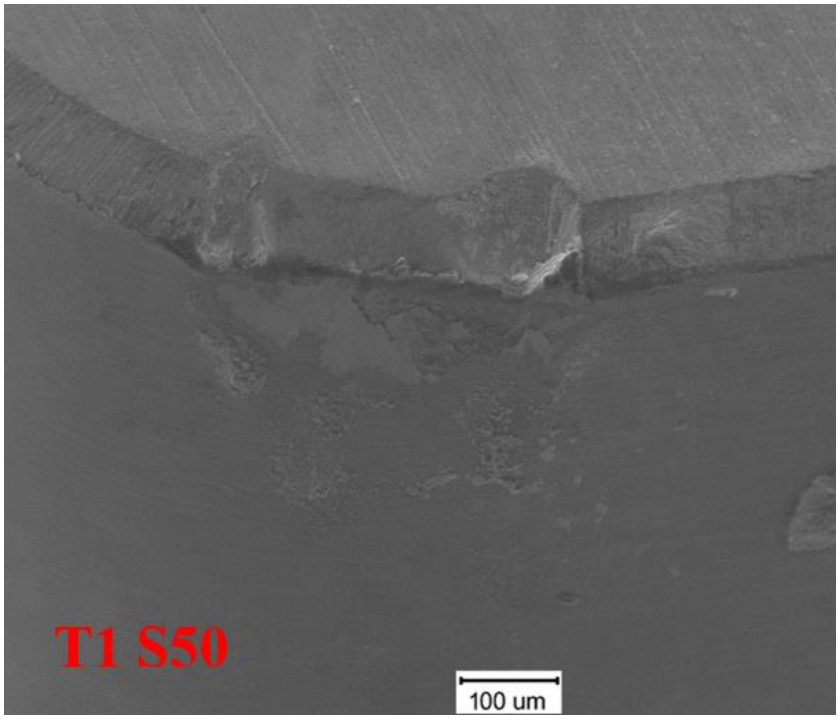
T1 S50
100 um

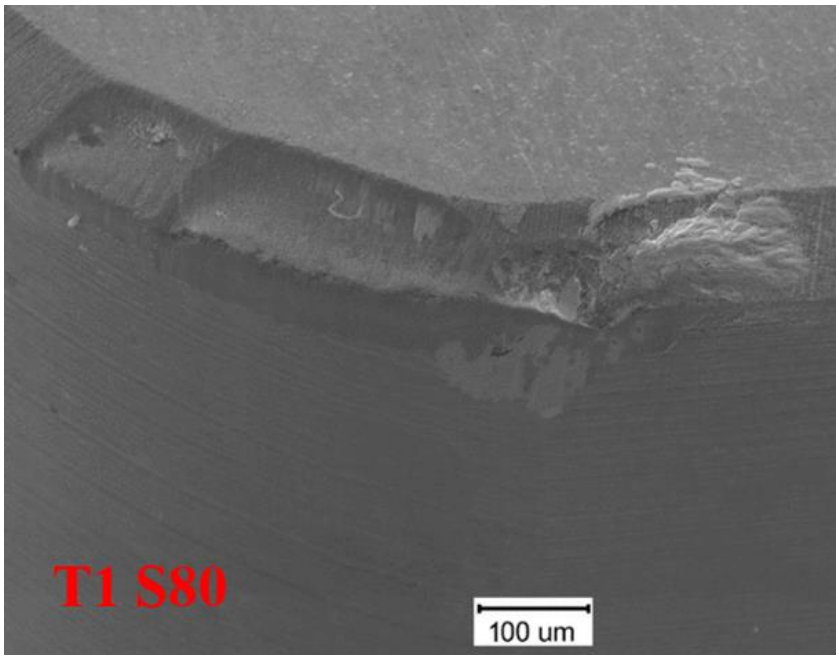
T1 S80
100 um

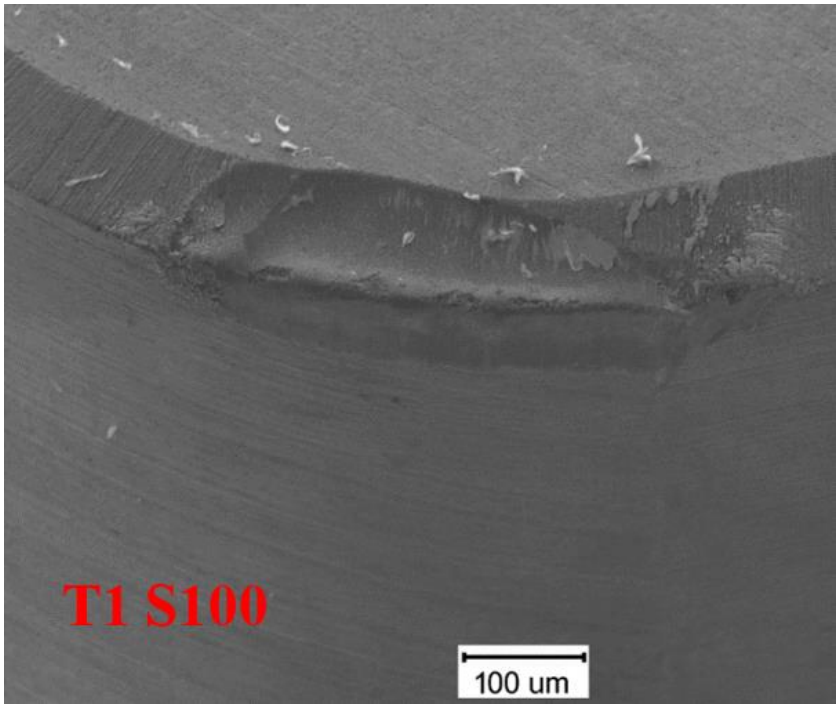

Figure 3.3 SEM of ceramic inserts in turning T1 steel at S50, S80 and S100

Figure 3.4 shows SEM images of ceramic tools after tuning D2 at the same three cutting speeds and up to the same approximate 850 m length of cut. Similar to machining T1, fractured areas were only observed on the S50 insert, on both flank and rake surfaces. At higher cutting speeds (S80 and S100), grooves were identified, showing evidence of abrasion wear on both flank and rake face; however, crater wear was much less pronounced.

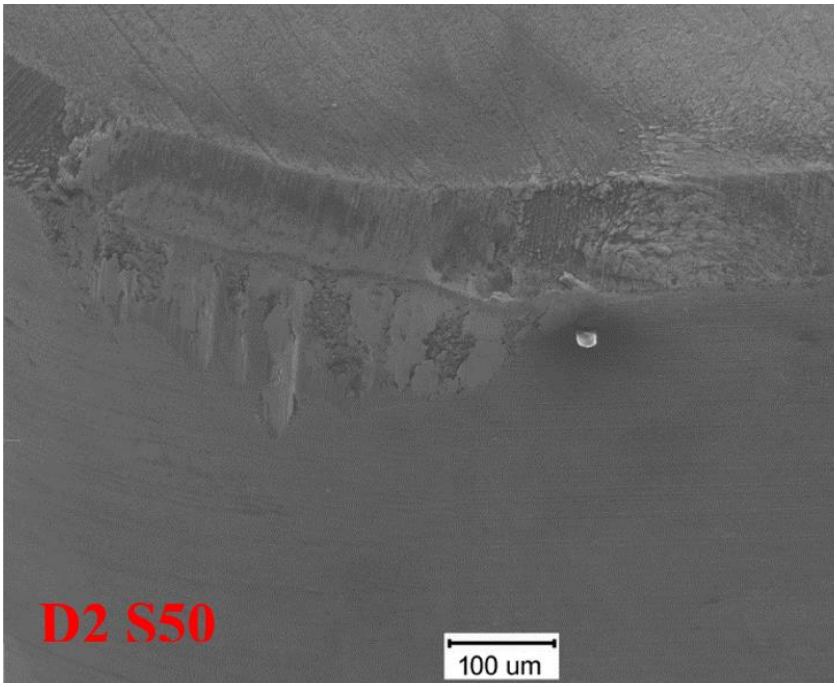
D2 S50
100 um

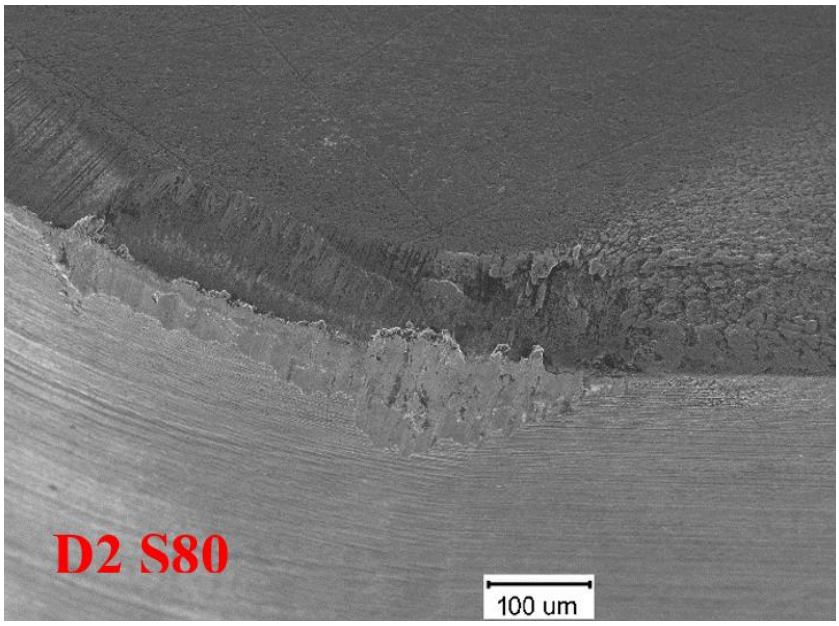
D2 S80
100 um

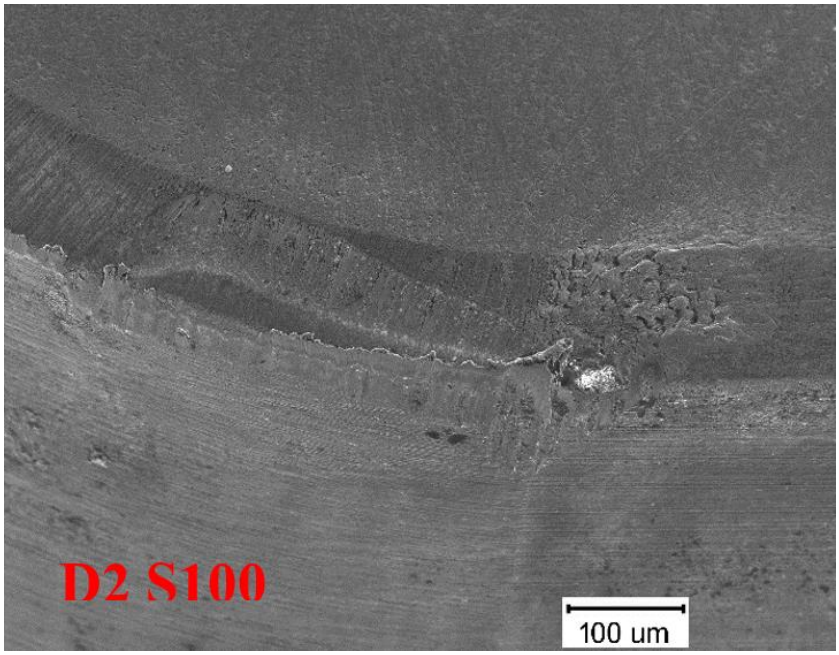

Figure 3.4 SEM of ceramic inserts in turning D2 steel at S50, S80 and S100

3.3.2 Adaptive behaviour

In machining of hardened material, which is a heavily loaded tribo-system, tribofilms formation plays an important role in friction and wear behaviour [26, 27]. Tribofilms are dynamic structures forming at the tool/chip or tool/workpiece interface and they can offer protection to the underlying coating and/or tool substrate. Tribofilms enhance the wear behavior of cutting tools in two ways: (1) working as a thermal barrier between the chip and cutting tool due to their lower thermal conductivity; and/or (2) acting as an in-situ lubricant to reduce the intensity of work material sticking [15].

Considering the wear mechanism , fractured areas were obseved in machining of both T1 and D2 at S50 and tool life was much worse compared to that of other cutting

speeds. But at S80 and S100, abrasive wear dominated the tool wear and tool life was elavated compared to S50. Therefore, 80m/min and 100m/min cutting speeds were used to study the adaptive behavior in machining of T1 and D2 steels. XPS data was used to characterize the tribofilms formed on the worn rake surfaces of the cutting inserts after 850 m of length of cut. In agreement with the predominant alloying elements listed in Table 3.1, the survey spectra of inserts used for machining T1 showed significant tungsten (W) signal, while spectra from the D2 insert was dominated by a chromium (Cr) signal at both cutting speeds. Different types of chemical bonds of tungsten and chromium from oxide tribofilms were revealed in high resolution spectra of XPS on the insert's surface after machining T1 and D2 steel at S80 and S100 respectively. In agreement with the predominant alloying elements listed in Table 3.1, survey spectra of the insert that was used to cut T1 at both cutting speeds showed a significant tungsten (W) signal, while spectra from the D2 insert at both cutting speeds were dominated by a Cr signal. Different types of chemical bonds of tungsten and chromium from oxide tribofilms were revealed in the high resolution spectra of XPS on the insert's surface after machining T1 and D2 steel at S80 and S100, respectively. Figure 3.5(a) shows the high resolution spectra XPS on inserts after cutting T1 at S80 and S100 while Figure 3.5(b) reveals them after cutting D2. In previous studies of different machining processes, similar meta-stable phases have been observed on the worn surface of coated tools [28, 29], and uncoated tools [17]. Various degrees of oxidation

with the formation of non-equilibrium phases and 'non-phase' clusters may occur within the tribo-oxides [29], and the same phenomena were observed in this study.

In Figure 3.5, various offsets of both W-O and Cr-O photoelectron lines were slightly shifted from the binding energy values of pure elements tungsten and chromium. In previous studies of tribofilms, both W-O based and Cr-O based tribofilms have been demonstrated to improve the wear behavior during the cutting processes. W-O tribo-oxides carry energy dissipating properties [27] and, due to its lower shear strength [30], WO_3 is a high-temperature lubricant [31]. Chromium has been reported as forming high-temperature stable oxides which would serve to enhance the formation of protective triboceramic films [15]. A variety of Cr-O oxides have also been previously revealed to provide a lubricious function at friction surfaces [14, 32].

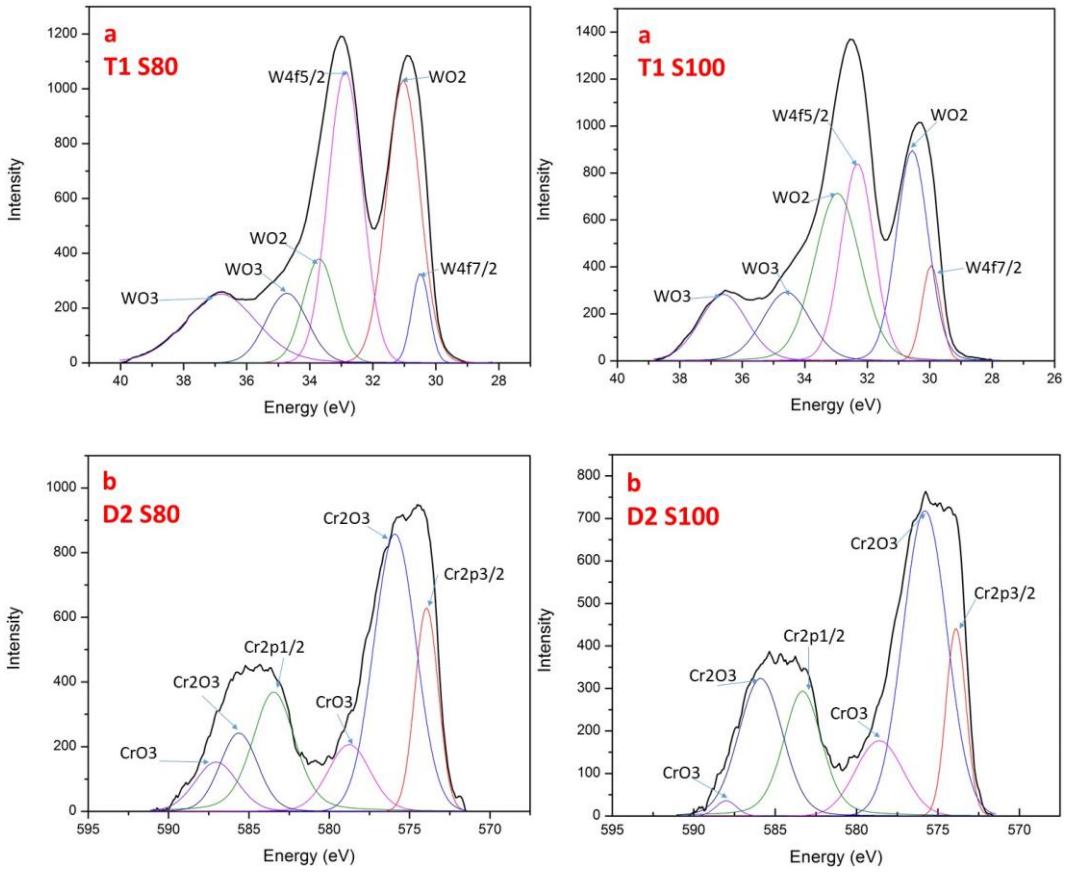

(a) W in cutting T1 steel, (b) Cr in cutting D2 steel

Figure 3.5 High resolution spectra on tool rake face after 900 meters cutting length

Table 3.2 and Table 3.3 presents the summarized data on the chemical composition of the tribo-oxides based on an XPS analysis performed after 900 m length of cut for T1 and D2, respectively. For both work materials, the relative amount of beneficial tribo-oxide relative to the pure metal (alloy) form is distinguishably greater at S100. Despite this, overall tool life was better at S80, although the initial wear rate in cutting D2 at S100 was lower than at S80.

Table 3.2 XPS on insert for T1 after 900m turning

T1	WO2	WO3	Total%
80m/min	49.1	11.5	60.6
100m/min	49.9	22.4	72.3

Table 3.3 XPS on insert for D2 after 900m turning

D2	Cr2O3	CrO3	Total%
80m/min	56.3	10.9	67.2
100m/min	60.2	11.9	72.1

3.3.3 Cutting temperature and friction at chip/tool interface

The relation between cutting temperature and chip color has been used in the past to estimate process temperature [33, 34], especially in machining of steel. In this study chips were collected after the first cutting pass performed with an unworn tool for both work materials and under both S80 and S100 cutting conditions. In this way, the influence of tool wear on cutting temperature was mitigated. Despite their differences in chemical composition, the color of chips resulting from both work materials were very similar for a given cutting speed. Chips exhibited a mixture of purple, blue and brown after machining at 100 m/min, corresponding to tool-chip interfacial temperatures of roughly 900-950°C. At 80 m/min, the resulting chips were predominantly light green and light brown in colour, corresponding to an approximate tool-chip interface temperature of 700-750°C[33, 34].

Figure 3.6 shows SEM images of the undersurface of chips resulting from the above tests performed using unworn inserts. In general, the undersurface of chips resulting from machining T1 is smoother than for D2, whether for S80 or S100 cutting conditions, suggesting better tool-chip lubrication [35]. Additionally, the SEM images show less micro cracking or tears in the T1 chips resulting from S80 conditions in Figure 3.6.

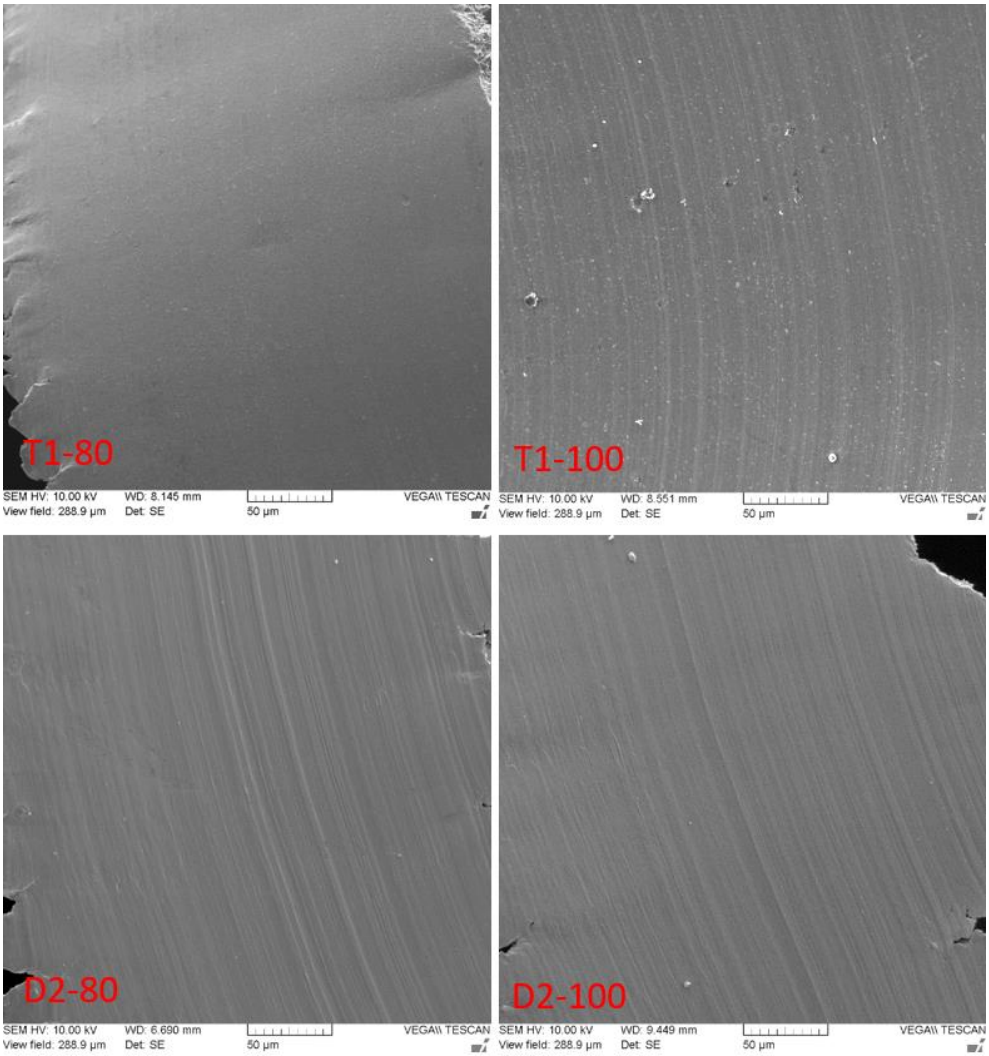

Figure 3.6 Chip undersurface morphology at 80 and 100 m/min

3.3.4 Discussion

Compared to S80, cutting both workpiece materials under the higher cutting speed of S100 resulted it more intensive tribo-oxide formation. The total amount of W-O was 72.3% at S100 compared to 60.6% at S80 in machining T1; while Cr-O was 72.1% at

S100 and 67.2% at S80 for D2. It is believed that W-O would perform as a lubricant during machining, especially at higher temperatures, which is consistent with the relatively smooth chip under surface (Figure 6). Cr-O, on the other hand, is a protective triboceramic and would be expected to beneficially reduce the wear of the tool during machining; as seen in Figure 2 and Figure 4. Cutting at S100 resulted in a lower wear rate and smaller level of flank wear within the stable wear stage compared to S80.

Even though a higher amount of tribofilms was formed during machining both steels at S100, overall tool life was still inferior as compared to cutting at S80. On the one hand, more intensive tribofilms can provide an enhanced thermal protective and/or lubricating function at the tool-chip interface and thereby reduce the severity of tribological processes during machining. However, cutting at higher speeds tends to trigger higher temperatures, making the tool more susceptible to thermal and mechanical damage. It is believed this latter effect is ultimately responsible for the accelerated wear rate in the later stages of the wear curve for T1 as well as the earlier tool failure due to massive peeling of the surface in the case of D2 (Figure 2). Lubricants offer limited protection against thermal damage of the tool. Crater wear was more severe (Figure 3) and chip undersurface was less smooth (Figure 6) when cutting T1 at S100 as compared to S80, despite the more intensive formation of tribofilms (Table 2). In-process adjustment of cutting conditions (cutting speed) has been applied with

coated carbide inserts and demonstrated as a means of extending tool life [20]; a similar strategy would likely improve overall machinability with ceramic tools as well.

There are a number of factors determining tool life. Traditionally, the nature of carbide phase and hot hardness of the work material have been considered the major factors determining wear rates and tool life in machining hardened steels. However, tribofilms formation provides a significant complementary explanation to the observed results from a nano-scale perspective. Tribofilms generation during machining can be affected by cutting conditions and it plays an important role in determining tribological conditions and overall tool life.

3.4 Conclusions

50 m/min, 80 m/min and 100 m/min cutting speeds were used with uncoated alumina ceramic tools in hard dry turning of AISI T1 and AISI D2 steels at comparable hardness. The microstructure of the workpiece materials, the wear mechanisms acting on the tools, and the tribofilms formed on the tools under different cutting speeds as well as their influences on friction and wear were studied with an optical microscope, SEM, and X-ray photoelectron spectroscopy. In cutting T1 and D2 steels at 50 m/min, both flank and rake faces showed relatively large fractured zones. Tool life at 50 m/min was less than half of tool life at 80 m/min and 100 m/min. At higher cutting speeds of 80 m/min and 100 m/min, abrasion dominated at the tool flank in dry hard machining both

T1 and D2 steels, while crater wear of the tool rake was more severe in machining T1, especially at the highest cutting speed. Tool life at 100 m/min was lower than at 80 m/min because of accelerated wear rate or massive chipping in the later stages of the wear curve.

Cutting conditions strongly affect the wear mechanism and tribofilms generation on the friction surface of alumina ceramic tools with higher cutting speeds triggering a more intensive formation of beneficial tribofilms. The higher amount of Cr-O triboceramics reduced the wear rate when machining D2 steel and W-O tribofilms where observed to improve the tribological conditions when cutting T1 steels; however, more intensive formation of lubricating tribofilms at higher cutting speeds had no effect on reducing wear due to the elevated temperature and heavier loading experienced under these more aggressive conditions. In addition to traditionally considered micro-scale wear mechanisms affected by carbide phase distribution in the machined workpiece and accumulation of mechanical and thermal damages on the surface of cutting tools; tribofilms generation provided a nano-scale approach for further examination of the friction/wear performance as well as tool life in machining of hardened steels under different conditions.

Acknowledgement:

The authors wish to acknowledge the financial support of the Natural Science and Engineering Research Council (NSERC) of Canada Discovery grants program.

References

[1] Byrne G, Dornfeld D, Denkena B. Advancing cutting technology. CIRP Annals-Manufacturing Technology 2003;52:483-507.

[2] Dudzinski D, Devillez A, Moufki A, Larrouquère D, Zerrouki V, Vigneau J. A review of developments towards dry and high speed machining of Inconel 718 alloy. International Journal of Machine Tools and Manufacture 2004;44:439-56.

[3] Sreejith P, Ngoi B. Dry machining: machining of the future. J Mater Process Technol 2000;101:287-91.

[4] Davim JP. Machining of hard materials: Springer; 2011.

[5] Hashimoto F, Guo Y, Warren A. Surface integrity difference between hard turned and ground surfaces and its impact on fatigue life. CIRP Annals-Manufacturing Technology 2006;55:81-4.

[6] Ezugwu E, Bonney J, Yamane Y. An overview of the machinability of aeroengine alloys. Journal of Materials Processing Technology 2003;134:233-53.

[7] Claudin C, Rech J, Grzesik W, Zalisz S. Characterization of the frictional properties of various coatings at the tool/chip/workpiece interfaces in dry machining of AISI 4140 steel. International Journal of Material Forming 2008;1:511-4.

[8] Chou YK, Evans CJ. White layers and thermal modeling of hard turned surfaces. International Journal of Machine Tools and Manufacture 1999;39:1863-81.

[9] Matsumoto Y, Hashimoto F, Lahoti G. Surface integrity generated by precision hard turning. CIRP Annals-Manufacturing Technology 1999;48:59-62.

[10] Grzesik W. Influence of tool wear on surface roughness in hard turning using differently shaped ceramic tools. Wear 2008;265:327-35.

[11] Lahiff C, Gordon S, Phelan P. PCBN tool wear modes and mechanisms in finish hard turning. Robotics and Computer-Integrated Manufacturing 2007;23:638-44.

[12] Barry J, Byrne G. Cutting tool wear in the machining of hardened steels: part II: cubic boron nitride cutting tool wear. Wear 2001;247:152-60.

[13] El Hakim M, Abad M, Abdelhameed M, Shalaby M, Veldhuis S. Wear behavior of some cutting tool materials in hard turning of HSS. Tribology International 2011;44:1174-81.

[14] Fox-Rabinovich G, Totten GE. Self-organization During Friction: Advanced Surface-engineered Materials and Systems Design: CRC Press; 2010.

[15] Fox-Rabinovich GS, Yamamoto K, D Beake B, S Gershman I, I Kovalev A, C Veldhuis S, et al. Hierarchical adaptive nanostructured PVD coatings for extreme tribological

applications: the quest for nonequilibrium states and emergent behavior. Science and Technology of Advanced Materials 2012;13:043001.

[16] Franz R, Mitterer C. Vanadium containing self-adaptive low-friction hard coatings for high-temperature applications: a review. Surf Coat Technol 2013;228:1-13.

[17] Fox-Rabinovich GS, Gershman I, Hakim MAE, Shalaby MA, Krzanowski JE, Veldhuis SC. Tribofilm Formation As a Result of Complex Interaction at the Tool/Chip Interface during Cutting. Lubricants 2014;2:113-23.

[18] Yuan J, Boyd JM, Covelli D, Arif T, Fox-Rabinovich GS, Veldhuis SC. Influence of Workpiece Material on Tool Wear Performance and Tribofilm Formation in Machining Hardened Steel. Lubricants 2016;4:10.

[19] Shalaby M, El Hakim M, Abdelhameed MM, Krzanowski J, Veldhuis S, Dosbaeva G. Wear mechanisms of several cutting tool materials in hard turning of high carbon–chromium tool steel. Tribology International 2014;70:148-54.

[20] Yuan J, Yamamoto K, Covelli D, Tauhiduzzaman M, Arif T, Gershman IS, et al. Tribo-films control in adaptive TiAlCrSiYN/TiAlCrN multilayer PVD coating by accelerating the initial machining conditions. Surf Coat Technol 2016.

[21] Özel T, Karpat Y, Figueira L, Davim JP. Modelling of surface finish and tool flank wear in turning of AISI D2 steel with ceramic wiper inserts. J Mater Process Technol 2007;189:192-8.

[22] Gaitonde V, Karnik S, Figueira L, Davim JP. Machinability investigations in hard turning of AISI D2 cold work tool steel with conventional and wiper ceramic inserts. Int J Refract Met Hard Mater 2009;27:754-63.

[23] Arsecularatne J, Zhang L, Montross C, Mathew P. On machining of hardened AISI D2 steel with PCBN tools. Journal of Materials Processing Technology 2006;171:244-52.

[24] Geller Y. Tool steels, Moscow, Mashinostroenie 1979:353.

[25] Zhangxiao Z. Enginerring Material: Tsinghua University; 2001.

[26] Jacobson S, Hogmark S. Tribofilms—on the crucial importance of tribologically induced surface modifications. Recent developments in wear prevention, friction and lubrication 2010;661:197-225.

[27] Bouzakis K-D, Michailidis N, Skordaris G, Bouzakis E, Biermann D, M'Saoubi R. Cutting with coated tools: Coating technologies, characterization methods and performance optimization. CIRP Annals-Manufacturing Technology 2012;61:703-23.

[28] Lehn J-M. Toward self-organization and complex matter. Science 2002;295:2400-3.

[29] Fox-Rabinovich G, Kovalev A, Veldhuis S, Yamamoto K, Endrino J, Gershman I, et al. Spatio-temporal behaviour of atomic-scale tribo-ceramic films in adaptive surface engineered nano-materials. Scientific reports 2015;5.

[30] Fox-Rabinovich GS, Yamamoto K, Veldhuis SC, Kovalev AI, Shuster LS, Ning L. Self-adaptive wear behavior of nano-multilayered TiAlCrN/WN coatings under severe machining conditions. Surface and Coatings Technology 2006;201:1852-60.

[31] Kovalev A, Wainstein D, Fox‐Rabinovich G, Veldhuis S, Yamamoto K. Features of self‐organization in nanostructuring PVD coatings on a base of polyvalent metal nitrides under severe tribological conditions. Surf Interface Anal 2008;40:881-4.

[32] Fox-Rabinovich G, Kovalev A, Aguirre M, Yamamoto K, Veldhuis S, Gershman I, et al. Evolution of self-organization in nano-structured PVD coatings under extreme tribological conditions. Appl Surf Sci 2014;297:22-32.

[33] Ning Y, Rahman M, Wong Y. Investigation of chip formation in high speed end milling. J Mater Process Technol 2001;113:360-7.

[34] Gorczyca FE. Application of metal cutting theory: Industrial Press Inc.; 1987.

[35] Fox-Rabinovich G, Dasch J, Wagg T, Yamamoto K, Veldhuis S, Dosbaeva G, et al. Cutting performance of different coatings during minimum quantity lubrication drilling of aluminum silicon B319 cast alloy. Surf Coat Technol 2011;205:4107-16.

Chapter 4

Tribofilms Control in Adaptive TiAlCrSiYN/TiAlCrN Multilayer PVD Coating by Accelerating the Initial Machining Conditions

Complete citation:

Yuan, Junfeng, Kenji Yamamoto, Danielle Covelli, Mohammed Tauhiduzzaman, Taib Arif, Iosif S. Gershman, Stephen C. Veldhuis, and German S. Fox-Rabinovich. "Tribofilms control in adaptive TiAlCrSiYN/TiAlCrN multilayer PVD coating by accelerating the initial machining conditions." Surface and Coatings Technology 294 (2016): 54-61.

Copyright:

Relative Contributions:

Junfeng Yuan:	Designed and performed all experiments, interpretation and analysis of the data and wrote the manuscript including all figures and text.
Kenji Yamamoto:	Deposited PVD coatings as requirements.
Danielle Covelli:	Performed XPS analyses and assigned peaks.
M. Tauhiduzzaman:	Assisted with the experiments and with surface characterization.
Taib Arif:	Assisted in cutting experiments and SEM characterization.
Iosif S. Gershman:	Provided valuable suggestions regarding the design of experiments
S. C. Veldhuis:	Provided thesis supervisor for the experiments and was responsible for the final draft submitted to the journal.
G. S. Fox-Rabinovich:	Offered help and suggestions for experiments and with writing.

Preface:

This chapter studied the control of tribofilms formation when machining DA 718 with a CrTiAlSiYN coated tool. All cutting inserts were prepared with the same coating so that the coating itself wouldn't affect the process other than serve as a source for tribofilms formation.

K313 CNGG 432FS cutting inserts were chosen to match the available tool holder, material code and edge geometry. The binding component of this inserts is WC-Co.

The decreased initial wear rate for the S60 case was more evident in the optical and EDX images of the crater wear and less by the flank wear rate which is shown in the wear curve provided.

Even though the amorphous Al-Al dangling bonds had lubricious properties, the amount present was much lower than Al-O and Cr-O protective tribofilms. For this reason these lubricious tribofilms were not discussed in this chapter.

Tribo-films control in adaptive TiAlCrSiYN/TiAlCrN multilayer PVD coating by accelerating the initial machining conditions

Junfeng Yuan [a], Kenji Yamamoto [b], Danielle Covelli [c], Mohammed Tauhiduzzaman [a], Taib Arif [a], Iosif S. Gershman [d], Stephen C. Veldhuis [a], German S. Fox-Rabinovich [a]

a Department of Mechanical Engineering, McMaster University, 1280 Main St., W. Hamilton, Ontario L8S 4L7, Canada

b Kobe Steel Ltd., Kobe, Hyogo 651–2271, Japan

c Biointerfaces Institute, McMaster University, 1280 Main St., W. Hamilton, Ontario L8S 4L7, Canada

d Railway Transport Research Institute, Moscow 29851, Russia

Keywords:

Nanolaminate TiAlCrSiYN/TiAlCrN PVD multilayer coating; tribo-oxidation; X-ray photoelectron spectroscopy; Auger Electron Spectroscopy; Inconel 718; acceleration of initial conditions;

Abstract

A nano- multilayer TiAlCrSiYN/TiAlCrN was deposited by Physical Vapor Deposition (PVD) on cemented carbide turning inserts. Assessment of the performance of the coated inserts in machining of DA718 Inconel was made at various cutting speeds during the initial, running-in stage of wear. Three types of machining conditions were used: i. Regular cutting speed (40 m/min) used in industrial practice; ii. Higher cutting speed of 60 m/min, and iii. Accelerated (higher speed followed by regular cutting speed). Comprehensive characterization of the tribofilms formed on the surface of the worn cutting tools was made using Auger Electron Spectroscopy and X-ray Photoelectron Spectroscopy analyses. SEM/EDS elemental mapping was used for evaluation of the wear patterns. It was shown that an initial short-term increase in the cutting speed during the running-in stage (condition iii) noticeably improves tool life. This is because during initial cutting at high speed, enhanced formation of protective/lubricious tribo-ceramic films on the friction surface takes place, with the subsequent slowdown in speed preventing total wearing out of the beneficial tribofilms. In this way, the tribofilms formation process can be enhanced at the start of the process and the benefits of these films can be realized over the life of the tool.

4.1 Introduction

The application of high speed machining processes to hard-to-machine aerospace materials brings a number of clear benefits; however it results in harsh tribological conditions and a very intensive tool wear rate [1, 2]. In addition to the heavy cutting loads and elevated temperature, strong built up edge formation makes the processes more complicated. From a tribological viewpoint, built up edge is related to seizure on the friction surface, which is a catastrophic failure mechanism [3]. This leads to strong gradients in the characteristics on the friction surface, combined with significant instability of the frictional process [4, 5]. Novel methods of cutting tool surface engineering, which are the major method of tool life improvement, have been applied to address these challenges to provide efficient protection of friction surfaces under operation[4, 6, 7].

There are two approaches in the design of wear resistant coatings [6]. First, the coating is considered as a completely artificial system with minimal changes in its structure taking place through its interaction with the environment. In this case the hardness, oxidation, and thermal stability of the coating layer as deposited is used to consider the major properties responsible for wear resistance [8, 9]. In contrast, the second approach involving an adaptive coating design, regards a coating as a surface-engineered tribological system that combines an artificial system (coating) and

beneficial processes associated with friction and interaction with the environment that results in its adaptation to its environment. Adaptability, which significantly increases tool life, is a consequence of the beneficial structure and phase transformations that take place on the friction surface [10]. During the cutting process, tribo-oxidation of the coating layer plays a significant role in frictional behavior and wear resistance of the entire surface-engineered layer. During permanent tribofilms formation and wear, the coating layer is efficiently protected and lubricated. These processes provide tribological compatibility between the tool/workpiece system and resulting in reduced levels of surface damage of the cutting tool, generated in a longer tool life [11, 12].

Physical vapour deposited (PVD) adaptive nanocrystalline multilayer TiAlCrSiYN/TiAlCrN coatings exhibit excellent tool life under severe cutting conditions [13]. This is true for the cutting of hard-to-machine materials; in particular for the machining of Ni-based superalloys [17]. Nickel-based superalloys have been widely applied for some demanding applications [3]. Inconel 718 superalloy, especially direct aged Inconel 718, belongs to the family of the most difficult-to-machine alloys due to high-temperature strength [3, 4], low thermal conductivity, and propensity to work-harden during machining [5-9].

A special challenge for tribological compatibility is thus the ability to control tribofilms regeneration on the friction surface. This is related to the concept of adaptability [14] and is done by shifting the system, in the short-term, to severe

frictional conditions during the running-in stage. This accelerates the formation of beneficial oxide on the surface of a tool in service.

This research is aimed to investigate the effect of initial high cutting speeds during the running-in stage when machining Ni-based super alloys using cutting tools with self-adaptive nanocrystalline multilayer TiAlCrSiYN/TiAlCrN coatings. This approach could provide the possibility of enhanced tribofilms formation on the tool initially and then prevent excessive wear of the tribofilms by slowing down to 'regular' machining conditions to prevent intensive wearing-out of the tribofilms layer. In this way the tribofilms formation can be controlled to improve the wear resistance of the surface engineered layer and thus enhance the productivity of the machining process by improving tool life.

4.2 Material and Methods

4.2.1 Coating deposition

Nano-multilayered Ti0.2Al0.55Cr0.2Si0.03Y0.02 N/Ti0.25Al0.65Cr0.1 N coating was deposited using Ti0.2Al0.55Cr0.2Si0.03Y0.02 and Ti0.25Al0.65Cr0.1 targets, which were fabricated through a powdered metallurgical process. The thickness of each alternating nano-layer in the multilayer coatings was approximately 20-40 nm (Table 4.1) [13, 15]. All inserts in this study were coated with the same coatings.

Table 4.1 Structure and micro-mechanical characteristics of TiAlCrSiYN/TiAlCrN coatings at room and elevated temperatures

Grain size, nm		20-40
Thickness, μm		2
Crystal structure		FCC nano-crystalline/laminated
Nano-layer thickness, nm		20-40
Micro hardness, GPa	Room temperature	30
	500°C	28

Coatings were deposited in an R&D-type hybrid PVD coater (Kobe Steel Ltd.) with a plasma-enhanced arc source. Samples were heated up to about 500 °C and cleaned through an Ar ion etching process. Ar–N_2 mixture gas was fed to the chamber at a pressure of 2.7 Pa with an N2 partial pressure of 1.3 Pa. The arc source was operated at 100 A for a 100 mm diameter×16 mm thick target. Other deposition parameters were: bias voltage 100 V and substrate rotation 5 rpm. The thickness of the coatings studied was around 2 μm for the film characterization and cutting test work. Table1 shows the structure and micro-mechanical characteristics of TiAlCrSiYN/TiAlCrN coatings at room and elevated temperatures [16].

Coated K313-CNGG432FS (in short CNGG) inserts with chip breaker (industry standard) were chosen for cutting tool life studies on a CNC lathe. The coated K313-SPG 422 flat inserts (in short SPG) were used for process characterization and additional laboratory studies to explain the nature of tool wear and tribofilms formation. The

flatness of the SPG inserts allowed the accuracy of the data collected to be significantly improved. Since SPG inserts do not have a chip breaker with a complex shape, and the data obtained by surface analysis is much more accurate on this flat, mirror-polished rake face.

4.2.2 Cutting experiments

Cutting experiments were performed at speeds of 40 m/min, 60 m/min and on accelerated test conditions (60 m/min at the beginning of machining followed by slowing down to 40 m/min for the remainder of the tool's life), which were designated as S40, S60 and S60/40 respectively. A cutting speed of 40m/min can be characterized as usual industry practice. All cutting experiments were performed under wet machining conditions. All of the turning tests were carried out on the same Boehringer VDF 180 CNC lathe. The combination of feed=0.1225mm/rev and DOC=0.25mm was used for all experiments. Flank wear land width (Vb) was measured by a Mitutoyo Toolmaker's Microscope. Tool failure was determined to be at 300 microns and the tool life was characterized by its cutting length. The tool holder used in this work is a Kenna clamp DCLNL166DKC4. The major characteristics of the turning inserts, tool holder and the workpiece material are presented in Table 4.2.

Table 4.2 Cutting experiments

Machining operation	Cutting tool substrates	Workpiece material	Workpiece Hardness	Tool holder
Single point turning	Kennametal K313 turning inserts	Direct aged Inconel 718	HRC 47-48	Rake angel -5°; clearance angle 0°; setting angel 95°

4.2.3 Cutting Tool Surface Characterization

Initial cutting using SPG inserts was performed in order to characterize the topography and to do the elemental mapping at 200m length of cut in order to study the effects of tribofilms on tool wear. A TESCAN VEGA LSU scanning electron microscope (SEM) and EDX mapping were used for studying the microstructure and investigating wear mechanism of the worn tools. A Nikon Optical Microscope was used to study in the morphology of the rake face and for measuring the area of the crater wear.

To understand the mechanisms of tribofilms that take place at different cutting speeds, the SPG surfaces at the running-in stage were characterized by X-ray photoelectron spectroscopy (XPS). The XPS equipment consisted of a Physical Electronics (PHI) Quantera II spectrometer with a hemispherical energy analyzer, an Al anode source for X-ray generation, and a quartz crystal monochromatic for focusing the generated X-rays. The X-ray source was from a monochromatic Al K-α (1486.7eV) at 50W-15kV and the system base pressure was between 1.0x10-9Torr and 2.0x10-8 Torr. At the beginning, the samples were sputter-cleaned for 4 minutes with a 4kV Ar+ beam

before collecting the data. The beam for data collecting was 200 microns and all spectra were obtained at a 45˚ take off angle. A dual beam charge compensation system was utilized to ensure neutralization of all samples. The pass energy to obtain all survey spectra was 280eV, while to collect all high resolution data it was 69eV. The instrument was calibrated with a freshly cleaned Ag reference foil, where the Ag 3d5/2 peak was set to 368eV. All data analysis was performed in PHI Multipak version 9.4.0.7 software.

Table 4.3 AES parameters

	Incident electron beam	Ar+ sputtering beam
Beam voltage	10keV	1keV
Beam diameter	100nA	25mA
Beam angle	30 degree from substrate normal	25 degree from substrate normal

Auger depth profile spectroscopy was used to analyze the thickness of the tribofilms on the worn SPG surface for the S60 samples. The sputtering rate and depth of tribofilms was calculated from the sputtering rate of SiO2. This was performed on a Palkin Elmer PHI650 scanning AES and the primary parameters are shown in Table 4.3.The sputtering rate was 1nm/min at the beginning and 2nm/min after 20min.The Auger signal was recorded in the mode CRR = 2 V at a speed of 2.1 eV/s and primary electron energy E = 2500 eV.

4.3 Results and Discussion

4.3.1 Effects of the initial high cutting speed on CNGG tool life

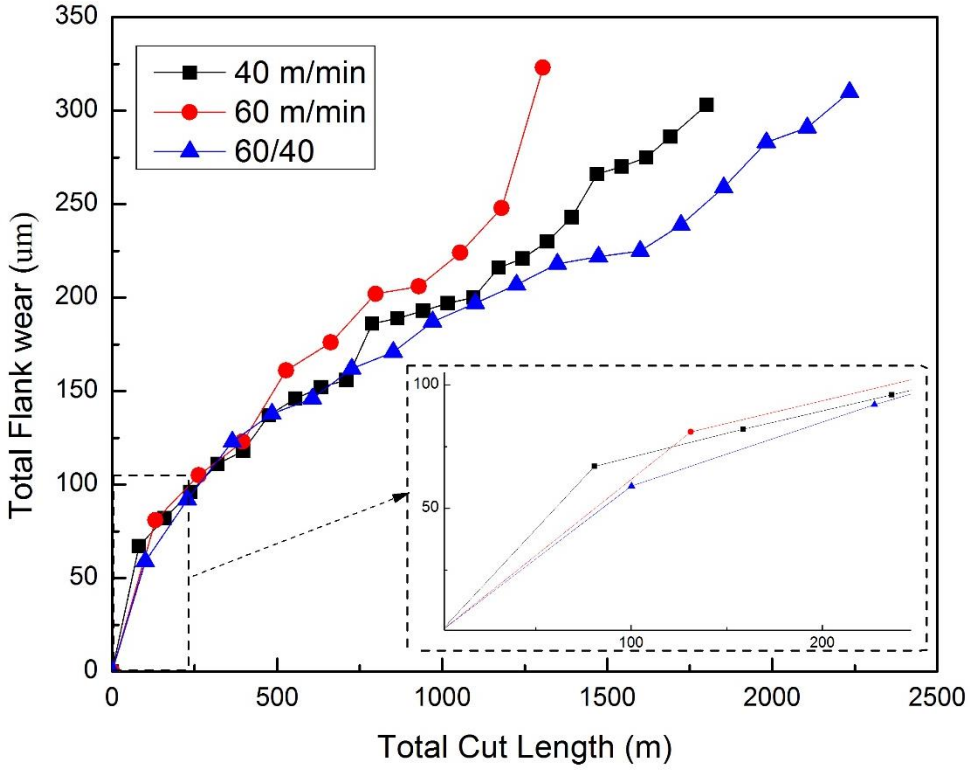

Figure 4.1 Wear curves at different cutting speed with CNGG inserts

Figure 4.1 illustrates flank wear as a function of cutting length at the three cutting conditions with cutting fluid used during machining. Although overall tool life is much higher at 40 m/min than at 60 m/min, the flank wear rate at 60 m/min is slightly smaller than that at 40m/min within the initial running-in stage (the first 121 meters in cutting length). Because of this reason, the accelerated test was designed to perform the higher speed at 60 m/min for 100 m length of cut, and then slow down to 40 m/min,

aiming to increase the overall tool life. It should be noted that the accelerated test resulted in a 24% tool life increase compared to the 40 m/min test and 71% tool life increase compared to the test at 60 m/min. The underlying reason why we chose to run the tool at 60m/min at the beginning is due to the rapid formation of beneficial tribo-oxides layer generated under these conditions. This tribo-oxides layer remains on the friction surface during the regular cutting speed and further improves the tool life as can be seen from Figure 4.1. The detail analysis on tribofilms formation has been explained using the SPG tool to support this observed improved performance and is discussed further in the following sections.

4.3.2 Wear mechanism and elemental mapping on SPG tools

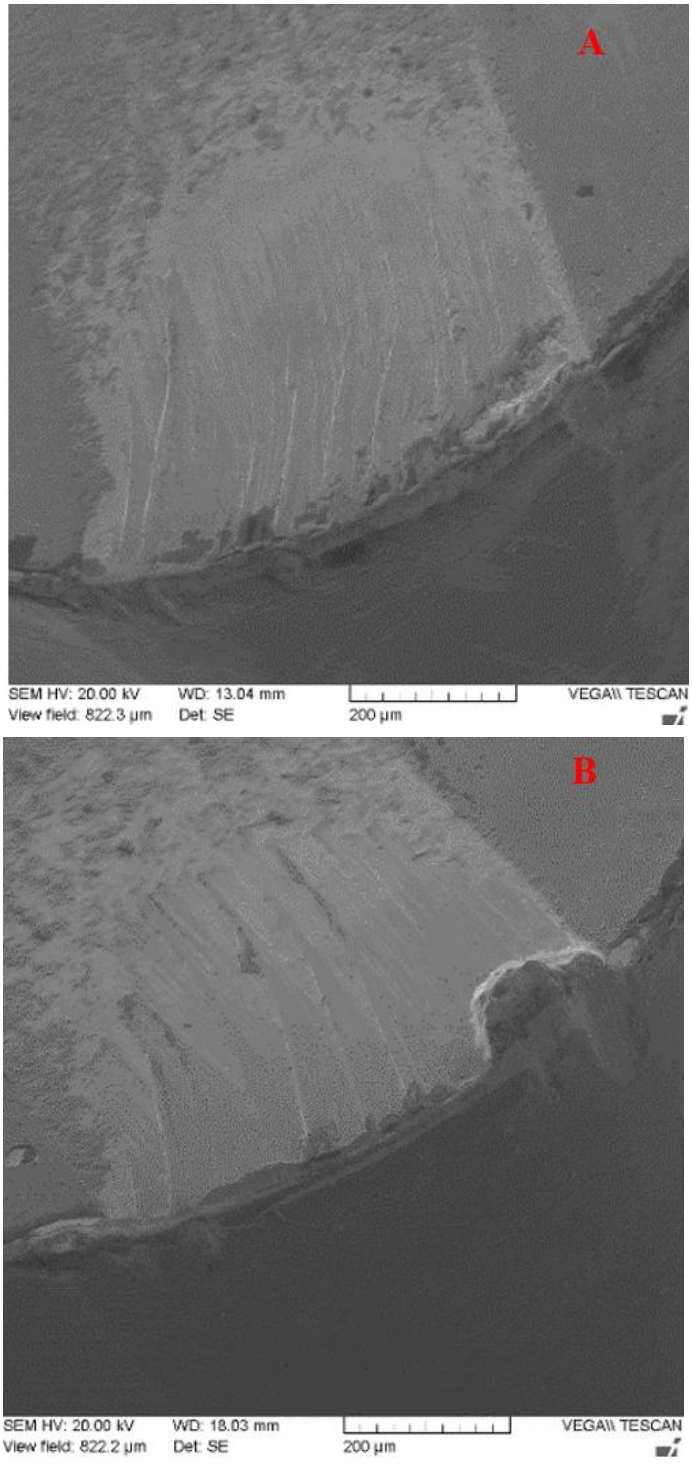

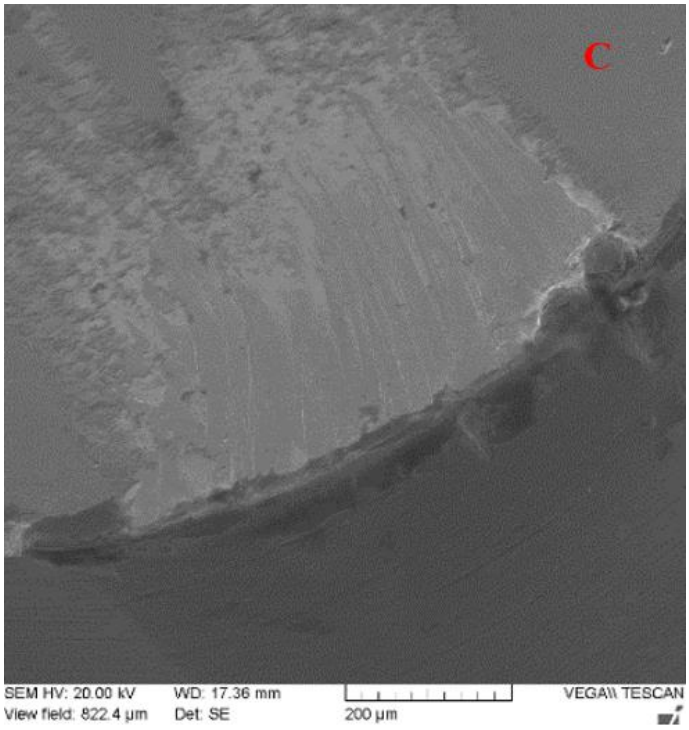

Figure 4.2 Cutting edge at 200 meters length of cut with SPG inserts.

(A-S40, B-S60, C-S60/40)

Figure 4.2 presents the SEM images of the S40, S60 and S60/40 of SPG tips after 200 meters of turning (running in stage). The S60/40 cutting experiment was performed with 100 meters of cut at 60 m/min followed by testing for another 100m length of cut at 40 m/min. The flank wear of all SPG inserts was small and similar due to the small cutting length (200 meters). Intensive built-up edge formation and severe notch wear were observed for all three samples even during the running-in stage.

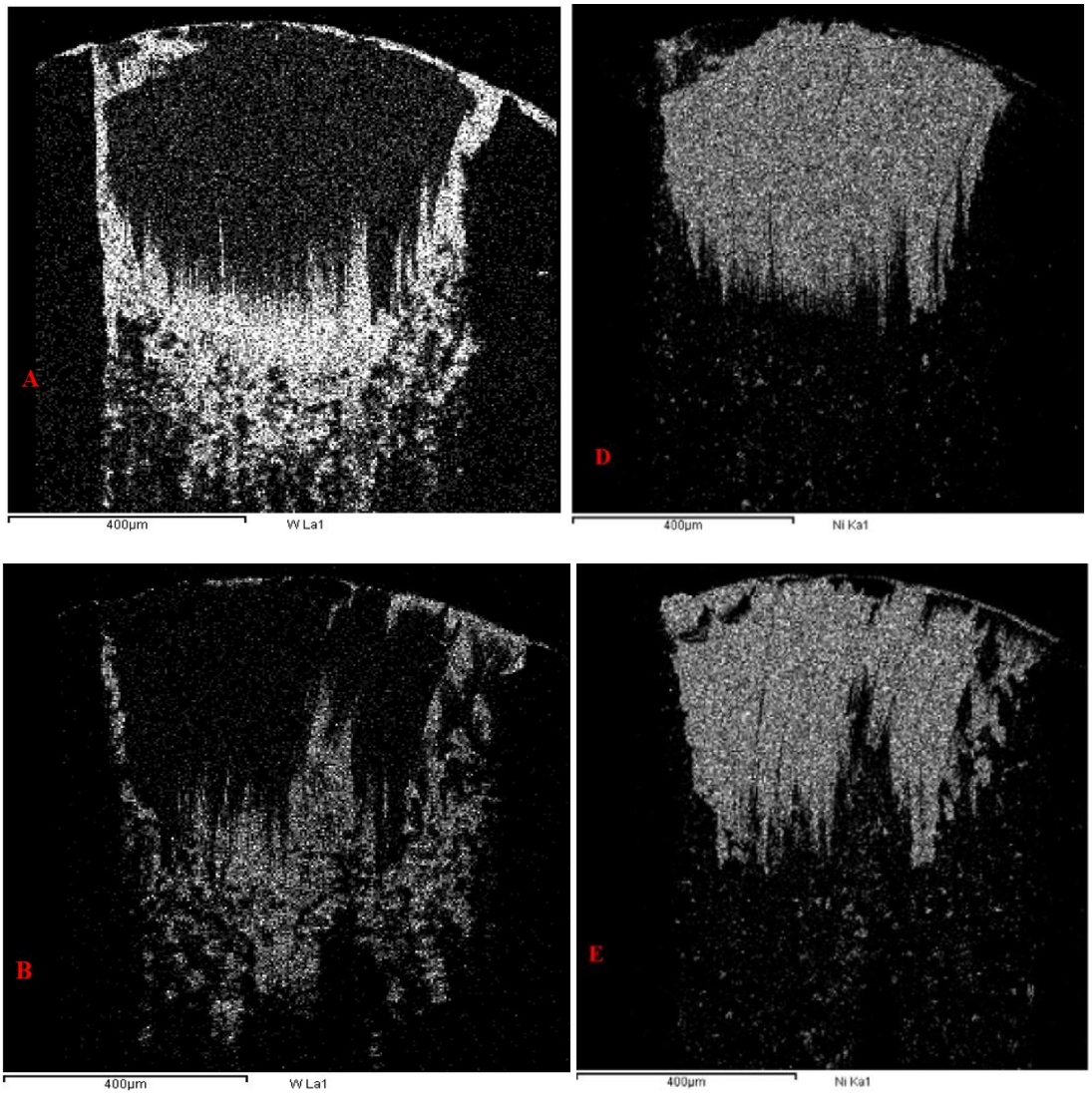
A
400µm
W La1
D
400µm
Ni Ka1
B
400µm
W La1
E
400µm
Ni Ka1

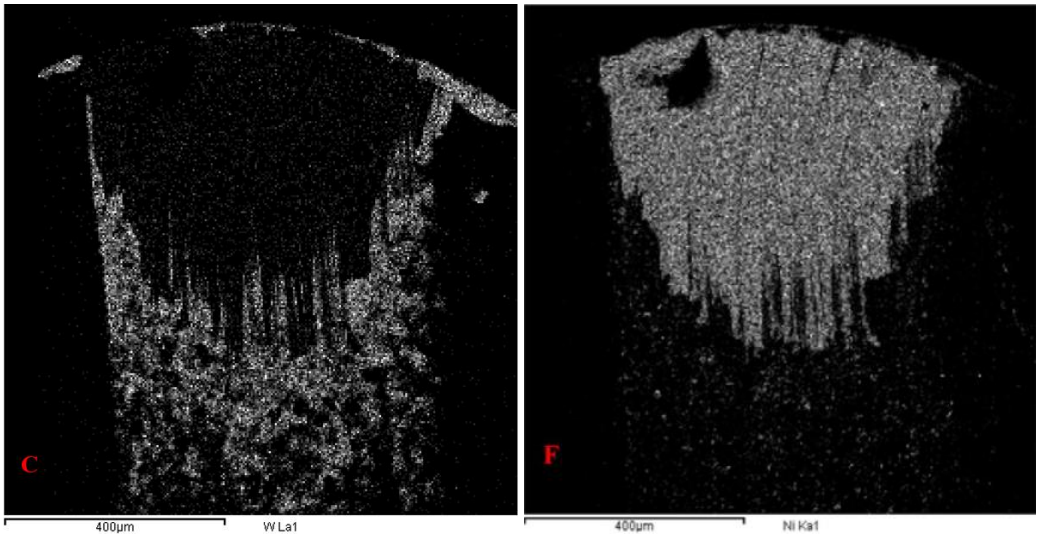

Figure 4.3 Elemental mapping of Tungsten (A-S40, B-S60, C-S60/40) and and Nickel (D-S40, E-S60, F-S60/40) on rake face.

Figure 4.3 shows EDX mapping spectra on the rake face of three inserts. Since Tungsten was only present in the insert substrate, this element was used as a monitor to indicate damage to the coatings. Nickel from the workpiece adhered heavily on the worn surface as built-up edge. In EDX elemental mapping analysis, the worn surfaces near the cutting edge were partially covered by Nickel, which was surrounded by Tungsten (in Figure 4.3).As shown in Figure 4.3, S40 showed the most intensive Tungsten signals among all the samples, which indicated S40 had more intensive wear.

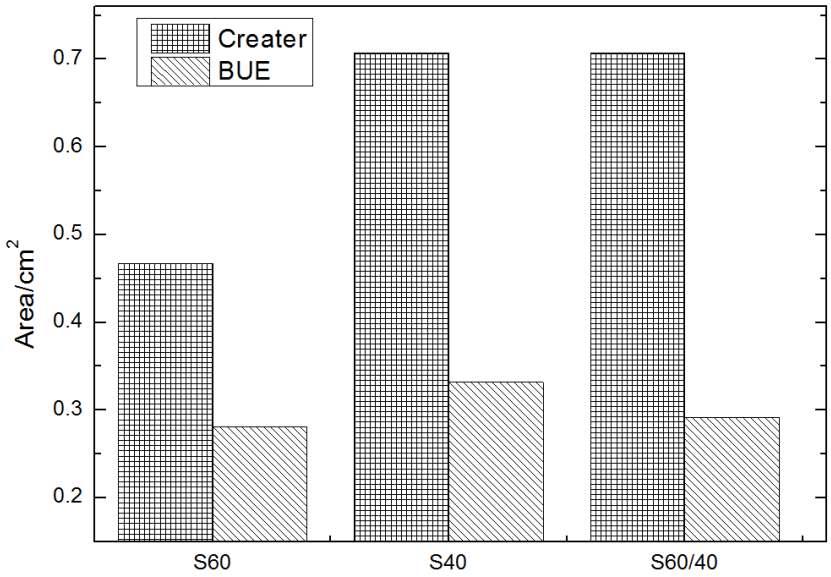

Figure 4.4 Areas of crater wear and build-up edge with SPG inserts

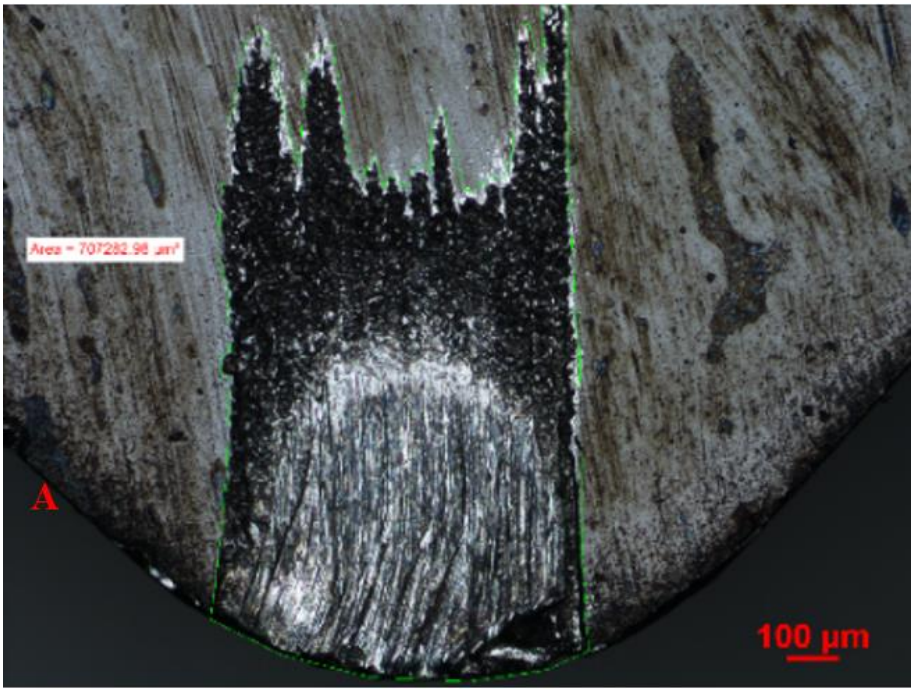

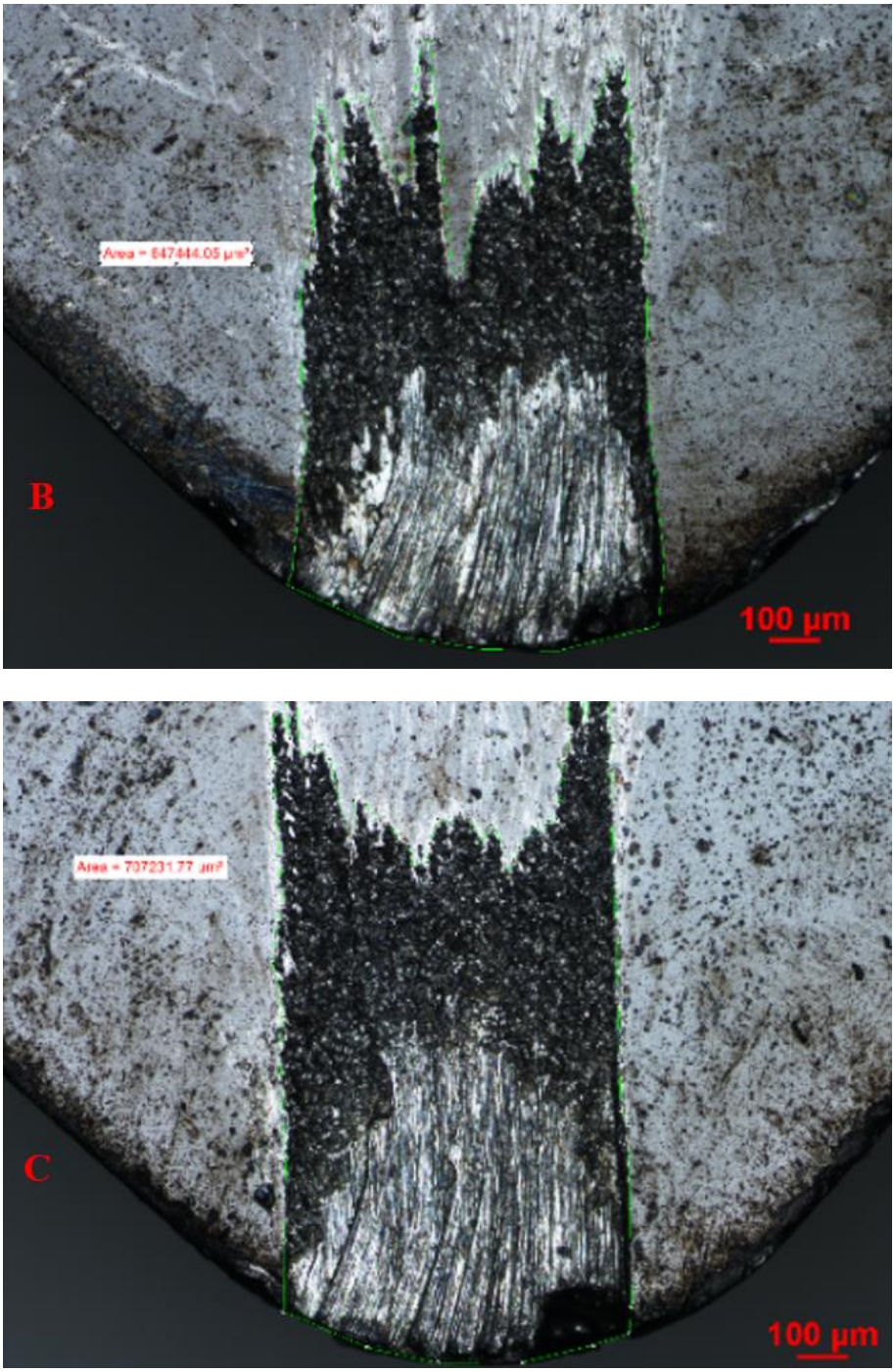

Figure 4.5 Area of crater wear. (A-S40, B-S60, C-S60/40)

Crater wear is crucial for tool life according to the ISO standard [17]. Figure 4.5 presents images of the crater wear of three inserts, which were also used to measure

the built-up edge. The crater wear areas of S60, S40 and S60/40 were around 0.647cm^3, 0.707cm^3 and 0.707cm^3 respectively, while the build-up edge areas were 0.281, 0.332 and 0.292 cm^3 respectively (Figure 4.4).

It was noticed that all three samples had the same wear mechanisms: abrasive wear on the flank surface and crater wear on the rake surface with intensive built-up edge formation. Among the worn inserts, the one at 40 m/min showed the largest crater wear intensity according to the images of the areas and the elemental mapping. The insert tested at 60 m/min had both the smallest crater wear and the smallest area covered by a built-up edge. Although no coating flaking was observed for the inserts, substrate (WC-Co) exposure was identified on the worn zone through the W signal. This indicates that the coating is missing in the observed area, including the built-up edge area. The worn coating area is the most intensive for the insert tested at 40 m/min and the least intensive for the insert tested at 60 m/min.

4.3.3 Adaptive behaviour

Tribofilms formation during friction plays a significant role in the wear behaviour of heavily loaded tribo-systems such as cutting tools [18, 19]. Different kinds of tribofilms can provide a protective, thermal barrier or lubricious functions to the frictional surface under operation [20].

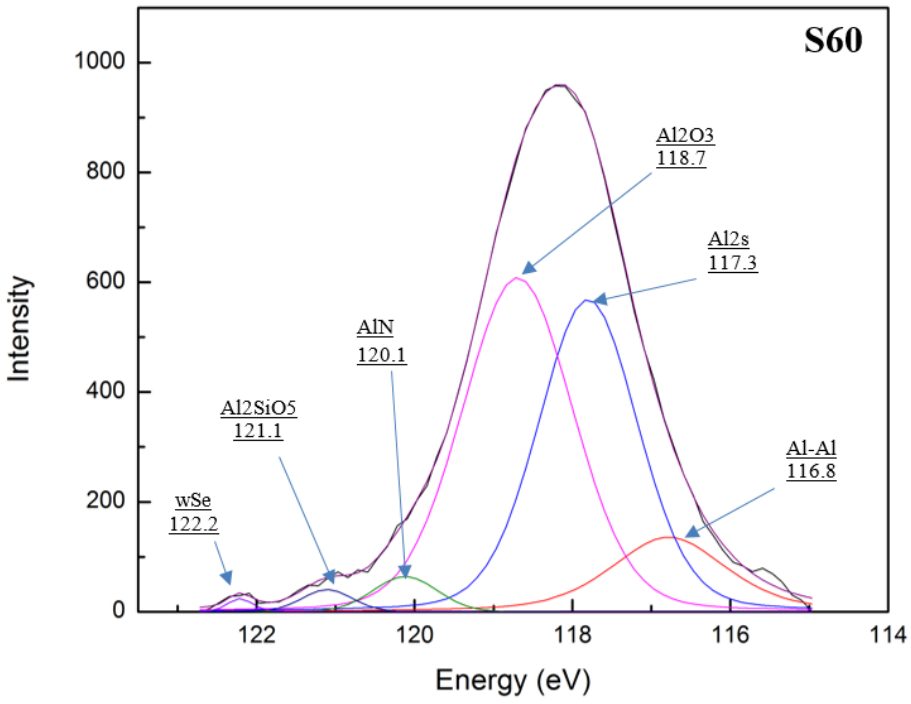
S60
Intensity
Energy (eV)
Al2O3
118.7
Al2s
117.3
AlN
120.1
Al2SiO5
121.1
wSe
122.2
Al-Al
116.8

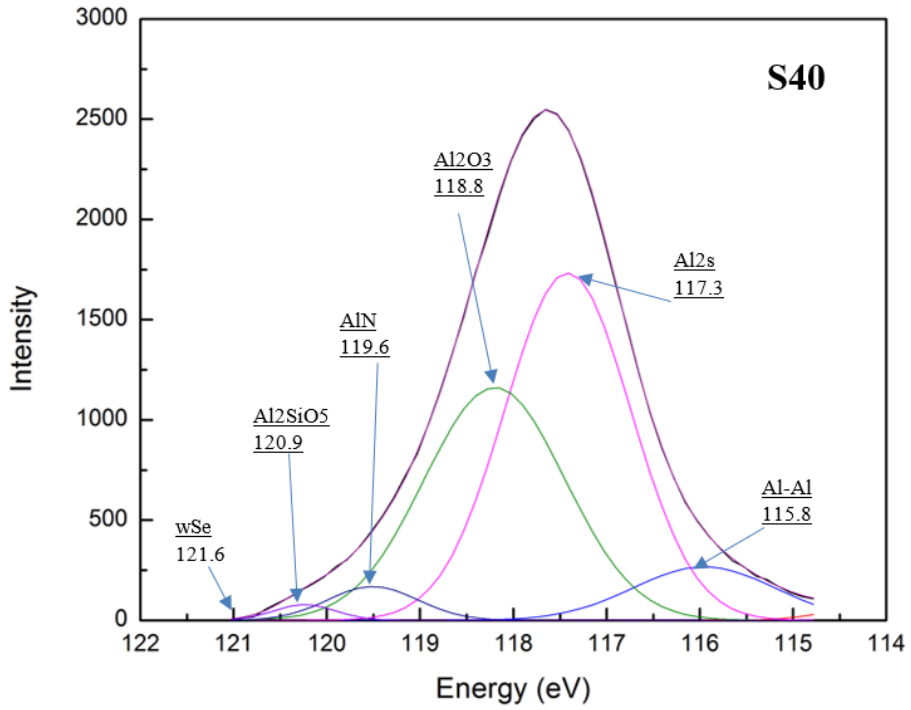
S40
Intensity
Energy (eV)
Al2O3
118.8
Al2s
117.3
AlN
119.6
Al2SiO5
120.9
wSe
121.6
Al-Al
115.8

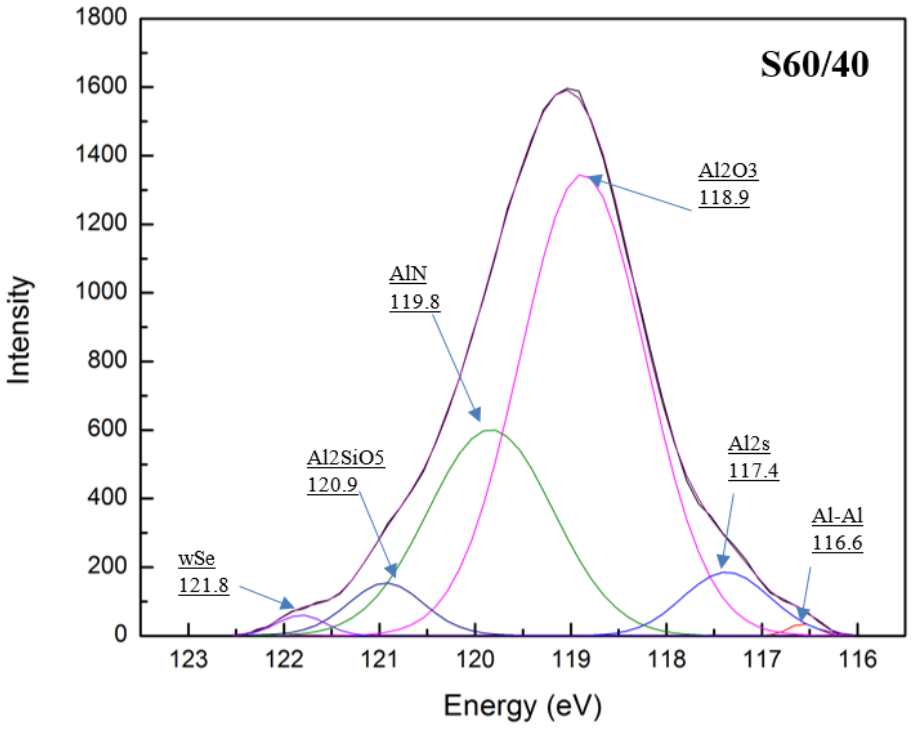
S60/40
Al2O3
118.9
AlN
119.8
Al2SiO5
120.9
Al2s
117.4
Al-Al
116.6
wSe
121.8
Intensity
Energy (eV)

(a) Al

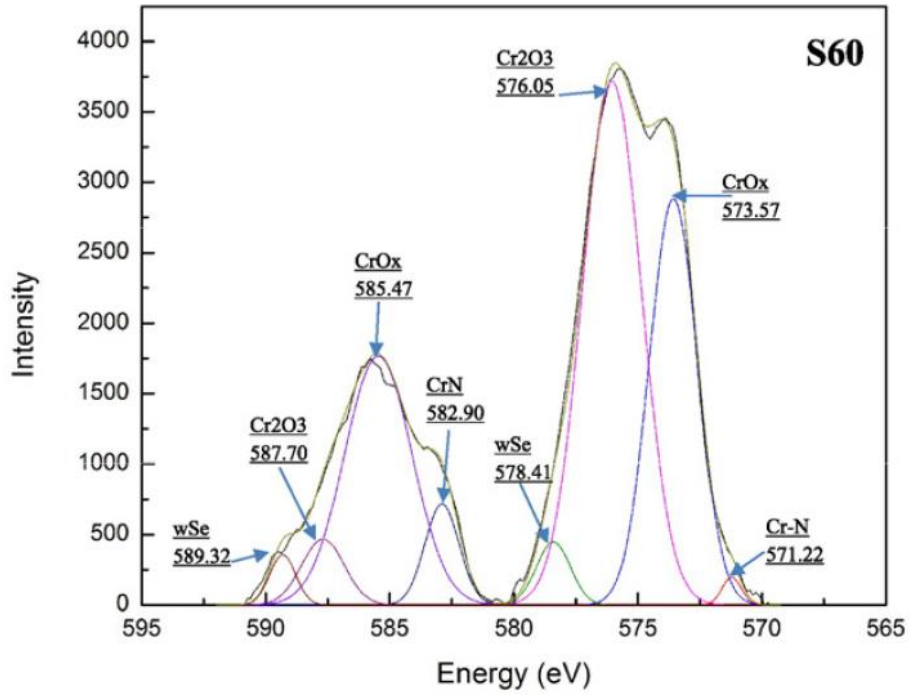
S60
Cr2O3
576.05
CrOx
573.57
CrOx
585.47
CrN
582.90
Cr2O3
587.70
wSe
578.41
wSe
589.32
Cr-N
571.22
Intensity
Energy (eV)

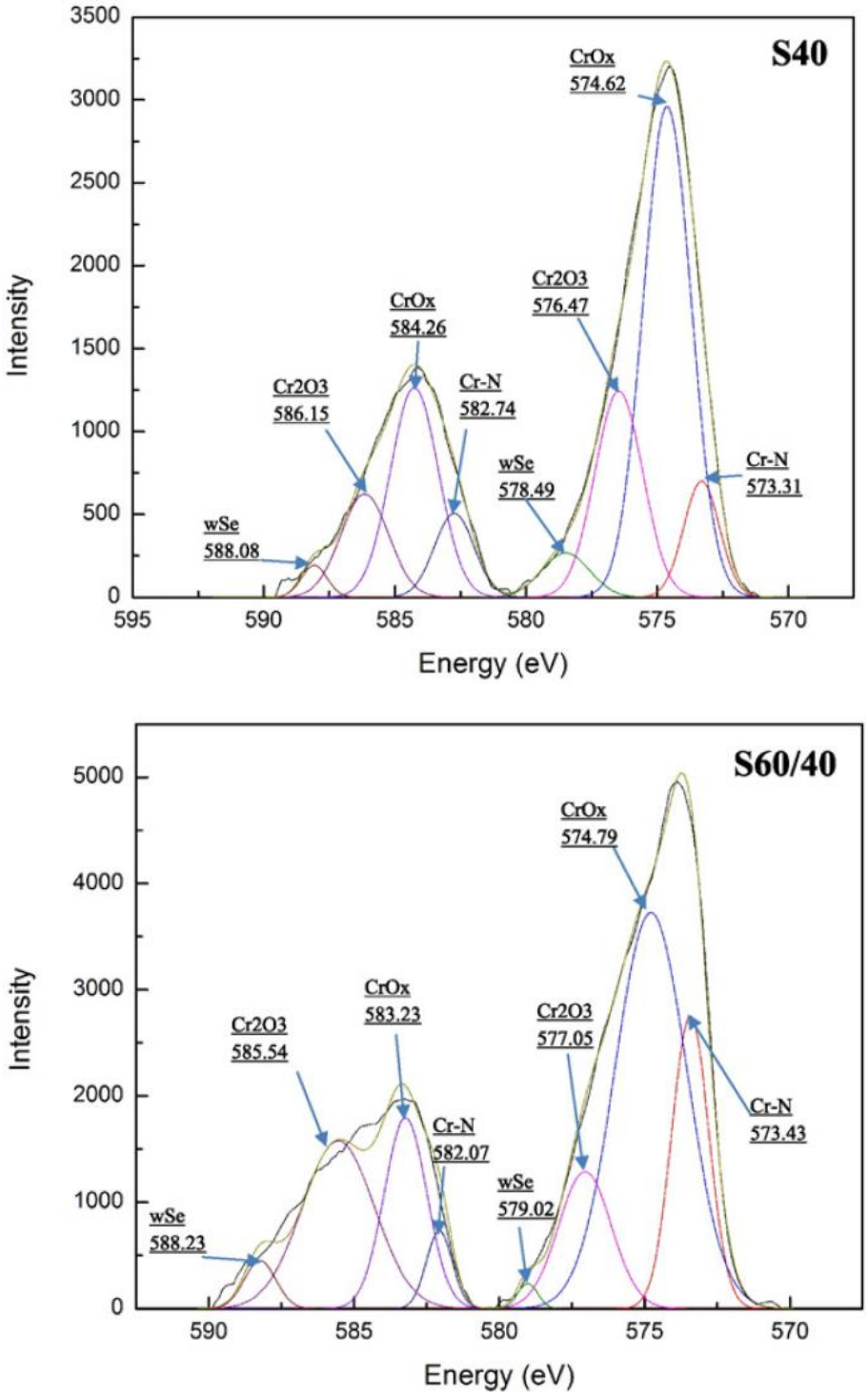
S40
CrOx
574.62
Cr2O3
576.47
CrOx
584.26
Cr2O3
586.15
Cr-N
582.74
wSe
578.49
Cr-N
573.31
wSe
588.08
Intensity
Energy (eV)
S60/40
CrOx
574.79
CrOx
583.23
Cr2O3
585.54
Cr2O3
577.05
Cr-N
582.07
Cr-N
573.43
wSe
579.02
wSe
588.23
Intensity
Energy (eV)

(b) Cr

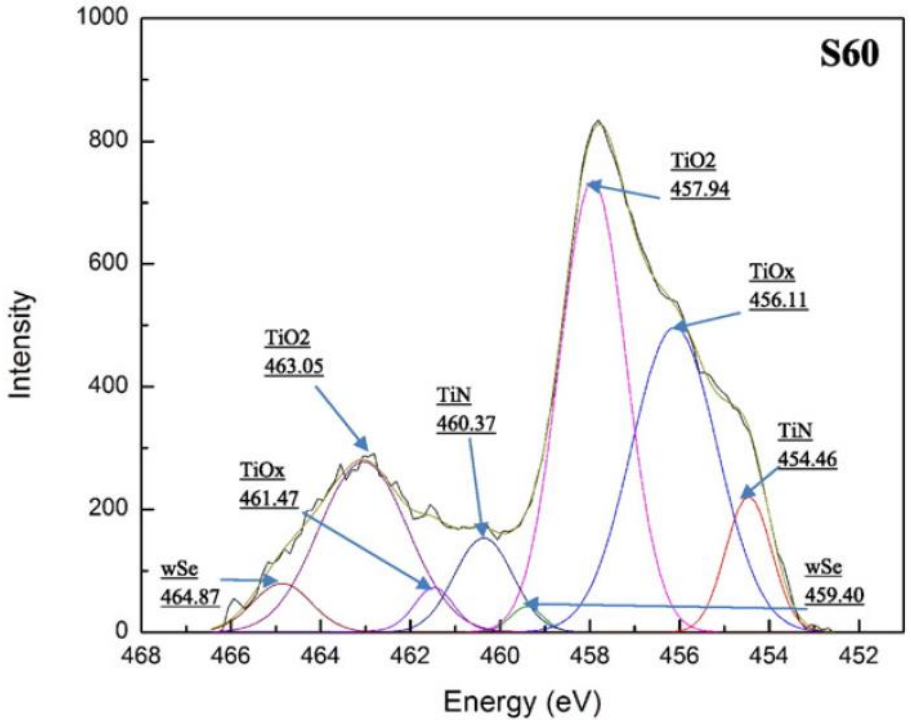
S60
TiO2
457.94
TiOx
456.11
TiO2
463.05
TiN
460.37
TiN
454.46
TiOx
461.47
wSe
464.87
wSe
459.40
Intensity
Energy (eV)
1000
800
600
400
200
0
468
466
464
462
460
458
456
454
452

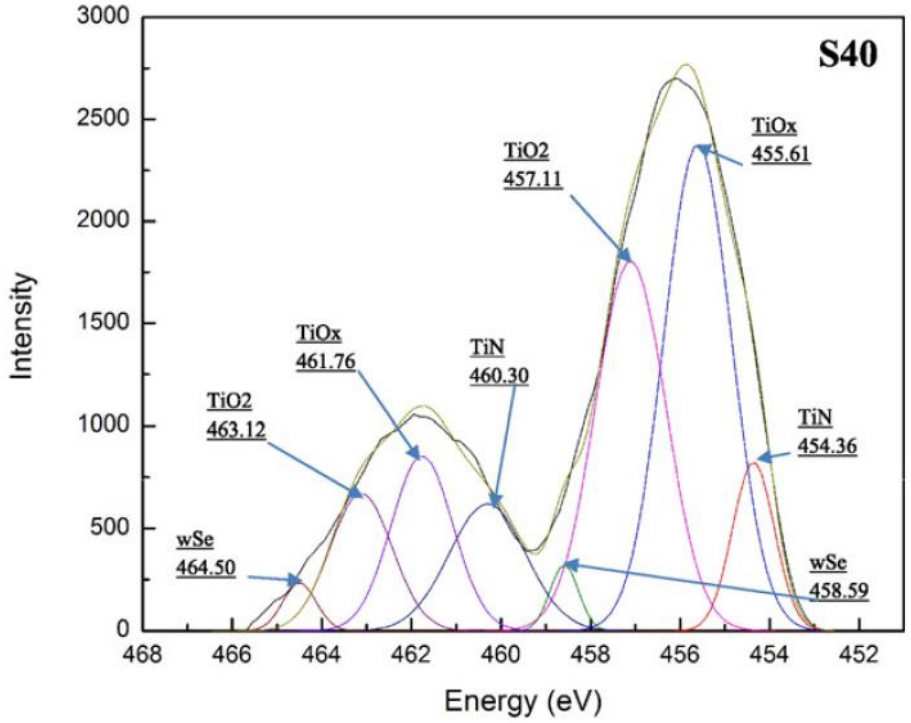
S40
TiOx
455.61
TiO2
457.11
TiOx
461.76
TiN
460.30
TiO2
463.12
TiN
454.36
wSe
464.50
wSe
458.59
Intensity
Energy (eV)
3000
2500
2000
1500
1000
500
0
468
466
464
462
460
458
456
454
452

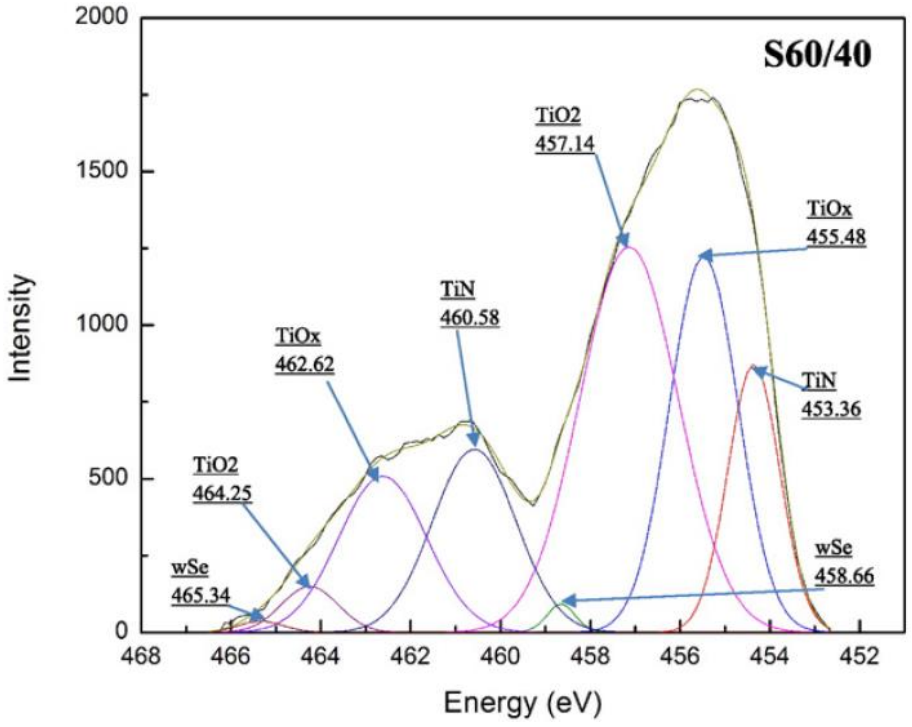

(c) Ti

Figure 4.6 Photoelectron spectra of Al2p Cr2p and Ti2p on rake face after turning of 200 meters

The tribofilms characteristics were studied by XPS. The high resolution spectra on the phase composition of different tools' rake faces after 200 meters of turning are presented in Figure 4.6. Figure 4.6 a-c shows different types of chemical bonds of aluminum, chromium and titanium in simple and complex oxide tribo-films and nitride coatings. These meta-stable phases have been observed on the worn surface of coated ball nose end mills during both the running-in and post-running-in stages of wear [21, 22]. Photoelectron lines are seen slightly shifted from the binding energy values of pure elements in various offsets. Different offset positions indicate various degree of

oxidation with the formation of nonequilibrium phases and 'nonphase' clusters in these three situations [11].

It was previously shown for nano-multilayered TiAlCrSiYN/TiAlCrN coatings (for different cutting conditions [23]) that a variety of tribofilms form on the friction surface. They include protective triboceramics with sapphire and mullite crystal structure, protective and lubricious amorphous-like Al-O phase, and a variety of Cr-O triboceramics. The Mullite phase has a noticeably lower thermal conductivity than sapphire [24]. The amorphous-like Al-O phase, with its lack of a crystalline order, has lower thermal conductivity as compared to the crystalline phase [25]. This low thermal conductivity is attributed to the smaller crystal size and strong phonon scattering at the poorly interconnected nano-crystal boundaries of amorphous-like phases (boundary scattering)[26]. The amorphous-like tribofilms also exhibit super-plasticity [27]. This type of tribofilms, in conjunction with the lubricating chromium oxides, promotes energy dissipation [3]. Together, the synergistic, multi-functional, behavior of the tribofilms results in a high thermal barrier and provides energy dissipative properties on the frictional surface. In addition, non-protective, Ti-based tribo-ceramics were observed [20]. Table 4.4 presents the summarized data on the chemical composition of the tribofilms based on the XPS analysis.

Table 4.4 Phase and chemical composition of worn surface

	Aluminum at%				Titanium at%			Chromium at%	
Sample	Al-Aldangling bonds	Al2O3	Mullite	Nitride	TiOx	TiO2	Nitride	CrxOy	Nitride
S60	6.73%	25.74 %	0.70 %	1.50%	6.90 %	7.90 %	1.60 %	6.77 %	0.10 %
S40	0.40%	28.20 %	1.90 %	21.00 %	7.80 %	6.20 %	1.68 %	2.80 %	1.20 %
S60/40	0.23%	34.80 %	2.60 %	15.50 %	8.03 %	8.05 %	2.90 %	1.70 %	2.60 %

At the higher cutting speed of 60 m/min, a noticeable amount of various Al-O-based phases was observed (Al2O3 and Mullite) during the running-in stage. The formation of lubricious Cr-O phases was also relatively intensive (6.77%). Complex Al-O/Cr-O tribo-oxides formed, resulting in lower thermal conductivity and better surface protection [20]. At the same time, a high amount of dangling bonds (6.73%) indicates the formation of amorphous-like tribo-ceramics with high thermal protection and energy dissipation [28]. The formation of non-protective Ti-O phases is also considerable. This will eventually result in intensive cratering on the rake surface and a reduction in tool life (Figure 4.1).

At the lower cutting speed of 40 m/min, Al-Al dangling bonds were generated in very small amounts. A similar amount of protective Al-O phases formed as compared

to S60. The generation of Cr-O lubricating phases was also similar. In addition, high amounts of the non-protective Ti-O phases were observed as well.

Compared to S40, S60 resulted in a relatively accelerated rate of tribo-oxidation during the running-in stage. Even though S60 generated slightly smaller amounts of the various protective Al-O phases compared to S40, the S60 sample formed significantly higher amounts of Al-Al dangling bonds, which are related to an amorphous phase formation with high thermal protection [29, 30]. This results in overall better surface protection/lubrication during the running-in stage of wear (Figure 4.2, Figure 4.3, Figure 4.4, Figure 4.5). Higher amounts of energy-dissipating tribo-phases result in better tribological performance at the chip/tool interface. However, a slightly diminished amount of the protective Al-O phases in S60 along with a somewhat increased amount of non-protective Ti-O phases resulted in worse tool life in the long run; S60 performed at only 80% of the tool life of S40.

Cutting at 60 m/min with subsequent slow down to 40 m/min resulted in intensive tribo-oxidation activity, with the formation of an increased amount of protective Al-O phases as compared to both the S60 and S40 samples. Formation of the mullite phase was limited but slightly higher than in the S40 sample. Only a small amount of Al-Al dangling bonds was observed, which indicated that energy dissipative tribo-phases could not stay on the surface or be generated when a lower cutting speed of 40 m/min was used. Formation of the various protective Al-O tribo-phases in the

beginning of wear resulted in enhanced surface protection. Lubricating tribo-oxides and non-protective Ti-O phases were lower than S60 but similar to S40 samples. Most importantly, in the 60/40 test, protective alumina tribo-films were intensively formed during the initial speed up and were not completely worn out in the following slow down to 40 m/min. In this way, better surface protection was established leading to the observed longer tool life.

Under a higher cutting speed, less intensive built-up edge formation can be explained by the higher temperature reached at the tool/chip interface. At higher cutting speeds, the tool/chip interface becomes hot enough to reduce seizure and diminish the formation of built-up edge. But this does not improve tool life at 60 m/min. In this case another variable has to be considered: the properties of the tribofilms. One important feature of the tribofilms generated on the friction surface of the adaptive coatings is their extremely high protective ability. The thermal properties and lubrication conditions are changed radically on the friction surface once the tribofilms are formed [31, 32]. In our research these dynamically re-generating surface films have been studied by Auger Electron Spectroscopy (AES) depth profiling. S60 showed the best tribological/wear behavior at 200 meters of cut, so it was chosen to be studied for Al-O tribofilms by AES (Figure 4.7).

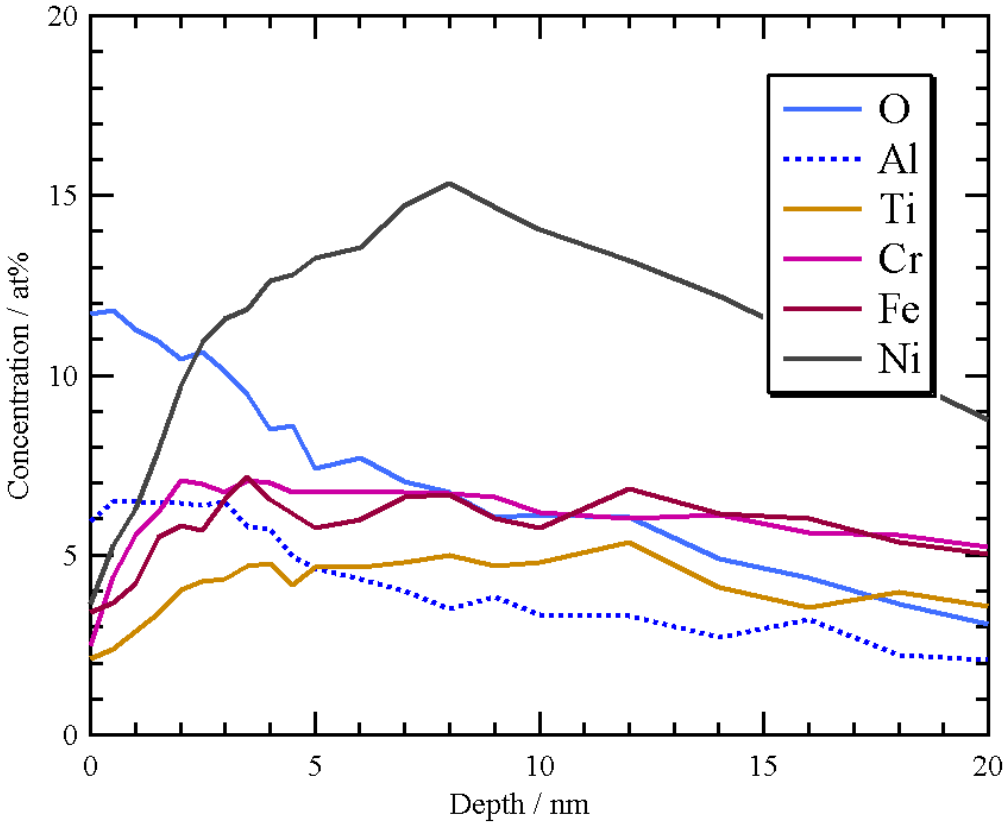

Figure 4.7 Auger depth profile for Thickness of the tribo-films

The thickness of the Al-O tribofilms, which are the major tribo-phase formed during friction, can be measured through AES depth profiling as presented in Figure 4.7. The surface of the worn coating close to the area of built-up edge formation on the rake face was studied. An increase in Ni content, which is a major element of the workpiece material, shows the area of built-up edge. The concentration of Oxygen and Aluminum indicate that the thickness of the protective Al-O tribo-ceramic is around 5 nanometers. Based on this it is concluded that the thickness of the tribo-films is within the nano-scale level.

4.4 Conclusions

A method to improve the adaptive performance of wear resistant coatings during machining of hard-to-cut DA 718 aerospace alloy with intensive built-up edge formation was achieved through the optimization of machining conditions. Cutting conditions strongly affect the generation of tribofilms on the friction surface of adaptive coatings. Using an initial elevated cutting speed during the running-in stage of wear followed by a subsequent slow down results in a noticeable tool life increase for a cutting tool when using an adaptive TiAlCrSiYN/TiAlCrN multilayer PVD coating when machining the DA718 alloy.

AES depth profiling was used to evaluate the spatial characteristics of the tribofilms formed. It was shown that nano-scale tribofilms were formed during operation. XPS analysis was used to detect the variety of tribofilms formed during cutting, including sapphire-like Al2O3, mullite-like Al6Si2O3, TiOx, TiO2, and polyvalent chromium oxides in three cutting conditions. An SEM/EDX and an Optical microscopy were used to assess wear mechanisms.

It was shown that using elevated cutting speed at the beginning of the wear process results in intensive formation of thermal protective tribo-ceramic phases and lubricious tribo-films, which results in better frictional conditions at the chip/tool interface. With a subsequent slow down the protective tribo-ceramics generated at the

beginning of cutting process are prevented from being totally worn out and thus partially stay on the friction surface, which leads to an overall increase in tool life. In this way, it was shown that optimizing the cutting conditions is a good method of controlling tribofilm formation in order to achieve better tool life for the entire surface engineered system.

Acknowledgement

Authors gratefully acknowledge funding support from the NSERC discovery grant program.

References

[1] P. Fallböhmer, C. Rodríguez, T. Özel, T. Altan, High-speed machining of cast iron and alloy steels for die and mold manufacturing, Journal of Materials Processing Technology, 98 (2000) 104-115.

[2] J.P. Davim, Machining of hard materials, Springer2011.

[3] G. Fox-Rabinovich, G.E. Totten, Self-organization During Friction: Advanced Surface-engineered Materials and Systems Design, CRC Press2006.

[4] G. Fox-Rabinovich, G.E. Totten, Self-organization During Friction: Advanced Surface-engineered Materials and Systems Design, CRC Press2010.

[5] E. Ezugwu, J. Bonney, Y. Yamane, An overview of the machinability of aeroengine alloys, Journal of Materials Processing Technology, 134 (2003) 233-253.

[6] G.S. Fox-Rabinovich, K. Yamamoto, B. D Beake, I. S Gershman, A. I Kovalev, S. C Veldhuis, M. H Aguirre, G. Dosbaeva, J. L Endrino, Hierarchical adaptive nanostructured PVD coatings for extreme tribological applications: the quest for nonequilibrium states and emergent behavior, Science and Technology of Advanced Materials, 13 (2012) 043001.

[7] G.S. Fox-Rabinovich, K. Yamamoto, B.D. Beake, A.I. Kovalev, M.H. Aguirre, S.C. Veldhuis, G.K. Dosbaeva, D.L. Wainstein, A. Biksa, A. Rashkovskiy, Emergent behavior of nano-multilayered coatings during dry high-speed machining of hardened tool steels, Surface and Coatings Technology, 204 (2010) 3425-3435.

[8] D.-Y. Wang, Y.-W. Li, W.-Y. Ho, Deposition of high quality (Ti, Al) N hard coatings by vacuum arc evaporation process, Surface and Coatings Technology, 114 (1999) 109-113.

[9] J. Woo, J. Lee, S. Lee, D. Lee, High-temperature oxidation of Ti0. 3Al0. 2N0. 5 thin films deposited on a steel substrate by ion plating, Oxidation of Metals, 53 (2000) 529-537.

[10] A. Kovalev, D. Wainstein, G. Fox‐Rabinovich, S. Veldhuis, K. Yamamoto, Features of self‐organization in nanostructuring PVD coatings on a base of polyvalent metal nitrides under severe tribological conditions, Surface and Interface Analysis, 40 (2008) 881-884.

[11] A. Kovalev, D. Wainstein, A. Rashkovskiy, G. Fox‐Rabinovich, S. Veldhuis, M. Agguire, K. Yamamoto, Investigation of electronic and atomic structure of tribofilms on the surface of cutting tools with TiAlCrSiYN and multilayer TiAlCrSiYN/TiAlCrN coatings during machining of hardened steels, Surface and Interface Analysis, 42 (2010) 1368-1372.

[12] A. Voevodin, J. Zabinski, Nanocomposite and nanostructured tribological materials for space applications, Composites science and technology, 65 (2005) 741-748.

[13] G. Fox-Rabinovich, B. Beake, K. Yamamoto, M. Aguirre, S. Veldhuis, G. Dosbaeva, A. Elfizy, A. Biksa, L. Shuster, Structure, properties and wear performance of nano-multilayered TiAlCrSiYN/TiAlCrN coatings during machining of Ni-based aerospace superalloys, Surface and Coatings Technology, 204 (2010) 3698-3706.

[14] I. Gershman, N. Bushe, A. Mironov, V. Nikiforov, Self-organization of secondary structures in friction, Trenie i Iznos, 24 (2003) 329-334.

[15] G. Fox-Rabinovich, K. Yamamoto, B. Beake, A. Kovalev, M. Aguirre, S. Veldhuis, G. Dosbaeva, D. Wainstein, A. Biksa, A. Rashkovskiy, Emergent behavior of nano-multilayered coatings during dry high-speed machining of hardened tool steels, Surface and Coatings Technology, 204 (2010) 3425-3435.

[16] G. Fox-Rabinovich, J. Endrino, M. Aguirre, B. Beake, S. Veldhuis, A. Kovalev, I. Gershman, K. Yamamoto, Y. Losset, D. Wainstein, Mechanism of adaptability for the nano-structured TiAlCrSiYN-based hard physical vapor deposition coatings under extreme frictional conditions, Journal of Applied Physics, 111 (2012) 064306.

[17] A.N.S. Institute, Tool Life Testing with Single-point Turning Tools, American Society of Mechanical Engineers1986.

[18] S. Jacobson, S. Hogmark, Tribofilms—on the crucial importance of tribologically induced surface modifications, Recent developments in wear prevention, friction and lubrication, 661 (2010) 197-225.

[19] K.-D. Bouzakis, N. Michailidis, G. Skordaris, E. Bouzakis, D. Biermann, R. M'Saoubi, Cutting with coated tools: Coating technologies, characterization methods and performance optimization, CIRP Annals-Manufacturing Technology, 61 (2012) 703-723.

[20] G.S. Fox-Rabinovich, K. Yamamoto, B.D. Beake, I.S. Gershman, A.I. Kovalev, S.C. Veldhuis, M.H. Aguirre, G. Dosbaeva, J.L. Endrino, Hierarchical adaptive nanostructured PVD coatings for extreme tribological applications: the quest for nonequilibrium states and emergent behavior, Science and Technology of Advanced Materials, 13 (2012) 043001.

[21] J.-M. Lehn, Toward self-organization and complex matter, Science, 295 (2002) 2400-2403.

[22] G. Fox-Rabinovich, A. Kovalev, S. Veldhuis, K. Yamamoto, J. Endrino, I. Gershman, A. Rashkovskiy, M. Aguirre, D. Wainstein, Spatio-temporal behaviour of atomic-scale tribo-ceramic films in adaptive surface engineered nano-materials, Scientific reports, 5 (2015).

[23] G. Fox-Rabinovich, A. Kovalev, M. Aguirre, K. Yamamoto, S. Veldhuis, I. Gershman, A. Rashkovskiy, J. Endrino, B. Beake, G. Dosbaeva, Evolution of self-organization in nano-structured PVD coatings under extreme tribological conditions, Applied Surface Science, 297 (2014) 22-32.

[24] R. Torrecillas, J.M. Calderón, J.S. Moya, M.J. Reece, C.K. Davies, C. Olagnon, G. Fantozzi, Suitability of mullite for high temperature applications, Journal of the European Ceramic Society, 19 (1999) 2519-2527.

[25] S. Grasso, N. Tsujii, Q. Jiang, J. Khaliq, S. Maruyama, M. Miranda, K. Simpson, T. Mori, M.J. Reece, Ultra low thermal conductivity of disordered layered p-type bismuth telluride, Journal of Materials Chemistry C, 1 (2013) 2362-2367.

[26] M. Barsoum, M. Barsoum, Fundamentals of ceramics, CRC Press2002.

[27] T.-G. Nieh, J. Wadsworth, O.D. Sherby, Superplasticity in metals and ceramics, Cambridge university press2005.

[28] B.D. Beake, G.S. Fox-Rabinovich, Y. Losset, K. Yamamoto, M.H. Agguire, S.C. Veldhuis, J.L. Endrino, A.I. Kovalev, Why can TiAlCrSiYN-based adaptive coatings deliver exceptional performance under extreme frictional conditions?, Faraday Discussions, 156 (2012) 267-277.

[29] F. Ma, K.W. Xu, Using dangling bond density to characterize the surface energy of nanomaterials, Surface and Interface Analysis, 39 (2007) 611-614.

[30] D. Wainstein, A. Kovalev, D. Tetelbaum, A. Mikhaylov, A. Belov, Investigations of SiC semiconductor nanoinclusions formed by sequential ion implantation and annealing in thermally oxidized Si, Surface and Interface Analysis, 40 (2008) 571-574.

[31] E.R. Dobrovinskaya, L.A. Lytvynov, V. Pishchik, Sapphire: material, manufacturing, applications, Springer Science & Business Media2009.

[32] R.J. Angel, C.T. Prewitt, Crystal structure of mullite; a re-examination of the average structure, American Mineralogist, 71 (1986) 1476-1482.

Chapter 5

Control of Tribofilms Formation in Dry Machining of Hardened AISI D2 Steel by Tuning the Cutting Speed

Complete citation:

Yuan, Junfeng, German S. Fox-Rabinovich, and Stephen C. Veldhuis. “Control of tribofilms formation in dry machining of hardened AISI D2 steel by tuning the cutting speed" Submitted to Wear, 2017.

Copyright:

Relative Contributions:

Junfeng Yuan:	Designed and performed all experiments, interpretation and analysis of the data and wrote the manuscript including preparing all figures and text.
G. S. Fox-Rabinovich:	Offered suggestions on the design of experiments and with writing.
S. C. Veldhuis:	Provided supervisor for the experiments and was responsible for the final draft submitted to the journal.

Preface:

This chapter studied the control of tribofilms formation when machining D2 steel. A Mitutoyo TM microscope was used to measure flank wear width. According to the ISO 3685, tool life should take both flank wear and crater wear into account. In this study flank wear was only considered as the major criteria of tool life. In the future more cutting tests are needed in order to develop this method into a statistical strategy to tune cutting speed.

Control of tribofilms formation in dry machining of hardened AISI D2 steel by tuning the cutting speed

Junfeng Yuan [a], German S. Fox-Rabinovich [a], Stephen C. Veldhuis [a]

a Department of Mechanical Engineering, McMaster University 1280 Main St., W. Hamilton, ON, Canada L8S 4L7

Abstract

This study focussed on the investigation of tribofilms which were formed as a result of mass transfer of workpiece material to the tool surface with further tribo-oxidation occurring through interaction with the environment. Based on the current understanding, the formation of tribofilms is enhanced by high temperatures which are brought on by higher cutting speeds with their beneficial properties further impacting the friction and wear process. Wear performance of uncoated ceramic (mixed alumina and TiCN) tools were studied at different constant cutting speeds (50; 80; 100 and 120 m/min) and tuned cutting speeds (120-100 and 120-100-80 m/min) during hard dry turning of AISI D2 tool steel. The tuning of the cutting speed was performed in order to enhance the generation of favourable tribofilms and obtain an extended tool life. During

the tuning of the cutting speed, tribofilms generated at higher speeds were not completely worn out and were found to improve the friction/wear process when subsequently shifting to a lower cutting speed. This study of tribofilms has offered better insight into the understanding of wear behaviour over a range of different cutting conditions and provides a novel approach to enhance the efficiency of the machining process.

Keywords:

Tribofilms; Tribo-oxidation; Hard turning of D2 steel; X-ray photoelectron spectroscopy; Auger Electron Spectroscopy; Tuning cutting speeds

5.1 Introduction

In some applications dry machining processes are preferred from a cost-saving, logistics and environmental perspective over conventional wet machining operations, as shown in the developments of dry machining [1-3]. Furthermore, avoiding the thermal shock associated with wet machining can greatly reduce the fatigue loading a tool experiences as demonstrated [2]. In addition improved surface integrity has also been

associated with dry machining, as presented by Davim in studies of dry machining of hardened steels [4-6].

In machining, coolant is involved in removing heat from the cutting zone and providing lubrication at the friction surface. When machining without coolant, especially during dry high speed machining of hard materials the tools are exposed to harsh tribological conditions and chips are not easily flushed out of the cutting zone, especially when machining sticky materials like aluminum or stainless steel or during deep hole drilling. Chip motion along the secondary shear deformation zone can generate extremely high temperatures at the cutting tool / chip interface that may reach or exceed the diffusion and bonding limits of the cutting tool materials. This situation leads to rapid tool wear and poor surface finish of the machined parts [4, 7, 8].

Among cutting tool materials such as high speed steel (HSS), poly-crystalline diamond (PCD), ceramics (based on alumina (Al_2O_3) or silicon nitride (Si_3N_4)) and polycrystalline cubic boron nitride (PcBN), PCD cannot be used to machine steel due to the reaction between carbon and iron at high temperatures [4, 9]. Coated HSS are widely used in drilling operations where additional toughness is needed [10], however they are not suitable to cut hardened workpiece material especially under aggressive dry machining conditions due to their relatively low hardness. Ceramic and PcBN are most widely used for machining of hardened steel, while more expensive PcBN are primarily used in finish hard turning [11, 12]. PVD/CVD coatings are widely used in these

machining applications due to their high wear resistance, thermal shock protection and lubricating properties, all of which serve to extend tool life under dry high speed machining. However under severe tribological cutting conditions, ceramic or PcBN tools with hard coatings sometimes perform even worse than uncoated tools [13]. For the testing performed in this study uncoated mixed ceramic cutting inserts (Al_2O_3+TiCN) were chosen as they are least likely to provide material that would impact tribofilms formation and thus the influence of the workpiece material on tribofilms formation could be studied [14, 15].

In general the formation of tribofilms plays an important role in friction and wear behaviour during dry machining of hardened material. This operation represents a high temperature and heavily loaded tribo-system where the formation of tribofilms has a large impact on tool life and process performance [16, 17]. Complex tribofilms are formed on the friction surface under severe cutting conditions. These thin films work as a dynamic nanostructure oxide film that serve to protect the underlying tool substrate at the tool/chip or tool/workpiece interface. Tribofilms are generated as a result of a self-adaptive process that occurs between the tool and the workpiece on the friction surface [18]. Tribofilms act as a thermal barrier and help eliminate thermal shock as well as protect the surface from oxidation wear. Thus both the physical and chemical properties on the friction surface are significantly improved due to the formation of beneficial tribofilms [19-21].

Formation of various tribofilms have been reported as a result of tribo-oxidation of cutting tools [22], as well as the result of workpiece material transfer during tool/chip interaction [19, 20]. There are three major sources of tribofilms: 1) tool surface modification with further tribo-oxidation resulting during the cutting process [22]; 2) workpiece material transfer during tool/chip contact in machining [19], and lastly tribofilms formation through the interaction between the tool surface and the cutting environment, for instance through material supplied through the coolant and other lubricants [18, chapter 12].

Hard to machine materials with hardness above 45 HRC have been increasingly applied in industry, such as hardened alloyed steels, tool steels, aerospace super alloys, with the machining of materials with the hardness of 58-68 HRC representing a significant challenge [4]. W Grzesik[10], V.N. Gaitonde [23] and Tugrul Ozel [24] investigated turning of hardened steels with hardness above 58HRC using different ceramic tools. Under dry cutting conditions, the range of cutting speeds was between 80 m/min and120 m/min. Within this range of cutting speeds for machining of hardened D2 (with the hardness around 58 HRC), 100 m/min is a level preferred by industry taking into account the balance between the relative lower wear rate and higher productivity. This value also considers the quality of the machined component's surface. Negative rake angles are preferred during hard machining to obtain maximum tool stiffness and cutting edge support, however the frictional interface area and

amount of heat generation during machining are intensified due to the use of negative rake angles. Simultaneously a larger feed rate and depth of cut can increase the probability of the immediate fracture of a tool insert. Therefore combinations of moderate feed rate and relatively small depth of cut are commonly used when machining hardened steels [25].

5.2 Experimental

5.2.1 Workpiece material

The high carbon and high chromium content AISI D2 steel is selected as the workpiece material in this experiment. Table 5.1 presents the chemical composition of this D2 steel. D2 steel was subjected to austenization at 1000-1040℃, oil quenching and two tempers at 430-450℃, leading to a hardness of 58.7 ± 0.5 HRC.

Table 5.1 Chemical composition of workpiece material

wt%	C	Si	Mn	S	P	Ni+Cu	Cr	Mo	V
D2	1.52	0.32	0.28	0.001	0.026	0.3	11.54	0.73	0.58

5.2.2 Cutting experiments

All turning tests were performed on an Okuma Crown L1060 CNC lathe. Cutting inserts were removed after each pass for inspection of the flank wear land width (Vb)

using a Mitutoyo TM microscope. The tool life was quantified as the accumulated length of cut upon reaching V_b = 300 µm. In this study, cutting speed for machining D2 steels were set in four stages; (1) Regular cutting speed is considered to be 100 m/min based on current industrial practice, (2) Higher cutting speed of 120 m/min was set to accelerate the formation of tribofilms, (3) lower cutting speed of 80 m/min was used to reduce the wear rate and (4) the lowest cutting speed of 50 m/min was chosen as a mild cutting condition which would minimize the intensity of wear. Tuning of the cutting speed at the beginning of the wear process was performed by using a higher cutting speed followed by a commonly used cutting speed. Two tuning methods were performed in this study; (1) 120 m/min in the beginning then down to 80 m/min, as shown in figure 4, (2) 120 m/min in the beginning, decreased to 100 m/min for a few paths and finally down to 80 m/min until the end of tool life as shown in figure 5.1.

Dry cutting conditions were used for all cutting tests, a constant feed rate (f) of 0.075mm/rev and the depth of cut of 0.10mm were used. Sumitomo CNGA432NB90S (70% Al_2O_3+ 30% TiCN) mixed alumina inserts were held in a Kenclamp DCLNL166DKC4 tool holder for all experiments. The following Table 5.2 showed the details for the ceramic tool inserts. Prior to each cutting pass, the workpiece was pre-machined using a separate insert at a relative lower cutting speed (V = 30 m/min) and higher depth of cut (DOC = 1 mm) to remove any possible work hardened layer from the previous pass.

Table 5.2 Tool inserts detail properties

Insert hardness	Nose radius	Rake angle	Clearance angle	Setting angle
2000HV	0.313inch	-5°	0°	95°

5.2.3 Tool surface characterization

A TESCAN VEGA LSU scanning electron microscope (SEM) was used to analyze tool wear mechanisms and assess the morphology of the worn cutting inserts. A JEOL JAMP-9500F EDX system with mapping capability was used for studying the chemical composition near the surface in the worn area on the cutting insert.

To understand the nature of tribofilms forming at different cutting speeds, the rake surface of the worn cutting inserts was characterized by using three methods: 1) XPS, 2) AES on the surface; 3) surface and subsurface layers were characterized by EDX. Even though XPS could obtain more accurate quantitative results as compared to AES, AES provides higher lateral resolution data on the tribofilms. The X-ray photoelectron spectroscopy (XPS) equipment consisted of a Physical Electronics (PHI) Quantera II spectrometer with a hemispherical energy analyzer, an Aluminum (Al) anode source for X-ray generation, and a quartz crystal monochromatic for focusing the generated X-rays. The X-ray source was from a monochromatic Al K-α (1486.7eV) at 50W-15kV and the system base pressure was between 1.0x10-9 to 2.0x10-8 Torr. At the beginning, the samples were sputter-cleaned for around 5 minutes with a 4kV Ar+ beam before

collecting the data. The beam diameter for data collection was 50 μm, and all spectra were obtained at a 45˚ take off angle. A dual beam charge compensation system was utilized to ensure neutralization of all samples. The pass energy to obtain all survey spectra was 280eV, while to collect all high-resolution data it was 69eV. The instrument was calibrated with a freshly cleaned Silver (Ag) reference foil, where the Ag 3d5/2 peak was set to 368eV. All data analysis was performed in PHI Multipak version 9.4.0.7 software.

Compared to the 50 μm beam diameter typical of the XPS, Auger electron spectra (AES) offers a better resolution down to a few tens of nanometers. AES spot analysis is the most direct and most often used mode for this instrument. This analysis was performed to collect the tribofilms information on the worn surface. Spot analysis AES data were collected from three sites on the rake face separately, using a JEOL JAMP-9500F Field Emission Auger Microprobe. The electron beam carried a 10 keV accelerating voltage and a 40 nA current, under which the lateral resolution was approximately 30 nm. An Argon ion beam was used for sputter cleaning at the beginning of the analysis. The Auger spectra were finally quantified in order to determine the atomic compositions of the tribo-oxides on the worn tool surface.

5.3 Result and Discussion

5.3.1 Tool life at different cutting speeds

Tool life and the quality of the machined surface are the main characteristics that are monitored during the machining process. Figure 5.1 illustrates tool life under four dry turning conditions employing different cutting speeds, in which flank wear, V_b, is a function of the length of cut. Because the recommended cutting speed for this ceramic insert during machining of the hardened D2 material is 100 m/min, the cutting speeds were selected for the experiments were 50, 80, 100 and 120m/min. With an increase in the cutting speed, flank wear rate tends to be lower within the initial (running-in) stage. The cutting inserts with 100 and 120 m/min cutting speed obtained a reduced tool life even though they experienced a lower flank wear rate as compared to the 80 m/min. This was due to catastrophic failure that may be attributed to chipping resulting from severe thermal and mechanical damage associated with the higher cutting speeds.

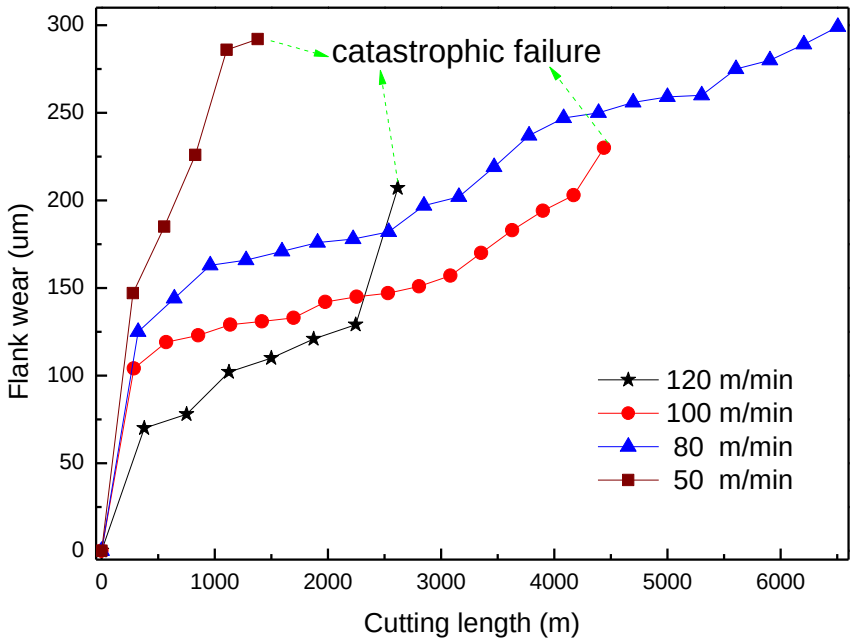

Figure 5.1 Wear curves at different cutting speeds

5.3.2 Wear mechanism under different cutting conditions

Figure 5.2 presents the SEM images of the inserts after 900 meters length of cut at the speeds of 50, 80, 100 and 120 m/min. With an increase in the cutting speed severe crater wear appeared while less intensive flank wear and a lower intensity of build-up edge formation was observed. Under the highest cutting speed of 120 m/min, the deepest crater wear with the largest area on the rake surface was observed; while at the lowest cutting speed 50 m/min, the crater wear was negligible. On the contrary the thickest build-up edge on the rake face was found to form, but the flank wear intensity was the highest with noticeable notch wear as compared to 120 m/min. This agreed with the results presented elsewhere [6], which show that at lower cutting speeds the

wear zone is located at the tool nose radius while it slides toward the secondary shear deformation zone with an increase in cutting speed. In all cases the flank wear was due to abrasion.

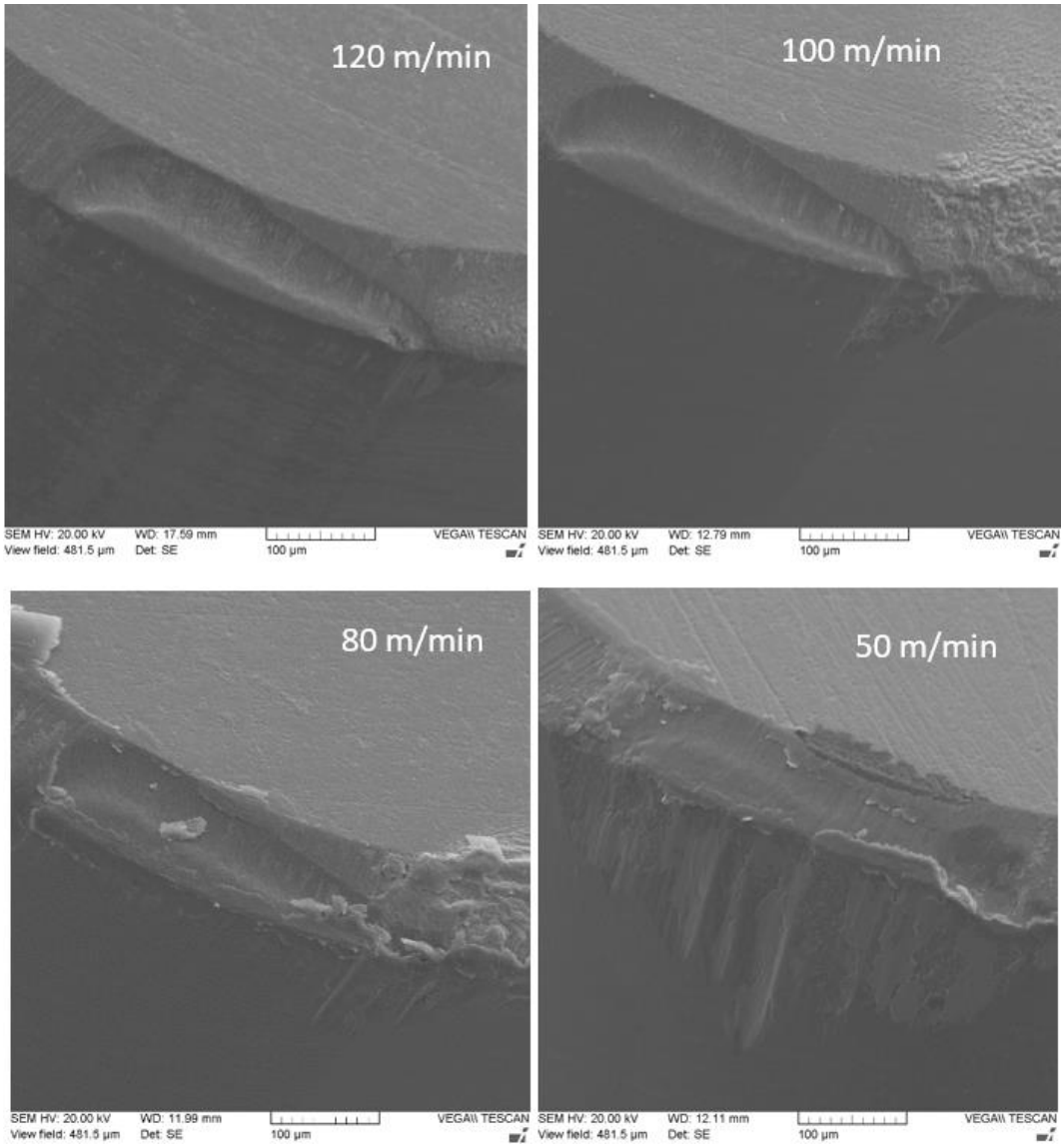

Figure 5.2 Cutting edge after 200 meter length of cut

5.3.3 Adaptive behaviour

The tribofilms were characterized by XPS on the tool tips after 900 meters of cutting length at different cutting speeds. XPS is a surface technique which is sensitive to the surface roughness condition. Therefore it was performed within the running-in stage where the surface geometry and roughness were comparable among the cutting tools tested at the different cutting speeds. In addition the surface roughness of the cutting edge was relatively better at the beginning of the cutting process, providing a more suitable surface condition to perform XPS characterization as XPS has tight surface finish requirements to achieve a reliable measurement.

Tribofilms enhance wear behaviour of cutting in two ways: (1) they work as a thermal barrier layer between the chip and cutting tool to lower the thermal conductivity of the corresponding tribo-oxides; and/or (2) by acting as an in-situ lubricant to reduce the intensity of workpiece material sticking [22]. Chromium promotes the formation of high-temperature stable tribo-oxides [22]. Cr_2O_3 has a corundum structure with the same order of magnitude in hardness and thermal properties as sapphire. These two characteristics promote reducing the adhesive interactions at the tool/chip interface and the heat generation during the cutting process. Meanwhile at high temperature, the Cr-O was also reported as a lubricous oxygen-containing tribofilms, which could prevent intensified chemical and oxidative

wear during high speed cutting [18, 26]. The cutting zone has a very strong temperature gradient, the highest temperature is reached on the rake face in the area where the depth of crater wear is maximum. CrO_3 has a low melting point and it could act as a lubricant especially within the sticking zone between the tool and the chips, where coolant cannot reach into this interface region even under high pressure wet machining conditions.

Table 5.3 XPS on tool tip for D2 within running-in stage

	Type and amount of tribo-oxide		
Speed	Cr2O3	CrO3	Total%
50 m/min	45.9	15.6	61.5
80 m/min	48.7	16.9	65.6
100 m/min	53.0	18.6	71.6
120 m/min	52.2	18.4	70.6
120-100 m/min	54.1	24.9	79.0

Table 5.3 showed the summarized results for the chemical composition of the tribofilms based on the XPS analysis. At all cutting conditions, protective and lubricating Cr-O tribofilms were observed during the running-in stage. When the cutting speed was increased up to100 m/min. the total amount of Cr-O tribofilms increased as well. However at the speed of 120 m/min the total amount of tribo-films was similar to the conditions found at 100 m/min. This is attributed to the higher speed of chip removal

and the shorter contact time between the chip and the tool which reduces the local intensity of all of the phases of the wear process.

Parameters affecting tribology during machining are complex. In general, with the increase in cutting speed, the temperature in the cutting zone and the material removal rate would be higher while the contact time between tool/chip and the cutting force would be lower. During the cutting of the hardened D2 steel, workpiece/chip would be soften at the elevated temperature associated with the higher cutting speeds, whereas the shorter contact time would make this tempering softening less impactful [27].

5.3.4 Tuning of cutting speeds for longer tool life

The results obtained could be used to enhance wear performance through the optimization of cutting conditions. A method was reported to improve tool life and machined surface through using an initial higher speed during the running-in stage of wear followed by a subsequent reduction in cutting speed for the remainder of the cutting time to reduce the intensity of wear [28]. A similar tuning method was applied in this study; performing higher cutting speed (120 m/min) after 900 meter of cutting length, then slowing down the cutting speed to a lower level (100 m/min). This tuning of speed from 120 to 100 m/min resulted in a 21.6% increase in tool life as compared to cutting at 100 m/min for the whole machining process. The results of the XPS analysis of

the Cr_2O_3 and CrO_3 are presented in Table 5.3. Tuning of the cutting speeds from an initial speed of 120 m/min with a subsequent reduction to 100 m/min resulted in the formation of protective/lubricating Cr-O tribofilms, compared to both 120 and 100 m/min conditions performed alone. After the initial high speed condition the formation of an increased amount of tribo-films was found to slowdown wear resulting in less intensive removal of the beneficial tribo-films from the friction surface over time leading to a larger magnitude of tool life increase.

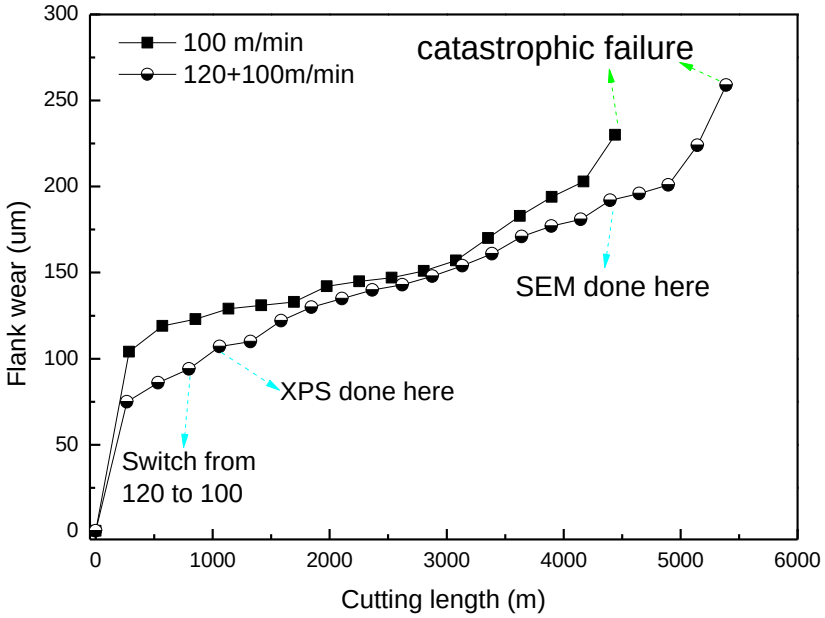

Figure 5.3 Wear curve and photoelectron spectra of tuned cutting speeds (120-100 m/min)

When altering the cutting speeds, more intensive protective/lubricating tribofilms formed during the higher cutting speeds were not completely worn away and would work in synergy with the newly generated tribofilms that would continue to form

under the subsequent lower cutting speeds. Based on the understanding of beneficial tribofilms generation the further tuning of the cutting speed was performed as shown in Figure 5.4. The first change in cutting speed occurred at the similar cutting length as in Figure 5.3; while the second adjustment was performed at 3953 meters of cutting length. Compared to a cutting speed of 100 m/min which is typical in industry, tool life at 120-100-80 m/min tuned cutting speed conditions was 99% longer as compared to the 100 m/min cutting speed alone; even compared with the cutting speed of 80 m/min, tool life was improved by 36%. Figure 5.5 presented SEM images of the worn corners after turning at 120-100 m/min at 4397 meter (Figure 5.3) and tuning of 120-100-80 m/min at 4307 meter (Figure 5.4) cutting length correspondingly. The flank wear was similar and associated mostly with abrasive wear while on the rake face of the tool under 120-100 m/min the wear condition had already started wearing aggressively near the notch wear zone. Nevertheless the tool performing under the 120-100-80 m/min condition showed smoother crater wear. At this cutting length, the tool tip geometry had changed significantly due to aggressive wear; neither the friction, cutting force nor heat flow at this point was considered to be comparable to that experienced during the running-in stage. Consequently neither XPS nor AES was performed at this stage, especially given the worse surface roughness and accumulation of mechanical damage both of which would affect the results of these surface characterization techniques. Repetition of this tuning procedure would further benefit the friction/wear process

during machining therefore it is expected that the tool life can be further improved by additional testing to improve the tuning of the cutting speeds over the full tool life.

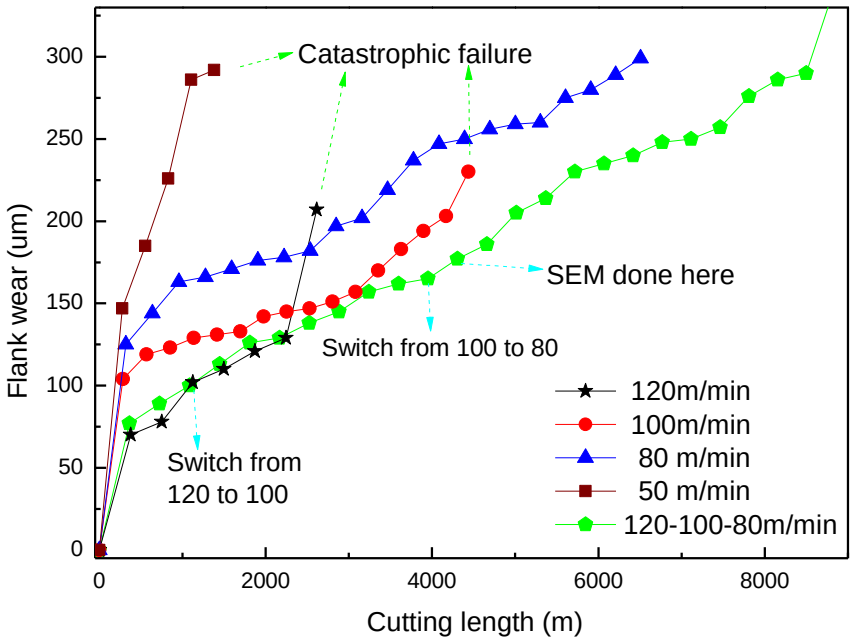

Figure 5.4 Wear curve of tuned cutting speeds 120-100-80 m/min

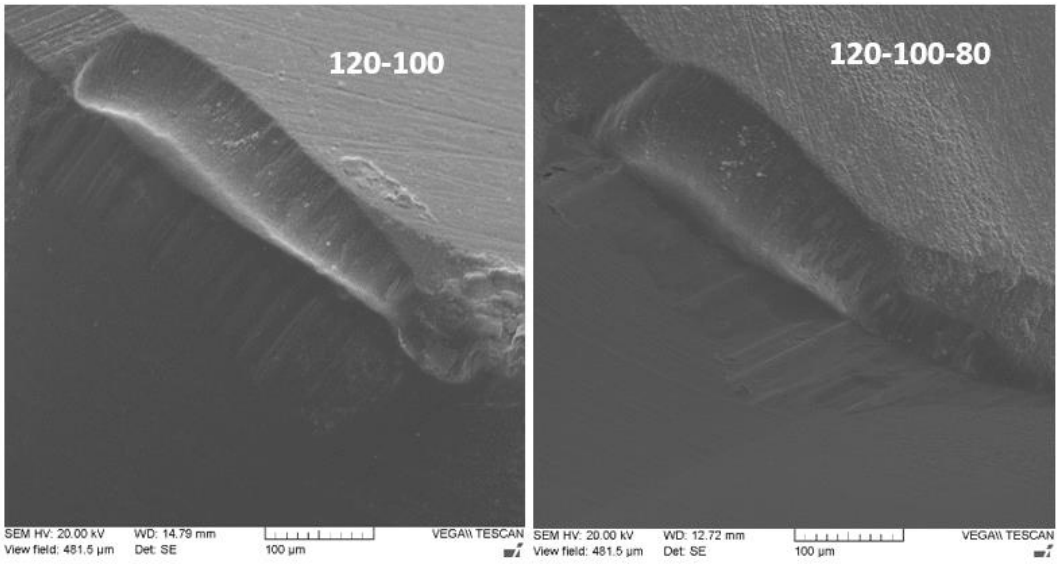

Figure 5.5 Cutting edge under different tuned cutting speeds around 4300 meters cutting length

5.3.5 Tribofilms characterization on top surface and near surface

Generation of tribofilms takes place at the tool/chip (workpiece) interface. The thickness of the tribofilms on the cutting tool is within the nano-scale range [18, 22, 29]. Considering the generation mechanism of XPS photon electron, Auger electron and Energy Dispersive X-Ray, the depth analysis volume of common XPS and AES techniques are around 10 nm while the EDX is between 0.5-3.0 microns. To get comprehensive information on the tribofilms' characteristics all these methods were tried. In this study given the nature of the tool material the tribofilms were generated through mass transfer from the workpiece material. AES and EDX were performed on the surface of the cutting tool at 100 m/min as this is the industrial recommended speed for this tool.

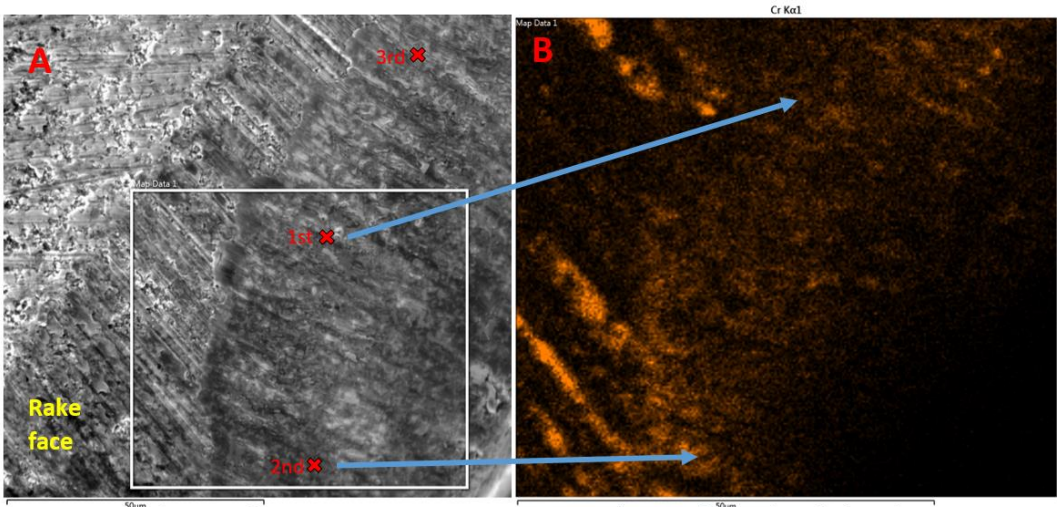

A: EDX mapping zone & AES spots B: Elemental mapping of Chromium

Figure 5.6 Rake face after 200 cutting length at 100 m/min

Rake face morphology after cutting 200 meters at 100 m/min was presented in Figure 5.6, in which A showed the EDX mapping zone (white box framed) and AES spots (three X makers) and B indicated the EDX mapping of chromium. It showed that at the near surface the distribution of chromium was not uniform. As a potential source of Cr-O tribofilms generation, it would affect the distribution of the tribofilms consequently making them uneven.

Table 5.4 Normalized AES results of O, Fe & Cr at 100 m/min

		1st spot	2nd spot	3rd spot
O		14.3 at%	26.0 at%	16.8 at%
Cr	Cr	4.0 at%	6.5 at%	0.7 at%
	Cr (Cr2O3&CrO3)	1.9 at%	11.0 at%	5.9 at%
Fe	Fe	23.5 at%	9.8 at%	15.1 at%
	Fe (Fe2O3)	0.9 at%	2.8 at%	5.1 at%

Compared to the large incident beam size of XPS at 50 microns, which shows an average amount of tribofilms formations, the better spatial resolution of AES would identify the tribo-oxides distribution on the surface within a scale of a few tens of nanometers. Table 5.4 summarized the normalized atom percentage of three different spots detected by AES, as shown in Figure 5.6. Oxygen shown in the results was from alumina in the tool substrate and hydrocarbons/organics are attributed to contamination, other than those from Fe-O and Cr-O. On average, a higher amount of chromium had been oxidized into Cr-O phases, which was significantly higher than the amount present from Fe-O phases. All characterization results indicated that the Cr-O tribofilms generation is a dominating tribo- oxidization process at the tool/chip (workpiece) interface in spite of the uneven distribution of the tribofilms on the surface of the tool.

5.4 Conclusion

Comprehensive characterization of the wear behaviour of ceramic metal cutting tools during hard turning of cold work die steel (AISI D2) was performed using uncoated ceramic (mixed alumina) inserts. The studies were performed at various cutting speeds during the initial, running-in stage of wear. Tools were tested at different constant cutting speeds of 50 m/min, 80 m/min, 100 m/min and 120 m/min to the end of tool life; to test the tuning of cutting speed and separate the role of other wear mechanisms from the higher cutting speeds a two-step cutting speed condition was tested. In the beginning of the test the cutting speed was set to 120 m/min to promote the formation of beneficial tribofilms then it was reduced to 100 m/min to reduce the aggressiveness of wear for the duration of the cut. This is referred to as the 120-100 m/min test. Similarly a three step 120-100-80 m/min test was also performed. The comprehensive characterization of the tribofilms formed on the tool's surface at different cutting speeds as well as their influence on tool life were performed using Scanning Electron Microscopy (SEM), Electron Dispersive Spectroscopy (EDX), Auger Electron Spectroscopy (AES) and X-ray Photoelectron Spectroscopy (XPS) analyses. Generation of tribofilms formed on the friction surface due to workpiece material mass transfer within the running-in stage was strongly affected by the cutting conditions.

A method to extend tool life during dry machining of hardened D2 was presented through the tuning of cutting speeds. Tool life of the 120-100-80 m/min tuned cutting speed was 99% longer as compared to the range obtained at 100 m/min (typical industrial cutting speed level); even compared to the lower cutting speed of 80 m/min, the tool life was improved by 36%. The underlying cause of this improvement at an elevated cutting speed was attributed to the intensive formation of protective/lubricating tribofilms. Their formation was accelerated by initially increasing the cutting speed during the running-in stage of wear; these highly beneficial tribofilms would partially stay on the friction surface during the subsequent slowdown in cutting speed.

When altering cutting speed, the changes in the cutting zone are complex affecting different characteristics of the cutting process such as cutting forces, temperature, etc., however tribofilms formation provides a nano-scale tribological approach to aid in better understanding of the wear behaviour under varying machining conditions. More importantly, the study of tribofilms generation offers a new strategy to improve tool life through the optimization of cutting conditions and the formation of beneficial tribofilms.

Acknowledgement

The authors would like to gratefully acknowledge the financial support received from the Natural Sciences and Engineering Research Council of Canada (NSERC) and Canadian Network for Research and Innovation in Machining Technology (CANRIMT). The authors would also like to express gratitude to Danielle Covelli for the assistance in X-ray photoelectron spectroscopy.

References

[1] Byrne G, Dornfeld D, Denkena B. Advancing cutting technology. CIRP Annals-Manufacturing Technology 2003;52:483-507.

[2] Sreejith P, Ngoi B. Dry machining: machining of the future. J Mater Process Technol 2000;101:287-91.

[3] Dudzinski D, Devillez A, Moufki A, Larrouquère D, Zerrouki V, Vigneau J. A review of developments towards dry and high speed machining of Inconel 718 alloy. International Journal of Machine Tools and Manufacture 2004;44:439-56.

[4] Davim JP. Machining of hard materials: Springer; 2011.

[5] Hashimoto F, Guo Y, Warren A. Surface integrity difference between hard turned and ground surfaces and its impact on fatigue life. CIRP Annals-Manufacturing Technology 2006;55:81-4.

[6] Fernández-Abia A, Barreiro J, De Lacalle LL, Martínez S. Effect of very high cutting speeds on shearing, cutting forces and roughness in dry turning of austenitic stainless steels. The International Journal of Advanced Manufacturing Technology 2011;57:61-71.

[7] Chou YK, Evans CJ. White layers and thermal modeling of hard turned surfaces. International Journal of Machine Tools and Manufacture 1999;39:1863-81.

[8] Matsumoto Y, Hashimoto F, Lahoti G. Surface integrity generated by precision hard turning. CIRP Annals-Manufacturing Technology 1999;48:59-62.

[9] Trent EM, Wright PK. Metal cutting: Butterworth-Heinemann; 2000.

[10] Grzesik W. Influence of tool wear on surface roughness in hard turning using differently shaped ceramic tools. Wear 2008;265:327-35.

[11] Lahiff C, Gordon S, Phelan P. PCBN tool wear modes and mechanisms in finish hard turning. Robotics and Computer-Integrated Manufacturing 2007;23:638-44.

[12] Barry J, Byrne G. Cutting tool wear in the machining of hardened steels: part II: cubic boron nitride cutting tool wear. Wear 2001;247:152-60.

[13] El Hakim M, Abad M, Abdelhameed M, Shalaby M, Veldhuis S. Wear behavior of some cutting tool materials in hard turning of HSS. Tribology International 2011;44:1174-81.

[14] Barry J, Byrne G. Cutting tool wear in the machining of hardened steels: Part I: Alumina/TiC cutting tool wear. Wear 2001;247:139-51.

[15] Ayas E, Kara A. Pressureless Sintering of Al2O3-TiCN Composites. Key Engineering Materials 2004;264:849-52.

[16] Jacobson S, Hogmark S. Tribofilms—on the crucial importance of tribologically induced surface modifications. Recent developments in wear prevention, friction and lubrication 2010;661:197-225.

[17] Bouzakis K-D, Michailidis N, Skordaris G, Bouzakis E, Biermann D, M'Saoubi R. Cutting with coated tools: Coating technologies, characterization methods and performance optimization. CIRP Annals-Manufacturing Technology 2012;61:703-23.

[18] Fox-Rabinovich G, Totten GE. Self-organization During Friction: Advanced Surface-engineered Materials and Systems Design: CRC Press; 2006.

[19] Fox-Rabinovich GS, Gershman I, Hakim MAE, Shalaby MA, Krzanowski JE, Veldhuis SC. Tribofilm Formation As a Result of Complex Interaction at the Tool/Chip Interface during Cutting. Lubricants 2014;2:113-23.

[20] Yuan J, Boyd JM, Covelli D, Arif T, Fox-Rabinovich GS, Veldhuis SC. Influence of Workpiece Material on Tool Wear Performance and Tribofilm Formation in Machining Hardened Steel. Lubricants 2016;4:10.

[21] Shalaby M, El Hakim M, Abdelhameed MM, Krzanowski J, Veldhuis S, Dosbaeva G. Wear mechanisms of several cutting tool materials in hard turning of high carbon–chromium tool steel. Tribology International 2014;70:148-54.

[22] Fox-Rabinovich GS, Yamamoto K, Beake BD, Gershman IS, Kovalev AI, Veldhuis SC, et al. Hierarchical adaptive nanostructured PVD coatings for extreme tribological applications: the quest for nonequilibrium states and emergent behavior. Sci Technol Adv Mater 2012;13:043001.

[23] Gaitonde V, Karnik S, Figueira L, Davim JP. Machinability investigations in hard turning of AISI D2 cold work tool steel with conventional and wiper ceramic inserts. Int J Refract Met Hard Mater 2009;27:754-63.

[24] Özel T, Karpat Y, Figueira L, Davim JP. Modelling of surface finish and tool flank wear in turning of AISI D2 steel with ceramic wiper inserts. J Mater Process Technol 2007;189:192-8.

[25] Arsecularatne J, Zhang L, Montross C, Mathew P. On machining of hardened AISI D2 steel with PCBN tools. Journal of Materials Processing Technology 2006;171:244-52.

[26] Fox-Rabinovich G, Kovalev A, Aguirre M, Yamamoto K, Veldhuis S, Gershman I, et al. Evolution of self-organization in nano-structured PVD coatings under extreme tribological conditions. Appl Surf Sci 2014;297:22-32.

[27] Pasko R, Przybylski L, Slodki B. High speed machining-The effective way of modern cutting. CA systems in production planning ISSN 2002:1335-3799.

[28] Yuan J, Yamamoto K, Covelli D, Tauhiduzzaman M, Arif T, Gershman IS, et al. Tribo-films control in adaptive TiAlCrSiYN/TiAlCrN multilayer PVD coating by accelerating the initial machining conditions. Surf Coat Technol 2016.

[29] Fox-Rabinovich G, Kovalev A, Shuster LS, Bokiy YF, Dosbayeva G, Wainstein D, et al. On characteristics features of alloying HSS-based deformed compound powder materials with consideration for tool self-organization at cutting 2. Cutting tool friction control due to the alloying of the HSS-based deformed compound powder material. Wear 1998;214:279-86.

Chapter 6 Conclusions and Future Work

6.1 General Conclusions

This thesis presented a new, nano-scale perspective to explain observed results: tribofilms generation on the friction surface of the tool insert significantly increases tool life. The aim of this research was to design a novel method to control beneficial tribofilms formation based on tuning of cutting parameters such as the selection of a specific cutting speed, in order to obtain improved cutting tool life, increased material removal rate, and a better machined surface quality. Comprehensive characterization of the tribofilms formed on the tool's surface as well as their influence on tool life were performed using multiple surface/near surface techniques such as AES and XPS, combined with SEM/EDS analysis.

In identifying tribofilms formation due to mass transfer from freshly cut workpiece material, dry turning of T1 and D2 steels at comparable hardness was studied under identical cutting conditions, with uncoated mixed alumina ceramic tools. A variety of lubricious Cr-O tribofilms was shown in turning of D2 while energy dissipating W-O and lubricious WO_3 were presented in turning of T1. The friction coefficient observed in

the tribo-meter tests agreed well with the analysis from hard turning, with a noticeably lower friction value for the T1 steel than D2 in the range of 800-900 °C.

In investigating the influence of cutting speed on tribofilms formation, cutting tests were performed at 50 m/min, 80 m/min and 100 m/min cutting speeds in hard dry turning of T1 and D2 steels of comparable hardness with uncoated alumina ceramic tools. Cutting conditions strongly affect tribofilms generation on the friction surface, with higher cutting speeds triggering a more intensive formation of beneficial tribofilms. In cutting D2, a higher amount of Cr-O protective and lubricating tribofilms reduced wear rate; while in cutting T1 lubricating W-O tribofilms improved tribological conditions; however, they had little impact on reducing the wear rate. In general, tribofilms formation in cutting D2 steel can be identified by the changes in wear rate, but it was very difficult to assess the coefficient of friction at different cutting speeds when cutting T1 steel. In addition, metallographic studies showed D2 steel features smaller and more evenly distributed carbide particles as compared with T1. Considering all of these factors, D2 is more suitable for studying tribofilms formation with easily measured wear rate and less influence from the distribution of carbides in the workpiece, as compared with cutting T1.

In studying the control of tribofilms formation, the tuning processes were applied to three different circumstances, which demonstrated control of tribofilms formation through 1) coated tools, 2) mass transfer from workpiece and 3) under

influence of cutting environment. When controlling the tribofilms formation through the tuning of cutting parameters or through the control of environmental factors, the changes in the cutting zone were found to be complex, affecting different characteristics of the cutting process such as cutting force, temperature, etc.

The control of the tribofilms formation with surface modification and further tribo-oxidation were performed in machining hard-to-cut DA 718 aerospace alloy with TiAlCrSiYN/TiAlCrN multilayer PVD coating under a wet condition. It was shown that using an elevated cutting speed at the beginning of the wear process resulted in intensive formation of thermal protective tribo-ceramic phases and lubricious tribofilms. Using an elevated cutting speed during the running-in stage of wear followed by a subsequent slowdown in cutting speed results in better thermal protective and frictional conditions at the chip/tool interface, and achieves improved tool life for the cutting tool.

Moreover, in studying the control of the tribofilms formation on a freshly cut workpiece due to material transfer, comprehensive characterization of tribofilms was performed in hard turning of cold work D2 steel using uncoated ceramic inserts. Two cutting strategies were applied in order to improve tribofilms formation; one is a two-step 120-100 m/min test and the other is a three-step 120-100-80 m/min test. The generation of tribofilms due to workpiece material mass transfer was strongly affected by the cutting conditions, which was revealed by the tool life extension that was achieved. As compared to the range obtained at 100 m/min which is a typical industrial

cutting speed level, tool life of 120-100 m/min tuned speed was 21.6% longer while 120-100-80 m/min tuned speed obtained a 99% increase in tool life.

In addition, when investigating controlling tribofilms formation with interaction between cutting tool surface and the cutting environment, cutting experiments were performed in machining of DA 718 with coated carbide tools under dry-wet conditions. Compared with wet cutting conditions during the running-in stage, the initial dry condition brought a lower wear rate which suggested the more intensive formation of protective tribofilms. Moreover, chip curl type and heat flow, chip under surface characteristics as well as cutting tool damage indicated that the process of tuning the cutting speed is more efficient under dry conditions than wet. This thesis highlights the importance of tribofilms, explains some aspects of their formation and demonstrates control over their formation through tooling, workpiece, process parameter and environmental control.

6.2 Research Contributions

The contributions of this thesis can be summarized as:

i. Tribofilms formation were used to explain friction and wear behaviour in machining hard materials from a nano-tribological approach. The formation of tribofilms offering thermal protection and/or in-situ

lubrication were analysed to explain some of the past performance improvements and more importantly, was designed in order to make further improvements in tool life, material removal rate and surface quality.

ii. Tribofilms generation due to mass transfer from workpiece material was validated in dry machining of hardened materials; Tribofilms formation under influence of changing cutting environment was investigated with preliminary results in dry-wet machining of Inconel DA 718 with TiAlCrSiYN/TiAlCrN multilayer PVD coated carbide tools. These studies of tribofilms formation laid the groundwork for designing a new approach to control tribofilms formation in machining.

iii. Most importantly, a novel method was presented for controlling the formation of tribofilms on the cutting tool surface during machining of hard materials. This approach was implemented by tuning the cutting speed in two separate groups of machining experiments with tribofilms generated from two different sources. 1) First was through material supplied by the base cutting tool material with coated cutting tools; and 2) the second was through the material transferred from a freshly cut workpiece with uncoated ceramic cutting tools.

6.3 Recommendations for Future Research

In addition to the tribological and wear behaviour, further study should be made into tribofilms generation under changing cutting environments, separate from the dry-wet switching condition as discussed in Section 6.1.

Moreover, a preliminary investigation of a stepwise tuned process involving cutting speed was made in Chapter 5, as 120 m/min –100 m/min – 80 m/min. This stepwise process could be further developed and applied to multiple cutting tools/workpiece materials, in order to accelerate the formation of beneficial tribofilms while decreasing the thermal or mechanical damage to cutting tools.

In addition to the XPS, AES and TEM analysis presented in this work; more surface techniques could be used to characterise tribofilms, such as Electron Energy Loss Fine Structure (EELFS), Secondary Ions Mass Spectroscopy (SIMS), Small Angle X-Ray Scattering (SAXS) and High Resolution Electron Energy-Loss Spectroscopy (HREELS) to better understand the formation of tribofilms and the role they play in friction and wear in machining.

Appendix

Preliminary Results of Tribofilms Control with Influence of Cutting Environment and Various Surface Techniques to Characterize Tribofilms

A.1 Tribofilms Formation under Influence of Cutting Environment

Preface

Chapter 4 studied control of tribofilms sourced from coated tools with further tribo-oxidation occurring during the cutting process. The formation of tribofilms is accelerated by high temperatures which are brought on by higher cutting speeds initially with their beneficial properties further impacting the friction and wear process. This work was under wet machining conditions with cutting coolant, but the higher temperature in the cutting zone could also be realized by switching from a wet environment to a dry one. The ideal tuning process would be to increase the formation of beneficial tribofilms, and at the same time to avoid the accumulation of mechanical or thermal damage to cutting tools as much as possible.

A.1.1 Experimental and Preliminary Wear Results

All cutting experiments were performed with the same tools, workpiece materials and machine, using the same parameters except cutting coolant. The cutting tests in chapter 2 were all wet with cutting coolant, while this work is using dry-wet conditions. The procedure for dry-wet cutting is to cut without coolant in the beginning for 100 meter cutting length, then switch to wet conditions with cutting coolant to the end of tool life.

Figure A.1 illustrates the flank wear as a function of cutting length under wet and dry-wet conditions. Even though the difference of tool life between these two processes is small, the wear rate of the dry-wet process is lower than the all wet process up to the 700 metre cutting length.

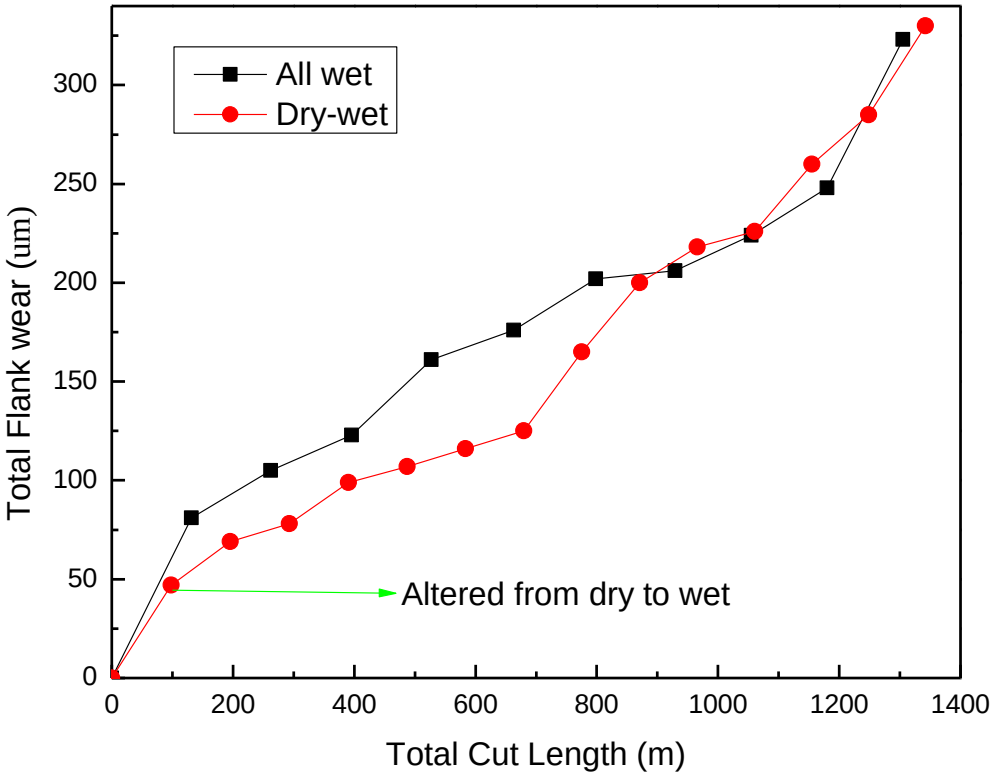

Figure A.1 Flank wear at wet and dry-wet conditions

According to the tuning processes in chapter 4 and chapter 5, a higher cutting speed within a proper range would enhance the generation of tribofilms. Similar to chapter 4, 40 m/min and 60 m/min are investigated under dry conditions in the running-in stage of the cutting process, in order to design a new cutting approach.

A.1.2 Tribological behaviour at the chip/tool interface: Chip characteristics, undersurface and cross-sectional studies

Type of chip is determined by comprehensive factors mainly associated with the workpiece properties, cutting conditions and tool properties such as geometry and

surface coatings. Material flow in single point hard turning, with a relatively larger nose radius tool, was not only along the feed marks but also in between the feed marks due to material side flow occurring during machining. It was noticed that the nose radius would lead to an increase in the plowing force. In addition, non-uniform displacement vertical to the chip length was facilitated due to the variation in the chip velocity. Chip edge serration at the trailing edge is a sign of material side flow. The retarded zone is heavily influenced by the thermal conductivity of the cutting tool, which is affected by the deformation and seizure of the workpiece material on the tool within the friction interface. The under-surface morphology and cross-sectional characteristics give a direct indication of the frictional conditions at the tool/chip interface.

The chips produced were collected in the beginning of the turning process from S40 and S60 with new inserts (less than 50m length of cut). To avoid the need for lubrication or cooling from a cutting fluid, the dry turning was performed with CNGG432FS inserts from Kennametal. Figure A.2 presents the SEM images of the chip curl which is an important property for practical machining. Both S60 and S40 showed continuous chip, but the chips at S60 are more regular. The uneven curling behaviour in S40 could be caused by the non-uniform displacement vertical to the chip length.

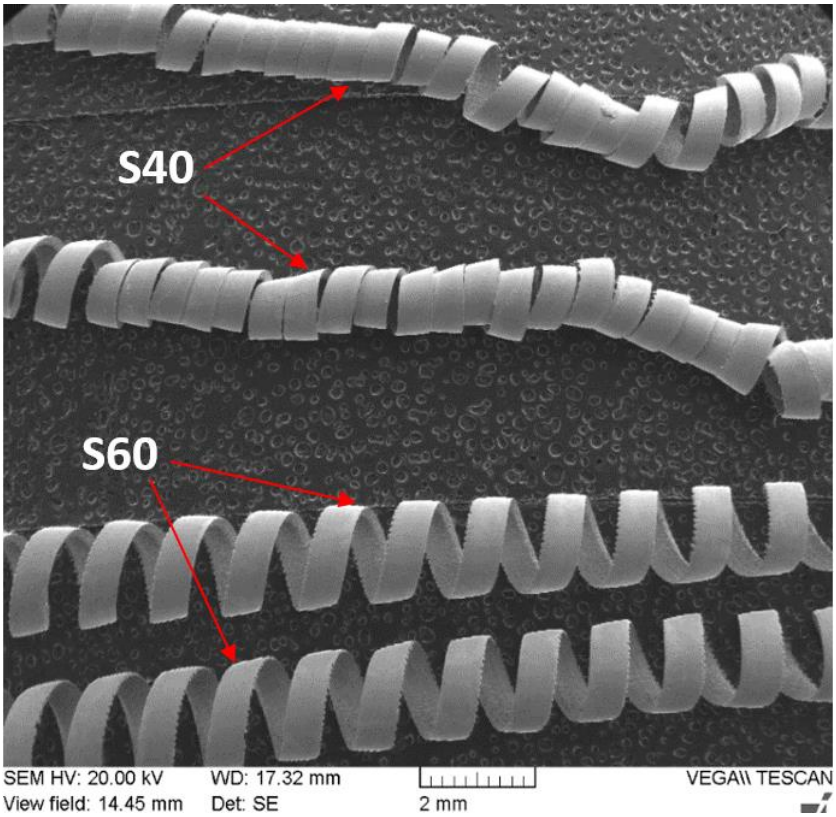

Figure A.2 Curling types of chips at S40 and S60

Figure A.3 presents the SEM images of the chips undersurfaces for S40 and S60 respectively. At a cutting speed of 40 m/min, the undersurface morphology shows some micro-cracks and tears, which caused by the seizure on the interface versus the potential metal flow. The chips generated at 60 m/min exhibit smoother morphology and groove. More serration is shown in S60 sample, which indicates more side flow. The markers on S60 surface exhibit more side flow as well.

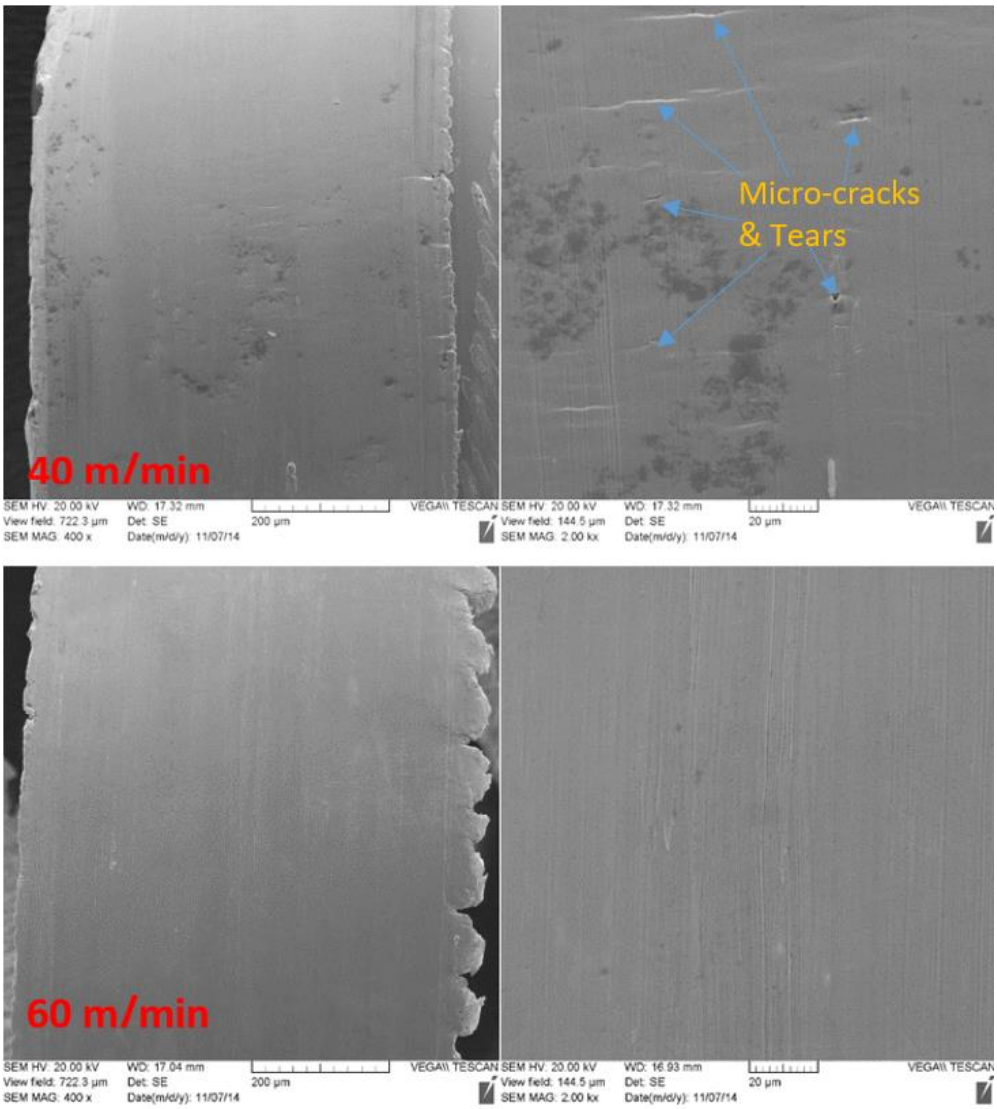

Figure A.3 SEM image of chip under surface

Figure A.4 presents the optical microphotograph of the chip cross-section. The retarded zone thickness is much thicker in the chip cross-section at 40 m/min than 60 m/min. A thicker section suggests higher friction at the interface which backs the chip material up contributing to the formation of a thicker chip. The metal flow in the cross-section distributes on the whole area of S60 while it is concentrated within a few

microns near the surface in S40. The seizure on the S40 surface limits the intensive deformation of chips within the near surface area, which is not seen in the S60 sample. This causes a thicker retarded zone in S40. Intensive deformation and dislocations originating from the near surface leads to more cracks and defects in the cross section which is more evident in the S40 sample.

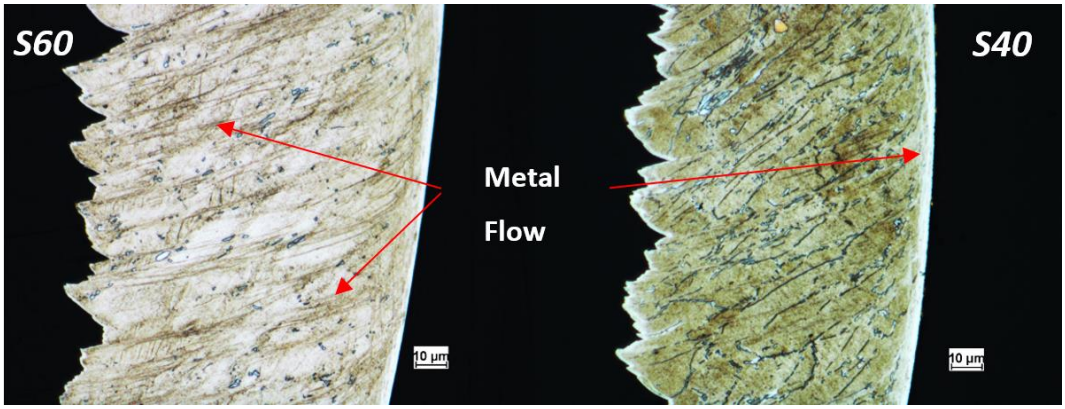

Figure A.4 Optical microphotograph of chip cross-section (etched by Aqua regia)

The optical images cannot present the deformation at the interface clearly. Figure A.5 shows the back-scattered electron images of the chip cross-sections at 40 m/min (S40) and 60 m/min (S60). The chip cross-section at 40 m/min shows more deformation and metal flow at the chip/tool interface, while less carbide is present in the 60 m/min chip cross-section.

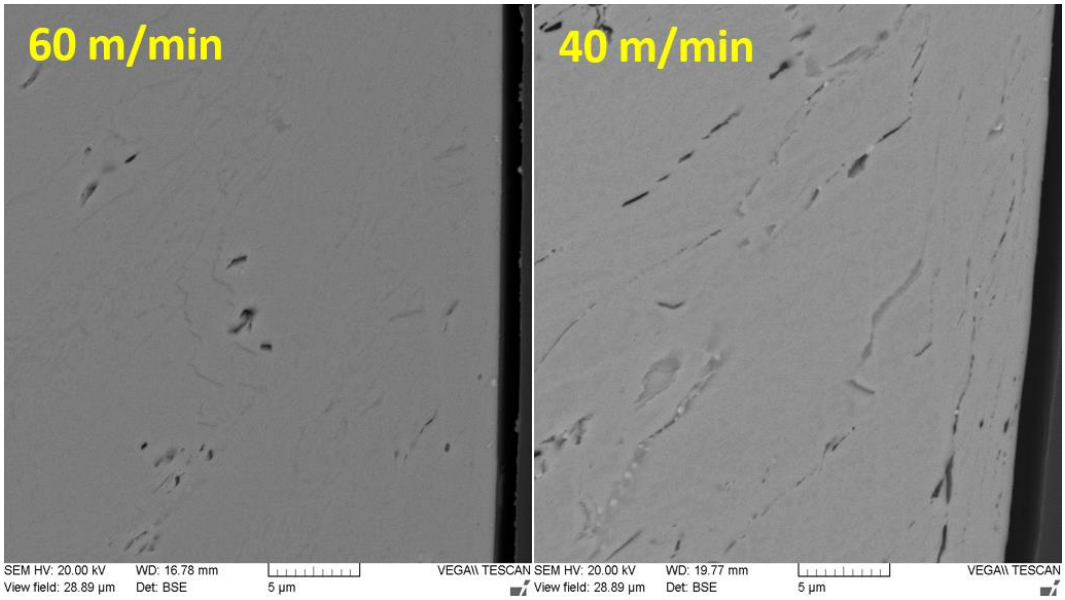

Figure A.5 BSE of chip cross-section (etched by 15ml HF+ 15ml 2% Acetic acid)

A.1.3 Wear Mechanism and Wear Patterns

Figure A.6 presents the SEM/EDS elemental maps of three worn inserts at S40 and S60 after 100 meters of turning (still within the initial running in stage) under dry conditions. Intensive buildup edge formation was observed for both samples. Since Nickel presents only in the workpiece material, this element was used as an indicator of the presence of adhered workpiece material on the worn surface. In EDX elemental mapping analysis, the worn surfaces were found to be mostly covered by Nickel transferred from the workpiece.

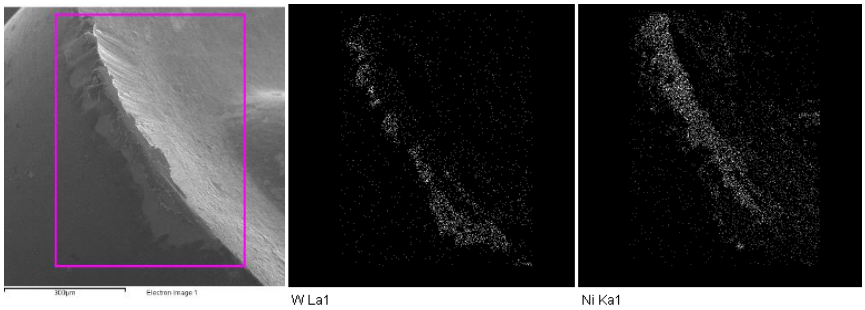

(a) S40 sample

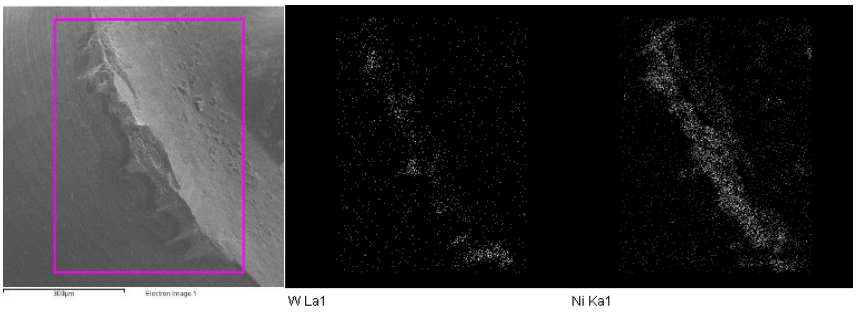

(b) S60 sample

Figure A.6 Cutting edge at 200m and elemental mapping of W and Ni

For both worn inserts, the Inconel buildup was etched out by swabbing with HF for 60 seconds. After etching, it was noticed that both samples have the same wear mechanisms: abrasive wear on the flank surface and crater wear on the rake surface. The tool used under 40 m/min showed a larger flank rake wear intensity than the tool used under 60 m/min. Figure A.7 shows the EDX mapping spectra of both inserts with the built up edge removed. Nickel still exists on the worn surface of all three inserts, but it does not cover the surface and prevent the detection of other elements as compared to the EDX spectra before etching. Nickel is clearly seen on the cutting edge for the insert used at 40 m/min, which indicates more severe built-up edge formation. Even

though no substrate coating flaking was observed for either insert, the substrate (WC-Co) exposure was identified on the worn zone based on the W signal. This means that the coating is gone in the observed area. The worn coating area is much more intensive for the insert tested at 40 m/min, as compared with 60 m/min.

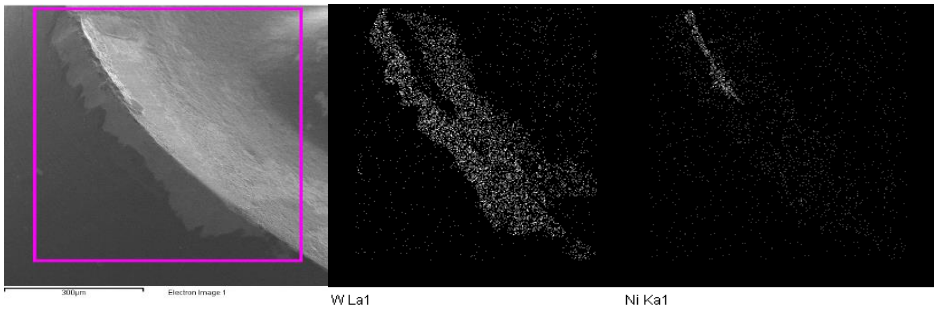

(a) S40 sample after etching

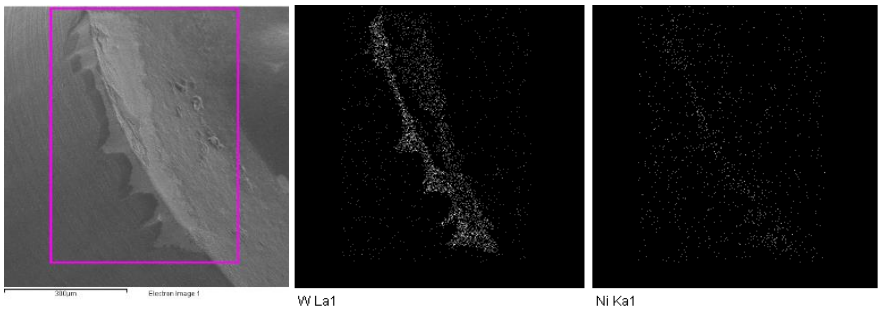

(b) S60 sample after etching

Figure A.7 Cutting edge at 200m after etching and elemental mapping of W and Ni

A.1.4 Remarks

The purpose of this work is to investigate tribofilms formation under the influence of a changing cutting environment. In the case of dry-wet cutting, tribofilms formation might be affected either by the temperature/heat flow during dry cutting or by the compounds changing due to the switching of cutting coolant. The tuning process

introduced in chapter 4 and 5 can be applied to multiple cutting tools and workpiece materials. The tribological and wear behaviour study indicated a better lubrication condition was provided at S60 than at S40 during the running-in stage, which is likely the result of the formation of lubricating tribofilms. Moreover, S60 presented less damage to the coated cutting tools which also benefited from the presence of the thermal protective tribofilms. Further characterization needs to be performed in order to confirm the assumption that acceleration produces beneficial tribofilms.

A.2 Various Methods to Characterize Tribofilms

Partial citation:

G. Fox-Rabinovich *a*,*, A. Kovalev *b*, M.H. Aguirre *c*, K. Yamamoto *d*, S. Veldhuis *a*, I. Gershman *e*, A. Rashkovskiy *b*, J.L. Endrino *f*, B. Beake *g*, G. Dosbaeva *a*, D. Wainstein *b*, Junfeng Yuan *a*, J.W. Bunting *a*, "Evolution of self-organization in nano-structured PVD coatings under extreme tribological conditions." Applied Surface Science 297 (2014): 22-32.

a Department of Mechanical Engineering, McMaster University, 1280 Main St. W., Hamilton, ON, Canada L8S4L7

b Surface Phenomena Researches Group, CNIICHERMET, 9/23, 2-nd Baumanskaya Street, Moscow 105005, Russia

c Laboratory of Advanced Microscopy, Institute of Nanoscience of Aragón, University of Zaragoza, 50018 Zaragoza, Spain

d Materials Research Laboratory, Kobe Steel Ltd, 1-5-5 Takatsuda-dai, Nishi-ku, Kobe 651-2271, Hyogo, Japan

e All-Russian Railway Research Institute, 10 Third Mytishchinskaya Street, Moscow 29851, Russia

f Albengoa Research, Energia Solar 1, Palmas Altas, Seville 41014, Spain

g Micro Materials Limited, Willow House, Yale Business Village, Ellice Way, Wrexham LL13 7YL, UK

Copyright:

Relative Contributions:

This article was led by Dr. Fox-Rabinovich. As a co-author of this journal article, the author of this thesis assisted in the machining tests, surface sample preparation and analysis of results in surface characterization.

Only the work that involved the author of this dissertation is included in this chapter with agreement from the lead author of the journal article. Even though the author of this dissertation gave assistance in the experiments and surface results analysis, yet the major discussion and the conclusion of this journal article were analyzed by the lead author, Dr. Fox-Rabinovich. The author of this thesis assisted with the SEM/EDX and XPS tests in this work which were already presented in the other chapters. The purpose of this section is to show the various surface techniques used to characterize tribofilms and to present a potential research direction for future research which can be applied for further research work on tribofilms. To avoid discussing the techniques already covered, only the results of the TEM and micro-mechanical tests are presented.

Evolution of Self-Organization in Nano-Structured PVD Coatings under Extreme Tribological Conditions

A.2.1 Experimental

Two different advanced coatings were compared, a TiAlCrSiYN monolayer and a TiAlCrSiYN/TiAlCrN multilayer. The monolayer $Ti_{0.2}Al_{0.55}Cr_{0.2}Si_{0.03}Y_{0.02}N$ and nano-multilayered $Ti_{0.2}Al_{0.55}Cr_{0.2}Si_{0.03}Y_{0.02}N/Ti_{0.25}Al_{0.65}Cr_{0.1}N$ coating was deposited using $Ti_{0.2}Al_{0.55}Cr_{0.2}Si_{0.03}Y_{0.02}$ and $Ti_{0.25}Al_{0.65}Cr_{0.1}$ targets correspondingly fabricated by a powder metallurgical process on a mirror polished cemented carbide WC-Co substrate and ball nose end mills in a R&D-type hybrid PVD coater (Kobe Steel Ltd.) using a plasma-enhanced arc source. Deposition parameters are shown in Table A.1. The thickness of the coating was around 3 microns for the film characterization and cutting test work.

Table A.1 Phase and chemical composition of the worn surface (XPS data) at the different stages of wear (15 m-running-in stage; 30 m-beginning of the stable stage).

Coating	Cutting length	Chemical elements content in the coating and tribo-films							
		Al, at%			Ti, at%			Cr, at%	
		Al_2O_3 tribo-films	Mullite tribo-films	Nitride coating	TiO_x tribo-films	TiO_2 tribo-films	Nitride coating	Cr_xO_y tribo-films	Nitride coating
Multilayer	15 m	14.9	20.4	20.4	0	0	0	10.1	9.9
Monolayer	15 m	19.8	10.2	25.0	5.36	4.04	10.6	7.22	12.38
Multilayer	30 m	29.1	6.6	19.3	7.3	5.5	7.2	15.9	4.1
Monolayer	30 m	8.8	17.6	28.6	6.8	7.2	6.0	16.0	4.0

Cross-sectional TEM observation was employed in combination with FIB (focused ion beam) for investigation of the coatings on the cemented carbide WC/Co substrates. Transmission electron microscopy, and selected area electron diffraction (SAED) were performed in a JEOL FS2200 microscope at an acceleration voltage of 200 kV. High annular angular dark field (HAADF) -STEM image of the coating was employed with EDAX profile of the coating layer (beam of 1 nm spot size).

The micro-mechanical characteristics of the coatings were measured on WC-Co using a Micro Materials NanoTest system.

Cutting tests have been performed during dry ball-nose end milling (Mitsubishi carbide ball nose end mills, D=10 mm) of the hardened AISI H13 tool steel with hardness HRC 53–55. Cutting parameters are outlined in Table A.2. The coated tool flank wear

was measured using an optical microscope (Mitutoyo model TM).A tool dynamometer (9255B, Kistler) was used to measure the cutting forces. At least three cutting tests were performed for each kind of coatings under corresponding operations. The scatter of the tool life measurements was approximately 10%.

Table A.2 Cutting parameters used for the tool life evaluation.

Machine	Cutting parameters				
Three-axis vertical milling center (Matsuura FX-5).	Speed, m/min	Feed, mm/tooth	axial depth, mm	radial depth, mm	Coolant
	500	0.06	5	0.6	Dry conditions

A.2.2 Results

A.2.2.1 Wear resistance of the coatings.

Tool life vs. length of cut data are shown in Figure A.8. The wear rate completely stabilizes after 20 m length of cut for the multilayer coating. In the monolayer, wear rate also decreases but with a lower wear rate stabilization.

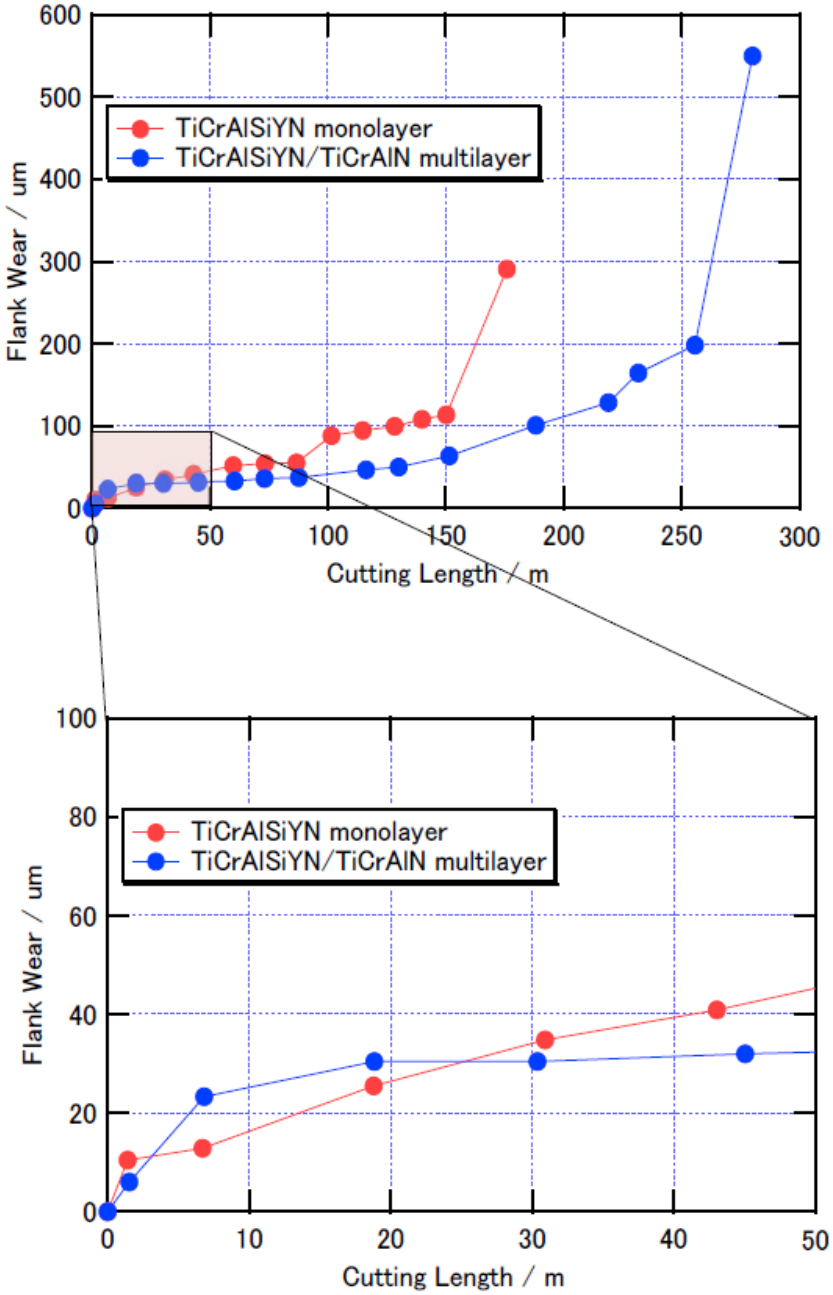

Figure A.8 Tool life of TiAlCrSiYN-based mono- and multilayer coatings vs. length of cut

A.2.2.2 Micro-mechanical characteristics of the coatings.

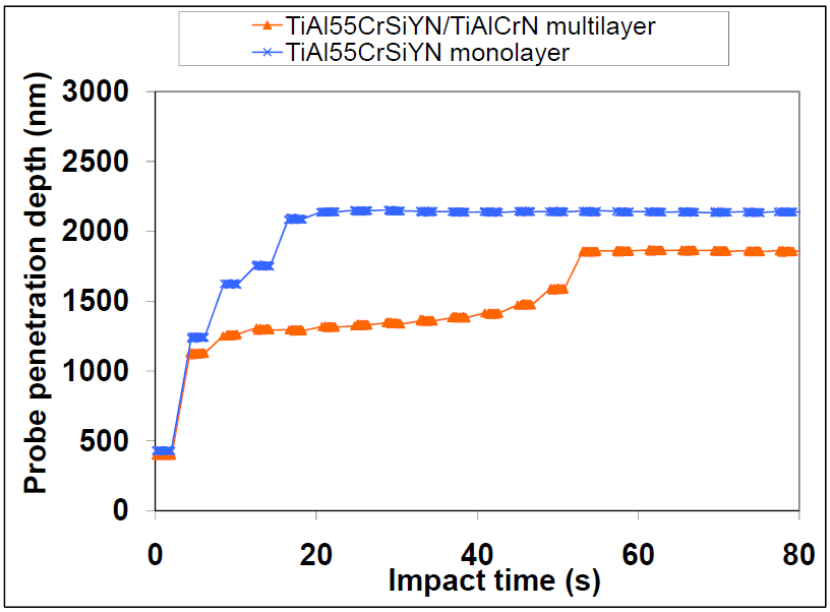

Figure A.9 SEM images of surface morphology vs. length of cut of the worn coated ball-nose end mills with a) TiAlCrSiYN mono-layered and b) TiAlCrSiYN/TiAlCrN multi-layered coatings during running-in stage

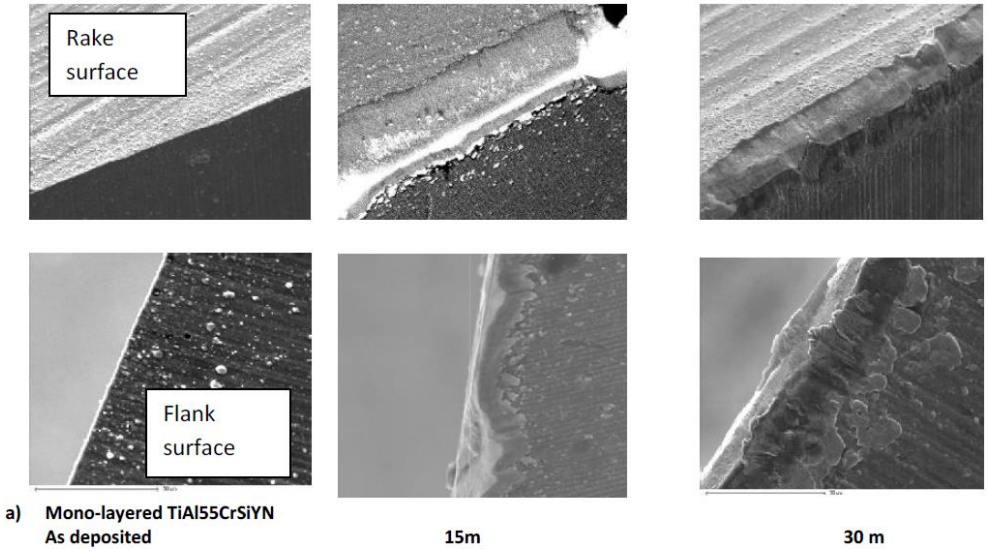

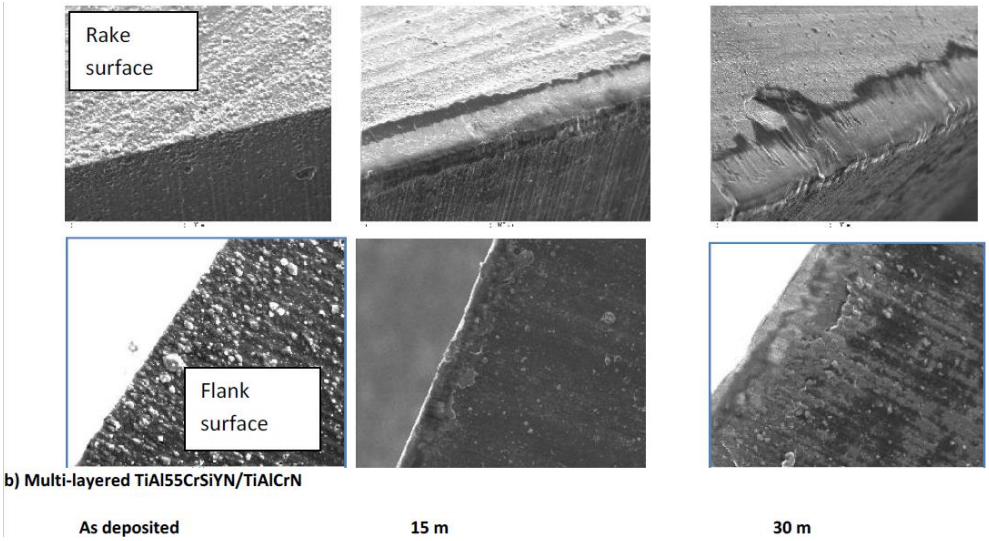

Figure A.10 Short time impact fatigue fracture resistance data at 25 mN for the TiAlCrSiYN and TiAlCrSiYN/TiAlCrN coatings that corresponds to the running in stage

The mechanical properties are a critical factor in providing a stable environment for the system to display adaptive behaviour that minimises wear. This is especially true for hard and brittle tribo-ceramics formed during friction. Rapid destruction of tribo-ceramics could be prevented with the proper design of the coating layer that can provide a low wear and surface damage resistant environment for the tribofilms to form and regenerate in order to sustain high temperatures/stresses under operation. Therefore, they can efficiently act as thermal barriers and in response, protect the underlying coating. Stability of the self-organization process could be controlled by dynamic self-regulation of the tribofilms generation and destruction. This could be realized in the multilayer coating as related in the short time impact data shown in Figure A.10. The impact fatigue data show that surface damage of the multilayer coating during the initial stage of testing is significantly lower than in the

monolayer. The micro-mechanical data shown in Figure A.9 are in full agreement with the SEM data shown in Figure A.10.

A.2.2.3 Microscopic evaluation of surface damaging processes

TEM analysis of worn surface for monolayer coatings after length of cut of 15 m (running-in stage) is presented in Figure A.11, and compared to the post running-in stage (Figure A.11, b). This analysis indicates deformation (bending of columns) during operation. Deformation takes place within relatively thick surface layer. Cracks are also forming below the surface. Quite strong surface damage is occurring. Similar (but somewhat less intensive) surface damage is observed after length of cut of 30 m when the running-in stage has completed (Figure A.11, b). More detailed HR TEM information on the monolayer coating after length of cut of 15 m is presented in Figure A.12. The figure shows the HRTEM of the first 50 nm of the spots marked 2-1; 2-2 (see TEM cross-section in the left upper corner). The coating layer includes a very thin superficial layer (around 20 nm thick) with a completely amorphous structure. Below this layer the structure is crystalline. Apart from the normal TiAlCrN-based structure with d_{111}~0.24 nm; d_{002}~0.20 nm; d_{022}~0.14 nm (ring pattern marked) two interplanar distances exist that cannot be assigned (~0.45 nm and ~0.35 nm) and coming from the marked regions. The possible nano-crystals marked could be Fe or Si content phases due to the enrichment of the surface layer by Fe (first 70 nm) and Si (110-60 nm).

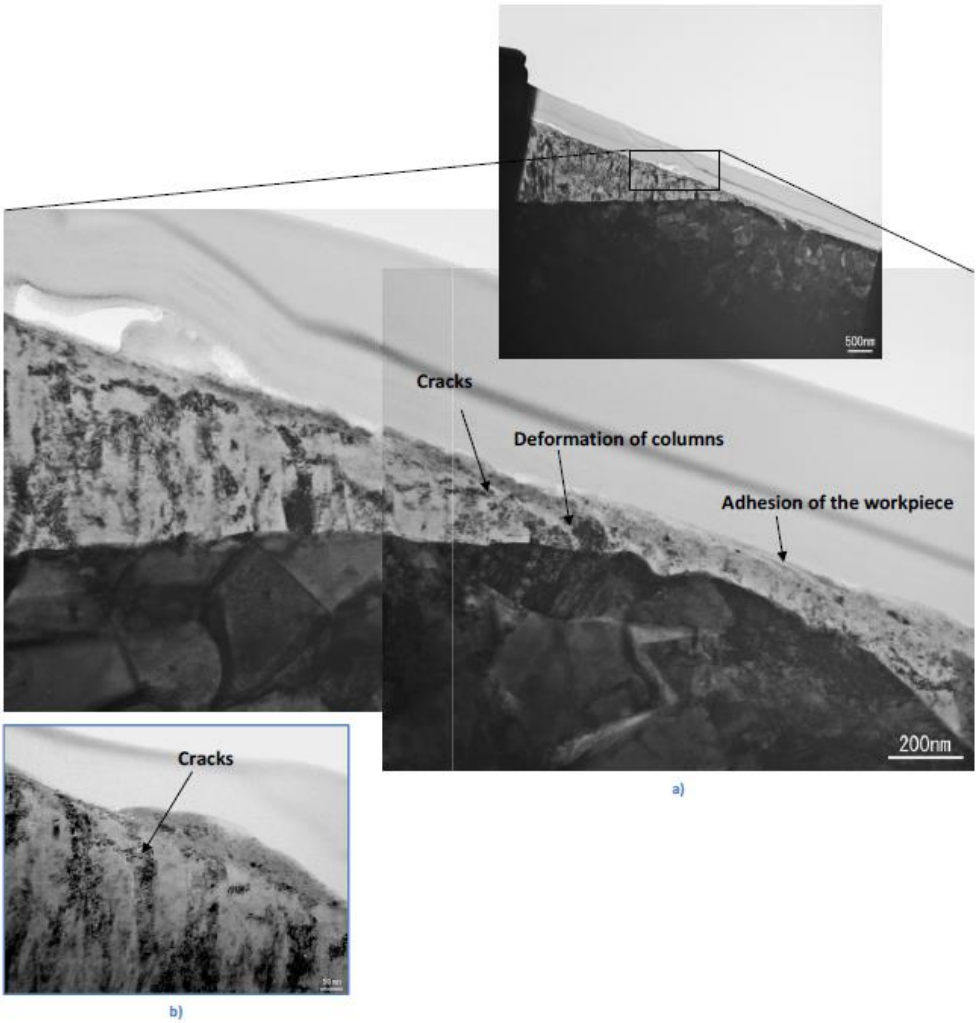

Figure A.11 TEM analysis of worn surface for monolayer coating a) at the length of cut of: a) 15m (running-in stage); b) 30 m (post running-in stage).

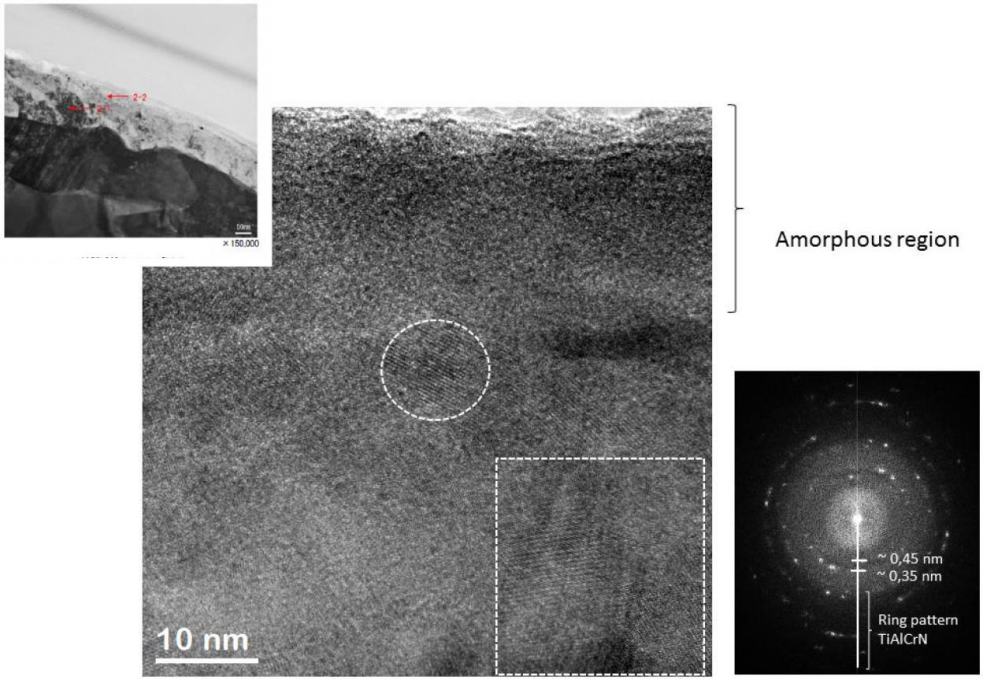

Figure A.12 HRTEM analysis of worn surface with SAED diffraction pattern for monolayer coating at the length of cut of 15m (running-in stage)

TEM analysis of worn surface after 15 m length of cut for the multilayer coatings is presented in Figure A.13, a. Deformation (bending of columns) takes place within the relatively thin surface layer compared to the monolayer (Figure A.11). Cracks also form but closer to the surface. Less intensive surface damage is taking place as related in the SEM data in Figure A.9. However, the worn surface of the multilayer coating in the post running-in stage (length of cut of 30 m) shows a minimum of surface damage indicating a milder wear mode (Figure A.13,b). Figure A.13, a) also shows SAED diffraction patterns of the marked areas. Spots 1, 2 correspond to build up edge. All other spots correspond to TiAlCrN-based structure of the coating layer. The outer surface layer of thickness 50-100 nm has an amorphous structure.

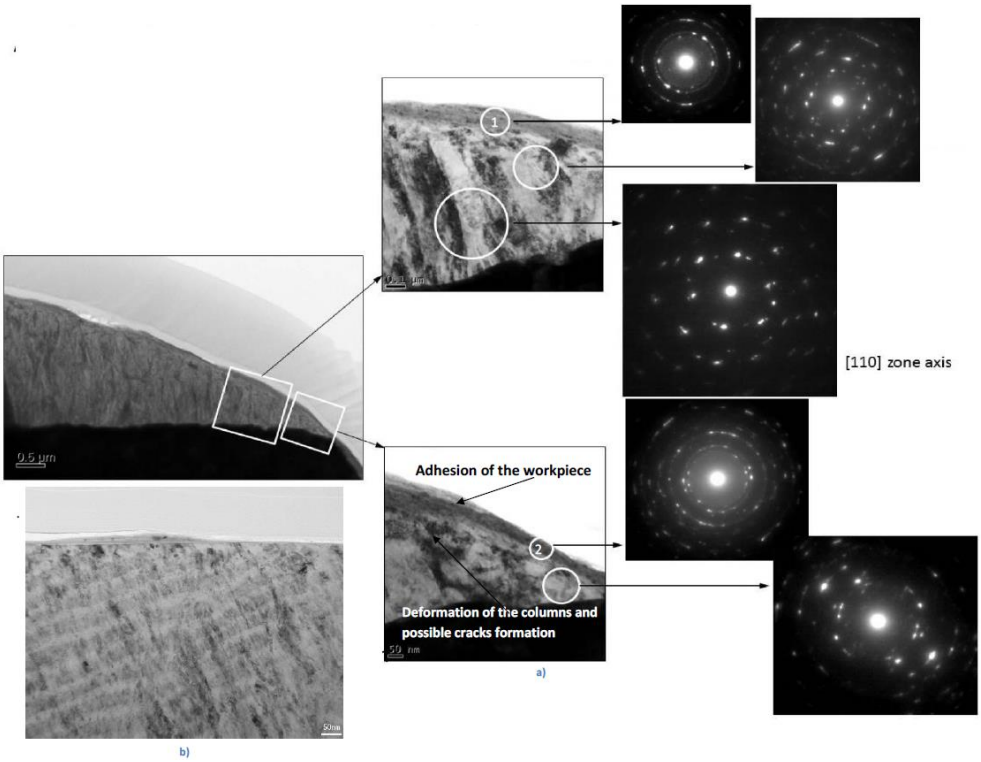

Figure A.13 TEM analysis of worn surface for multilayer coating. TEM cross-section with SAED diffraction patterns of the marked areas for multilayer coating at the length of cut of a) 15m (running-in stage,) in comparison to b) the post running-in stage (30 m length of cut)

Line scan profile of the multilayer coating is shown in Figure A.14. The analysis shows the elemental distribution on the worn surface. Elemental map and line scan analysis both indicate formation of a buildup edge. The Fe signal decreases once Ti signal grows at the position of about 150 nm on the line scan. This relates to the layer of the buildup and the coating correspondingly. The Si signal is somewhat higher at the buildup/coating interface (see elemental map).

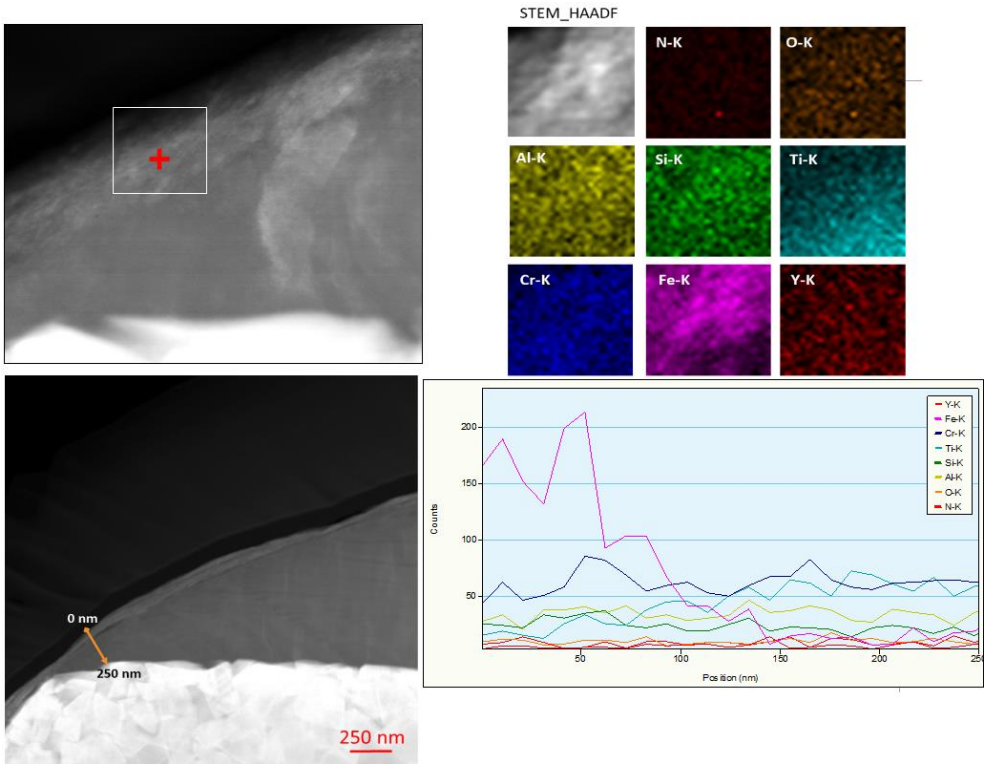

Figure A.14 EDS line scan profile of the multilayer coating at the length of cut of 15m (running-in stage)

Remarks

The purpose of this citation is to present a various and comprehensive characterization of tribofilms. Due to limitations of preparing and performing experiments at such a large scale, the other journal articles cited in this dissertation were only performed with XPS and AES in order to present quantitative and qualitative results in tribofilms characterization. XPS and AES could meet the basic requirements of this study, however, TEM and micro-mechanical characterization would provide a more data and an interesting viewpoint to better understand the tribofilms.